

# **Sustainable Nutrient Recovery Through Integrating Electricity-Assisted Membrane Processes**

---

A Dissertation

Submitted to

the Temple University Graduate Board

---

In Partial Fulfillment

of the Requirements for the Degree

DOCTOR OF PHILOSOPHY

(Environmental Engineering)

---

by

Kartikeya Kekre

December 2022

Examining Committee Members:

Heyang Yuan (Ph.D.), Advisory Chair, Civil and Environmental Engineering

Rominder Suri (Ph.D.), Civil and Environmental Engineering

Gangadhar Andaluri (Ph.D.), Civil and Environmental Engineering

Sujith Ravi (Ph.D.), Department of Earth and Environmental Science

## ABSTRACT

The rising use of mineral-based fertilizer and water for agricultural operations to feed a growing population has polluted water bodies and depleted resources. In addition, nutrient contamination has caused eutrophication and wastewater concerns that conventional wastewater treatment cannot solve. Thus, meeting new water treatment regulations and procuring more value-added products from these procedures is crucial. Conductive ultrafiltration membranes precipitate and extract struvite, an ecologically good fertilizer, from synthetic livestock effluent. This technique produces solid fertilizer and irrigation-quality water.

Since the recovery process relies on electrochemical hydrolysis and local pH modulation along the membrane surface, pH correction does not need chemical additions. The system was tested using cow effluent with up to 1,000 mg/L of nitrogen and phosphorus. Analytical tests showed that the precipitates were struvite and that up to 65% of the phosphorus and nitrogen were removed in the first 30 minutes of electrochemical filtration. Low membrane fouling and flux drop made the recovery technique successful. A mathematical model of N, P, and Mg ions in an external electric field explained the fouling and precipitation tests. Thus, precipitation happens near the membrane but not on it. This reduces surface fouling.

Forward osmosis was used to make struvite with less energy. A voltage near the FO membrane enabled magnesium to migrate opposite into the feed chamber, where it reacted with ammonium and phosphate in the feed solution to form struvite. Electrical charging increased struvite recovery by 77% and water recovery by 39%. Ion migration may have

reduced dilutive and concentrative polarization on the draw and feed sides of the FO membrane, causing the rise. High external voltage, draw concentration, and draw pH made water recovery and struvite precipitation simpler. This study suggests that reverse salt flow might improve FO systems' nutrition and water recovery. These devices were combined with microbial electrolytic cells to generate electricity and prevent biofouling. FO treatment was investigated using vacuum membrane distillation for sustainability and zero discharge. Constant draw solution reconcentration yields more steady flux values than the typical lowering flux. The research will increase knowledge of treatment system synergy in water reclamation and nutrient recovery. It also identifies possible obstacles to development.

## ACKNOWLEDGEMENTS

I would like to express my utmost gratitude and appreciation to my advisor, Dr. Heyang Yuan, for his guidance and wisdom throughout this project and his unwavering patience in working with me over the last two years. For me, you've been an excellent role model. Your guidance has been priceless, both in terms of research and my professional development. Additionally, I would not have been able to start this journey without the committee members Dr. Rominder Suri, Dr. Gangadhar Andaluri, and my former advisor Dr. Avner Ronen. Thank you for the chance to work in your labs when I first started at Temple University and for collaborating on projects.

Many Thanks to my fellow lab mates Dr. Arezou Anvari, Ying Yao, Katelyn Kahn, Shiyun Yao, Zhang Cheng, Diana Tiburcio, and Josh Simpson for your assistance and expert company. It was always a pleasure to work with such lovely and gracious people every day.

I would like to thank my family for their continued love and support through graduate school. I would like to thank my parents for their continuous support and motivation through this process. Thank you for not asking me how much longer it would take. I am grateful to my uncle and aunt for supporting me and being my parents away from home. Thanks to the food you made me, I didn't miss home. I also want to express my appreciation to my girlfriend, Veronica, for her support through this process.

## Table of Contents

ABSTRACT.....	ii
TABLE OF FIGURES.....	viii
LIST OF TABLES.....	ix
<b>1. WASTEWATER AS RESOURCE AND NUTRIENT IMBALANCE: AN INTRODUCTION.....</b>	<b>1</b>
1.1. Conventional Nutrient Pollution Treatment .....	2
1.2. Nutrient Recovery As Struvite.....	4
1.3. Current Knowledge About Struvite Precipitation .....	5
1.3.1. pH .....	5
1.3.2. Supersaturation Ratio (SSR).....	7
1.3.3. Temperature .....	8
1.3.4. Mixing .....	9
1.3.5. Induction Time .....	10
1.3.6. Foreign Ions And Impurities.....	10
1.3.7. Nucleation And Seeding.....	11
1.3.8. Effect Of Surface Area On Struvite Crystallization .....	12
1.4. Membrane-Based Nutrient Treatment .....	13
1.5. Objectives And Significance.....	14
<b>2. ENHANCED NUTRIENT RECOVERY FROM LIVESTOCK WASTEWATER WITH CONDUCTIVE ULTRAFILTRATION.....</b>	<b>17</b>
2.1. Introduction.....	18
2.2. Materials & Methods.....	21
2.2.1. Materials .....	21
2.2.2. Membrane Fabrication.....	22
2.2.2.1. Feed Solutions.....	22
2.2.2.2. Experimental Setup .....	23
2.2.2.3. Membrane And Struvite Characterization.....	24
2.3. Results And Discussion.....	26
2.3.1. Reactive Electrochemical Membrane Characterization.....	26
2.3.2. Struvite Recovery Cycles.....	27
2.3.3. Membrane And Particles Analysis .....	31

2.3.4.	Influence Of External Potential On pH Change .....	34
2.3.5.	Modeling Ions Concentration Near The Electrically Charged Membrane ....	37
2.3.6.	Estimated Cost Of Electrochemical Struvite Recovery .....	41
<b>3.</b>	<b>ENHANCED NUTRIENT RECOVERY FROM LIVESTOCK WASTEWATER WITH ELECTRICITY – ASSISTED FORWARD OSMOSIS.....</b>	<b>43</b>
3.1.	Introduction.....	44
3.2.	Materials and Methods.....	48
3.2.1.	Feed And Draw Solutions.....	48
3.2.2.	System Setup And Operation.....	48
3.2.3.	Measurement And Analysis .....	50
3.3.	Results And Discussion.....	51
3.3.1.	Enhanced System Performance Under External Voltage .....	51
3.3.2.	Struvite characterization.....	53
3.4.	Effects Of Operating Conditions On System Performance.....	55
3.4.1.	External Voltage.....	55
3.4.2.	Draw Concentration .....	58
3.4.3.	Draw pH.....	59
3.5.	Perspective.....	61
<b>4.</b>	<b>ENHANCED NUTRIENT RECOVERY FROM LIVESTOCK WASTEWATER BY COUPLING ELECTRICITY – ASSISTED FORWARD OSMOSIS &amp; MEMBRANE DISTILLATION .....</b>	<b>64</b>
4.1.	Introduction.....	65
4.2.	System Setup .....	71
4.2.1.	Forward Osmosis Setup.....	71
4.2.2.	Vacuum Membrane Distillation .....	72
4.2.3.	Measurement And Analysis .....	73
4.3.	Results and Discussion.....	74
4.3.1.	MD Setup Testing .....	74
4.3.2.	Hybrid FO-MD Operation .....	74
4.4.	Perspectives .....	77
<b>5.</b>	<b>FUTURE PERSPECTIVES: COUPLING MICROBIAL ELECTROLYSIS CELL, ELECTRICITY – ASSISTED FORWARD OSMOSIS &amp; MEMBRANE DISTILLATION FOR ZERO-CHARGE NUTRIENT RECOVERY .....</b>	<b>79</b>
5.1.	Introduction.....	80
5.2.	Nutrient Recovery In Bioelectrical Systems .....	82

<b>5.3. Combining BES With Forward Osmosis Processes.....</b>	<b>84</b>
<b>5.4. Methods.....</b>	<b>86</b>
<b>5.4.1 Fabrication Of MEC.....</b>	<b>86</b>
<b>5.4.2. System Operation.....</b>	<b>87</b>
<b>5.4.3. Analytical Measurements.....</b>	<b>87</b>
<b>5.4.4. System Perspective.....</b>	<b>88</b>
<b>5.5.1. Acidification.....</b>	<b>90</b>
<b>5.5.2. Osmotic Shock.....</b>	<b>90</b>
<b>5.5.3. Voltage Issues.....</b>	<b>92</b>
<b>5.5.4. Impact Of Separating Membrane.....</b>	<b>93</b>
<b>6. Executive Summary, Conclusions, and Future.....</b>	<b>95</b>
<b>REFERENCES.....</b>	<b>99</b>
<b>APPENDIX A. SUPPLEMENTARY MATERIAL.....</b>	<b>134</b>

## TABLE OF FIGURES

<b>Figure 1</b> Membrane Flow-cell design .....	<b>25</b>
<b>Figure 2.</b> Characterization of fabricated Conductive Ultrafiltration Membranes based on Carbon nanotubes. a) SEM images of the REM top surface; b) Conductive Ultrafiltration Membranes cross-section following freeze-fracture, showing the deposited Carbon nanotubes layer; c) wetting contact angle for pristine PES; d) wetting contact angle for CNT-polyvinyl alcohol coated PES.	<b>27</b>
<b>Figure 3.</b> Recovery cycles of 1mM and 10mM solutions. (a) 1mM flux and pH profile as a function of time: (b)10mM flux and pH profile as a function of time. Dotted lines represent shutting the permeate flux and washing the reactive electrochemical membranes with Deionized water.....	<b>29</b>
<b>Figure 4</b> Precipitated struvite by USB-microscopy at (a) 1mM solution and (c) 10mM solutions; (b) Scanning electron microscopy images of the precipitated particles at (c) 1mM solution and (d) 10mM solution; X-ray diffraction (e) commercial struvite and (f) precipitated sample ; Fourier transform infrared spectra for (g) commercial struvite (h) precipitated sample .....	<b>33</b>
<b>Figure 5</b> Schematic representation of struvite recovery by charged membranes. Electrochemical production of hydroxide at the membrane surface catalysis struvite formation while excess ammonium is turned into ammonia. ....	<b>34</b>
<b>Figure 6</b> Graphical description of concentration profile as a function of the membrane's surface charge: a), d) Ions concentration profile without voltage b) Ions concentration profile a function of distance from the charged membrane surface in 10mM solution c) Ions concentration profile as a function of distance from the charged membrane surface in 1mM solution e) schematic model describing the distribution of the ions in proximity to charged membranes. The nucleation zone is formed a few angstroms away from the membrane surface .....	<b>40</b>
<b>Figure 7</b> Schematic of the eFO system .....	<b>49</b>
<b>Figure 8</b> Water flux in the eFO and control systems. ....	<b>51</b>
<b>Figure 9</b> (A) The XRD spectra for samples collected from the eFO system (black) and commercial struvite (red). (B) The FTIR spectrum for samples collected from the eFO system. .	<b>54</b>
<b>Figure 10</b> (A) Water flux under different voltages. (B) Mass of struvite recovered and percentage of phosphate removed under different voltages.....	<b>57</b>
<b>Figure 11</b> (A) Water flux under different draw concentrations. (B) Mass of struvite recovered and percentage of phosphate removed under different draw concentrations.....	<b>59</b>
<b>Figure 12.</b> (A) Water flux under different draw pH conditions. (B) Mass of struvite recovered, and percentage of phosphate removed under different draw pH conditions.....	<b>60</b>
<b>Figure 13</b> A. FO flux and MD Flux characteristics at 80 C and 10KPa B. FTIR spectra of precipitates obtained in FO-MD processes. ....	<b>76</b>
<b>Figure 14</b> MEC-FO system for livestock wastewater treatment and biofilm development.....	<b>86</b>
<b>Figure 15</b> Schematic of microbial electrolysis system.....	<b>88</b>

## **LIST OF TABLES**

<b>Table 1.</b> The operating parameters under different experimental conditions.....	<b>50</b>
<b>Table 2</b> Struvite recovery and P removal in different units.....	<b>56</b>

# **1. WASTEWATER AS RESOURCE AND NUTRIENT IMBALANCE: AN INTRODUCTION**

The growing population has led to limited freshwater availability, increased food demands, and energy needs. Phosphorus and nitrogen are vital nutrients for agriculture. As a result, chemical fertilizers have increased demands and production to meet the ever-growing food requirements (Smil, 2000). The worldwide fertilizer demands have been growing by 2.4% annually (Heffer and Prud'homme, 2014). This has increased stress on high-quality phosphate minerals and the excess need for ammonia to meet crop production demands (Metson et al., 2016). Agricultural activities account for almost 85-90% of water consumption, and then these produce wastewater rich in phosphorus and ammonia as a result of chemical fertilizer and LWW (Qin et al., 2019; Smil, 2000).

By utilizing expansive and highly concentrated animal feeding facilities, the animal agriculture industry is growing to keep up with the demands of a growing population (Glibert et al., 2018). It is estimated that the annual production of livestock in the United States results in the release of 82,700 tons of nitrogen (N) and 26,000 tons of phosphorus (P) in the form of animal waste (Mallin et al., 2015). According to the findings of international studies, global livestock production will expand by 115% between the years 2000 and 2050, which will result in an increase of 23% and 54%, respectively, in the global surpluses of nitrogen and phosphorus. However, most excess nitrogen and phosphorus are lost to the ecosystem due to leaching into groundwater and runoff into surface waters (Bouwman et al., 2013). Therefore, nutrient contamination can result in eutrophication, which is a significant cause for concern in terms of the environment and may also threaten human health (Burkholder et al., 2018). In the meantime, the production of nitrogen-based

fertilizers worldwide has expanded by 1.5 over the previous few decades, reaching more than 150 million tons annually in 2013. (Glibert et al., 2014; Howarth, 2008).

Long-term predictions of water demand project that about 2.3 billion people will live in water-stressed areas and a 55% increase in global water demand (OECD, 2012). Existing water treatment models address this situation by using treated Livestock based wastewater for agricultural purposes and non-potable use (S.A, 2006). However, the application of fertilizers composed of phosphorus has also increased, albeit at a rate of approximately one-third that of nitrogen. Because of the excessive discharge and the rising demand for nutrients, there is an urgent requirement to recover nitrogen and phosphorus from Livestock based wastewater.

### **1.1. Conventional Nutrient Pollution Treatment**

Advancements in technologies for phosphate removal started in the 1950s; this was in response to the growing eutrophication issue and to control the phosphate levels in the surface waters (Morse et al., 1998). Some of the commonly used technologies include chemical adsorption, chemical precipitation, activated sludge processes, and crystalactor.

Chemical adsorption gained more popularity since it offers the option of adsorption of nutrients and regeneration of the same by desorption (Ramasahayam et al., 2014). The advantage of using adsorbents is that no extra reagents are needed to be added to control the pH, and there is no additional sludge production. A wide variety of materials like metal oxides and hydroxides (Golder et al., 2006), Fly ash (Chen et al., 2007), Furnace slag (Oguz, 2004), modified clay (Wu et al., 2006), and biological waste (Kse and Kivan, 2011) have been used as adsorbents. However, most materials used for chemical adsorption have

only been reported for bench-scale lab-based studies. Therefore, their practical efficiency and stability with livestock-based wastewater and wastewater treatment have still not been reported.

Chemical precipitation is one of the leading technologies. It employs the addition of metal salts, causing precipitation of an insoluble metal phosphate that is settled out by sedimentation. Unfortunately, this process leads to much-bonded phosphorus in the wasted sludge. These lead to the formation of a large amount of sludge which is primarily landfilled (Chimenos et al., 2003; Schuiling and Andrade, 1999; X. J. Wang et al., 2006; Yu et al., 2010; Zdybiewska and Kula, 1991). However, for agricultural use, the bioavailability of this sludge is inconclusive and still under study (Yeoman et al., 1988).

Activated sludge processes could take up phosphorus in considerable excess to that required for average biomass growth, which comprises biological phosphorus removal. Therefore, it is advantageous as it avoids using chemicals and prevents excess sludge production (Crocetti et al., 2000; Helmer and Kunst, 1998; Liu et al., 2007). However, on the contrary, the process requires complex plant configurations and operating parameters; the removal efficiency is variable and reaching low and consistent effluent standards would require simultaneous precipitation (Morse et al., 1998).

The Crystalactor method is based on crystallizing calcium phosphate on a seeding material. This method ensures short retention periods, hence a smaller reactor. Pellets are periodically removed, allowing continuous operation and automation of the plants (van Dijk and Braakensiek, 1985). This method requires the addition of additives to control the pH and enhance crystallization. Other wastewater approaches include ion exchange-precipitation using cationic resin. Most of the current phosphorus removal processes

mainly aim to improve the effluent quality, phosphorus removal is secondary, and the recovered sludge from backwashing is unsuitable for recycling (Morse et al., 1998).

## **1.2. Nutrient Recovery As Struvite**

Nitrogen and phosphorus are two of the three macronutrients required for life on earth (Smil, 2000). However, removing them from waste streams is also essential to reducing the environmental impact of eutrophication, which occurs when water-receiving bodies become too fertilized. Phosphate rock is in danger of running out of supply within the next half-century, mainly as a direct consequence of the increased demand in agricultural production (Luo et al., 2018). This crisis could be alleviated by recovering phosphate from wastewater rich in phosphate, such as digestates and urine that has been source-separated and then further reusing it as an alternative to manufactured phosphate fertilizer, which derives its primary component, phosphoric acid, from phosphate rock.

The precipitation of struvite, one of the most used methods for nutrient recovery, can achieve simultaneous recovery of ammonium and orthophosphate.  $\text{NH}_4^+$ -N and  $\text{PO}_4^{3-}$ -P can precipitate as struvite ( $\text{MgNH}_4\text{PO}_4 \cdot 6\text{H}_2\text{O}$ ) if a dependable supply of magnesium is added to the mix. Compared to typical chemical and liquid fertilizers, struvite exhibits a slow-releasing rate. This allows it to avoid burning crop roots and reduce nitrogen loss via leaching and surface runoff (Perera et al., 2019). The precipitation of struvite may also be used to successfully prevent the blockage of pipelines and other transportation equipment (De Paepe et al., 2020). Because of these apparent benefits, controlled struvite precipitation has been researched and utilized for several waste streams, including source-separated urine (Mu, 2012; Spångberg et al., 2014), anaerobic digestate (Wu and Modin, 2013),

swine wastewater (Osada et al., 1991), and municipal landfill leachate (Driver et al., 2010). Much research has been in the precipitation of struvite through existing physical and chemical methods to some degree of success. However, most of these depend on adding chemicals and chemical precipitation.

Apart from its use as an eco-friendly fertilizer, struvite has also been used as a potent fire retardant. Studies have looked at Struvite-based aerogels, where phosphoric acid released at elevated temperatures produces carbon char that smothers the flame. In addition, it uses significantly less phosphorus than conventional polyphosphate-based aerogels and is mined from wastewater sources, thus reducing the burden on phosphate-based mining. Authors also claim that using phosphate and ammonia as fire retardants increases economic profitability compared to being used as a fertilizer in the form of struvite (Kim et al., 2021).

### **1.3. Current Knowledge About Struvite Precipitation**

#### ***1.3.1. pH***

It has been observed that struvite crystallization occurs primarily in alkaline pH; thus, pH adjustment and control are the primary concern. The struvite precipitation is controlled by the ion solubility product (ISP) of  $Mg^{2+}$ ,  $NH_4^+$  and  $PO_4^{3-}$ ; the ISP depends on the pH of the solution. The yield of struvite of crystals increases with the change of pH from 8.0 to 9.0, and the system follows zero-order kinetics (Ch Bouropoulos et al., 2000; Le Corre et al., 2009; Nelson et al., 2003).

It has been reported that pure struvite does not exist above the pH of 10.0 (Hao et al., 2008); the presence of  $Ca^{2+}$  causes most phosphate-based precipitation after that. It can

also impact the struvite crystal characteristics. It has been reported that an increase in the pH from 8.0 leads to a decrease in the crystal size (Matynia et al., 2006).

Experiments on the effect on zeta potential revealed that pH is the most crucial factor in ensuring efficient agglomeration. The study attempted to quantify the impact of pH, ionic strength, and Mg dose. It was determined that even little pH changes might result in significant zeta potential changes, which would accelerate crystal growth through improved aggregation (Ch Bouropoulos et al., 2000).

Solution pH has also been reported to control the formation of ammonia gas from ammonium ions, affecting the molar concentration of the Mg:P:N affects the struvite precipitation process (Le Corre et al., 2009). In addition, the pH determines the range of solubility, an increase in pH value increases the phosphate ion concentration, while concentrations of Mg and  $\text{NH}_4$  decrease (M. S. Rahaman et al., 2008).

In studies by Ariyanto et al., the initial pH of the solutions varied to equilibrium pH, and the existing solution ions were reported. At lower pH (pH=3), it was observed that  $\text{H}_2\text{PO}_4^-$  dominates the phosphate concentration till pH 4. At pH 5 and 7,  $\text{H}_2\text{PO}_4^-$  and  $\text{HPO}_4^{2-}$  are the more prevalent species (Mijangos et al., 2004). At pH 9 and 11, the phosphate predominantly existed as  $\text{HPO}_4^{2-}$ . At extremely high pH ranges (pH>11),  $\text{NH}_4^+$  has the potential to transform into  $\text{NH}_3$  gas (Ali et al., 2005) (Ariyanto et al., 2014). It has been reported that the high solubility of ammonia does not affect the ammonia content of water and the volatilization of ammonia has no remarkable effect on total ammonia content (Wang et al., 2016).

The initial pH of the feed water is significant since pH, in some cases, cannot be maintained or controlled (Suzuki et al., 2007). The morphology, particle size, and thermal

properties of struvite can also be affected by initial pH (Ma et al., 2014). The addition of alkalinity and co-precipitation of carbonates are disadvantages of using high pH for struvite precipitation (Wang et al., 2010).

### 1.3.2. Supersaturation Ratio (SSR)

The rate of crystal synthesis and induction time vary based on changing supersaturation ratio. Supersaturation greatly depends on the ionic nature and strength of the system based on the ions taking part in it (Ch Bouropoulos et al., 2000; Kofina and Koutsoukos, 2005). Supersaturation can be explained by-

$$SSR = P_s/P_{s_{eq}} \quad Eq 1$$

$$P_s = [Mg^{2+}] [NH_3] [PO_4^{3-}] \quad Eq 2$$

Where  $P_s$  is the conditional solubility product, and  $P_{s_{eq}}$  is the equilibrium conditional solubility product. With the increase in ionic species, the  $P_s$  also increase. At higher pH, the value of  $P_{seq}$  decreases; hence it can be inferred that the SSR can be increased by increasing the concentration of struvite-forming ions and the pH of the solutions. In addition, Rahaman et al. reported that increasing the system's supersaturation ratio increases the removal of phosphate ions, resulting in a faster equilibrium rate. The experiments reported the highest phosphate removal rate at a supersaturation rate of 9.64 and the lowest at 1.13 (M S Rahaman et al., 2008a).

Ohlinger et al. observed the change in struvite supersaturation by varying mixing energy, experiment time, solution solubility, and pH. It was reported that the supersaturation ratio was higher in the system with moderate to high mixing. Experiments were conducted with a constant Supersaturation ratio and varying mixing energies. The results showed high dependence on struvite accumulation of the SSR value and a more

negligible dependence on mixing energy. Hence it was concluded that struvite precipitation is a diffusion-based process rather than an active transport-based product (Ohlinger et al., 1999).

In constant supersaturation conditions, the ionic activity in the system remained constant. Kofina et al. concluded that induction time depended on the supersaturation ratio. The threshold supersaturation was observed between SSR 3.18-4.45 for homogenous/heterogeneous nucleation. The parabolic dependence of the precipitation rates on relative supersaturation suggests a surface diffusion mechanism of precipitation (Kofina and Koutsoukos, 2005).

The total organic carbon in the system is also affected by the SSR and P-removal rate, which was attributed to the phosphate groups' tendency to form organic ligands. This effect seems to reduce above the pH of 8.1 (Bhuiyan et al., 2008b).

### ***1.3.3. Temperature***

With the increase in temperature, it has been observed that the solubility of struvite increases (Aage et al., 1997). On the contrary, studies reveal that the solubility of struvite increases up to 35°C. and then a drop in solubility was observed (Bhuiyan et al., 2007). Diffusion-controlled crystal growths are observed at high and low temperatures and are characterized as surface accumulation crystal growth (Jones, 2002). At higher temperatures, it has been reported that crystals other than Struvite might be formed at higher rates (Babi-Ivancic et al., 2002). Studies by Moussa et al. reveal that the increase in temperature after 20°C does not affect the critical pH. On the contrary, it affects the supersaturation coefficient and decreases with an increase in temperature (Ben Moussa et al., 2011). Although the equilibrium composition may be affected by the feed's

temperature, several published studies controvert results regarding the effect of temperature on struvite precipitation (Çelen and Türker, 2001).

#### ***1.3.4. Mixing***

The mixing speed has little to no effect on the intrinsic kinetics of struvite precipitation. The nucleation of struvite increases or is higher in the initial stages due to turbulent conditions of the feed solution, and this is because as the mixing energy increases, the induction time decreases. Rahman et al. observed no change in the nucleation rate above the threshold mixing energy of  $76\text{s}^{-1}$  for synthetic unseeded ALW (M. S. Rahaman et al., 2008). However, the removal and setting ability of phosphorus may be reduced by the excess mixing energy, which may cause the breakdown of crystals. Wang et al. report that mixing is vital for the initial crystal growth; mixing significantly affects struvite precipitation limited to a period of 60 mins (J. Wang et al., 2006). High mixing speed increases nucleation but simultaneously decreases crystal growth, and this specific phenomenon increases crystal breaking (Durrant et al., 1999). It has also been reported that the different mixing energies will impact the structure and size of the struvite crystals. Low growth rates were observed in low-mixing environments (Ohlinger et al., 1999).

Kim et al. carried-out experiments to correlate phosphorus and nitrogen removal rates to the mixing energy and duration. It was observed that the removal rates were lower than the predicted values. The study consolidated the conclusion that the struvite precipitation process remains unaffected beyond a particular threshold value for mixing energy and mixing duration. The struvite removal peaked at 80%. It was also observed that the struvite crystals' morphology depended on the changing mixing energies (Kim et al., 2009).

### ***1.3.5. Induction Time***

The time taken for struvite crystallization, i.e., crystallization, and induction time, controls the struvite precipitation process. It is defined as the time between mixing the constituents and forming the first precipitants (Ohlinger et al., 1999); as the parameters like pH and temperature increase, the induction time decreases (Abbona et al., 1982). Furthermore, the turbulence of the system also decreases the induction time, decreasing the time needed for nucleation (Ohlinger et al., 1999).

K.S. Le Corre et al. observed the relationship of Mg dosing to induction time. In lab-scale studies, induction time was observed to reduce from 125min to 6 min when the Mg dosage concentration varied from 1.2mM to 3.56mM. However, in pilot scale studies, it was observed that the increasing Mg dosage had little effect on the reduction of induction time (Le Corre et al., 2007).

### ***1.3.6. Foreign Ions And Impurities***

Crystal sizes and nucleation can be inhibited due to the deposition of impurities that block the crystal formation sites (Jones, 2002). It was observed that the presence of carbonate ions in the feed negatively impacts the growth rate and prolongs the induction time (Acelas et al., 2014). The presence of sodium, sulfate, and carbonate-bicarbonate impact struvite crystal size and structure. It was observed that sodium ions tend to reduce induction time. The presence of sodium ions increased the supersaturation levels. The crystal morphology was reported to be more comprehensive. Sulfate ions increased the induction time, even with a high comparable supersaturation level. Carbonate ions exert a negligible or marginal effect on the struvite precipitation and the supersaturation levels of the solution. Calcium

ions were expected to show a longer induction time, but this was not observed in higher concentrations.

The induction time decreased with an increase in calcium concentration. This study was done in lower ammonia levels (Kabdaşli et al., 2006). It has also been reported that excess calcium ions in the feed can reduce the struvite quality by forming other amorphous substances instead of crystalline struvite (Le Corre et al., 2005). Studies with Cadmium ions reported that the amorphous phase affects the purity of struvite from a  $\text{Cd}^{2+}$  concentration of 10mg/L. Aluminum ions did not affect the crystal purity, forming increasingly larger agglomerates with increased concentrations. Induction time was also decreased, and the phosphorus removal rate was significantly higher (Saidou et al., 2015)

### ***1.3.7. Nucleation And Seeding***

Crystal growth is one of the essential aspects of Crystal formation, which is controlled by mass transfer and surface deposition mechanisms (Le Corre et al., 2009). Wang et al. experimented with different seeding materials to enhance struvite precipitation. These experiments were done via jar testing using struvite, granite, and quartz sand as seeding material and unseeded solution as a control. It was observed that the struvite crystal showed the highest seeding capabilities because it has low specific gravity compared to other materials, providing it with more particles and enhanced surface area at the same mass addition (J. Wang et al., 2006). If a solution is already seeded, it does not need the nucleation process for crystal embryo formation (Ohlinger et al., 1998).

### ***1.3.8. Effect Of Surface Area On Struvite Crystallization***

Several published studies have attempted to highlight the role of surface area on struvite precipitation. These studies study surface area as surface roughness and the nature of surface material. It was observed that the steel-based rough surfaces had higher deposition. This suggests that highly porous materials aid the precipitation process. It was also observed that the regions of higher roughness had the highest struvite deposition by precipitation, irrespective of the material used for the experiment (Ohlinger et al., 1999) (Doyle et al., 2002). This study suggests that increased surface area leads to increased struvite crystallization.

Factors responsible for the deposition of struvite during wastewater treatment processes have been identified as following (Borgerding, 1972):

1. High surface area formation from the digester to sludge pipes is due to the high surface area to volume ratio.
2. The roughness of the pipes.
3. Increased energy for crystallization from vibrations of sludge filtration screens.

Metal hydroxide-based nanomaterials like aluminum and iron hydroxide have been used since they have solid affinities for orthophosphate. These materials are known to have higher phosphorus removal efficiency because they provide a higher surface area for reactions. However, on the contrary, it also acts as a disadvantage since it may limit hydraulic conductivity (Pratt et al., 2012).

#### **1.4. Membrane-Based Nutrient Treatment**

Coexisting heavy metals and toxic compounds significantly negatively impact recovering nutrients, such as lowering the caliber of the recovered nutrients. Due to its poor quality and purity, using such recovered struvite in agriculture can be prohibited. Separating the nutrients from the foreign material is crucial to increase the recovered nutrients' application potential. Water in the feed solution may pass through the membrane under pressure in a membrane filtration process, which mainly depends on the membrane's pore size (Gerardo et al., 2013). To recover nutrients from wastewater, several membrane approaches have been combined with chemical precipitation and biological processes called membrane hybrid systems (Gong et al., 2017; O. Ichihashi and Hirooka, 2012; Qiu and Ting, 2014). The technical and financial viability of the nutrient recovery system can be enhanced in such circumstances. The ability of membranes to selectively high-reject ions allows for the enrichment and separation of nutrients from foreign materials in streams (Gerardo et al., 2015).

Membrane-based separation technology provides a more comprehensive solution and grants treatment strategies that consider the salinity and the unique qualities of different pollutants. Due to increased membrane fabrication set-ups and more demand in treatment circles, the cost of membrane-based technologies has decreased (Chen et al., 2021; Okamoto and Lienhard, 2019). Membrane-based treatment systems have higher utility than conventional treatment systems because they can be easily attached to an existing system to enhance wastewater treatment and resource recovery (Adham et al., 2018; Nazir et al., 2019). The membrane system efficiency is also impervious to changes in the water quality. This makes it more stable than traditional methods, especially in biological treatment

systems. Several membrane units could be utilized simultaneously to treat multiple pollutants in the complex waste stream. Recent studies look at the potential of membrane technology in treating various sources of saline wastewater as an alternative solution for marine recirculating aquaculture systems (Ng et al., 2018) and membrane-based bioreactors for treating saline wastewater treatment (Tan et al., 2019). A combination of membrane separation treatments was used to treat concentrate-digested swine manure effluent, removing 97% of total ammonia, nitrogen, and organic matter (Ruan et al., 2015). Membrane-based filtration of wastewater can be classified based on the driving forces (pressure-driven, osmosis-driven, thermal-driven, and electrical-driven).

### **1.5. Objectives And Significance**

The overall objective of the research is to establish livestock wastewater treatment through electricity-assisted membrane treatment and the viability of electrochemical precipitation with membrane filtration.

The central research hypothesis is that applying an electric field on the conductive unit (conductive membrane or the stainless-steel mesh) leads to the production of alkaline pH and electrostatic attraction, thus, providing optimum conditions for nutrient precipitation. In order to meet to meet this objective, the following goals have been accomplished:

- 1) Development of conductive ultrafiltration membrane. Based on the discussion in the previous section, membrane-based treatment usually leads to nutrient stream concentration and not recovery. On the other hand, an electrochemical treatment system uses pH manipulation for nutrient precipitation. Based on this hypothesis, a conductive membrane was developed by coating a polyethersulphone membrane

with functionalized carbon nanotubes. The conductive membrane was characterized using the scanning electron microscope and goniometer.

- 2) Electrochemical performance of conductive membranes. The pH is the leading indicator of performance and nutrient precipitation. The impact of voltage, feed solution concentration, and nutrient analysis was done. The pH in the permeate was measured to ascertain the change in pH. The precipitate analysis was done by powder X-ray diffraction and Fourier transform infrared spectroscopy.
- 3) Development of electricity forward osmosis. Increased precipitation and fouling require increased pressure to maintain water flux efficiency. Increasing pressure over time can lead to excess energy requirements. In order to reduce the impact of pressure on the treatment process. Electricity-based forward osmosis was developed, and performance was tested for parameters such as voltage, draw solution concentration and draw pH solution.
- 4) Performance of eFO with membrane distillation. As the FO treatment progresses, the draw solution dilutes, leading to a drop in water flux efficiency. So heated draw solution was fed to the eFO and membrane distillation system in order to have draw solution reconcentration, and the impact of high-temperature draw solution on precipitate formation was studied.

In general, the results of this research will advance the understanding of electrochemical processes being combined with membrane processes. In particular, the research will produce an understanding of the electric field impact on water treatment and nutrient

recovery in order to enhance the treatment capabilities of ultrafiltration and forward osmosis applications. To the best of our knowledge, this research introduces electricity-assisted forward osmosis as a water recovery and struvite production technique.

Overall, this research will assess the potential and the ability of conductive ultrafiltration and eFO to treat nutrient-rich wastewater and optimize the system to increase nutrient and water recovery, specifically for applications that require nutrient removal before effluent release.

## **2. ENHANCED NUTRIENT RECOVERY FROM LIVESTOCK WASTEWATER WITH CONDUCTIVE ULTRAFILTRATION**

*(The Section has been published as “Kekre, K.M., Anvari, A., Kahn, K., Yao, Y., Ronen, A., 2021. Reactive electrically conducting membranes for phosphorus recovery from livestock wastewater effluents. J. Environ. Manage. 282, 111432. <https://doi.org/10.1016/j.jenvman.2020.111432>)*

This section aims to develop and optimize a conductive ultrafiltration system for novel nutrient recovery and livestock wastewater treatment. The ultrafiltration membrane was modified through the use of functionalized carbon nanotubes. The nutrient precipitates were investigated and quantified. The application of voltage on the cathodic membrane surface leads to the formation of an alkaline pH buffer layer leading to optimum precipitation conditions.

## **2.1. Introduction**

Animal farms, including those for swine, poultry, cattle, and dairy, discharge wastewater with high amounts of nitrogen, phosphorus, and organic compounds (Hooda et al., 2000; Rahman et al., 2014). According to studies by Hooda et al. (2000) and Wang et al. (2016), the direct discharge of animal effluent from farms to aquatic habitats is to blame for eutrophication and gas emissions (such as methane and carbon dioxide) (Zhu and Chen, 2002). Additionally, because livestock wastewater typically contains high concentrations of N, P, and organic matter, conventional wastewater treatment plants are ineffective at reducing these concentrations. As a result, treating livestock wastewater necessitates additional treatment facilities, which raises operational costs because denitrification requires external carbon sources and a longer hydraulic retention time (González et al., 2009; Yang et al., 2011). It was also demonstrated that using treated livestock wastewater effluents for irrigation gradually lowers the quality of soil, groundwater, and surface water resources due to residues of nitrate, nitrite, pharmaceutical byproducts, and antibiotics (Katz and Dosoretz, 2008; Mohammad and Mazahreh, 2003; Snyder et al., 2003; Ternes et al., 2007; Watkinson et al., 2007). Furthermore, despite the possibility that certain bacteria may employ these materials as electron acceptors or donors, the significant nitrogen/carbon loading and the quick interaction resulted in the contamination of groundwater sources, which is associated with risks to human health (Wick et al., 2012). Additionally, the discharge may alter the biodiversity of the soil (Guignard et al., 2017). Recycling and recovering P and N from waste streams, such as livestock wastewater, is an integral approach, even if it seems like there is no one answer to the complex problems surrounding the sustainability of nutrients (Childers et al., 2011; Cordell and White, 2013).

The generation of nutrients via energy-intensive mining and recycling techniques was decreased.

From animal effluent, phosphorus and nitrogen may be extracted as struvite, a crystalline salt made of magnesium, ammonium, and phosphorus. Due to its gradual release of P and N and low metal concentration compared to other commercial fertilizers, struvite is regarded as an environmentally beneficial fertilizer (Driver et al., 2010; von Münch and Winker, 2011).

Typical struvite recovery processes are based on crystallization (Ariyanto et al., 2014; Martí et al., 2010; Rahman et al., 2014; Ronteltap et al., 2010; Suzuki et al., 2005; Tao et al., 2016; Uysal et al., 2010) through multiple mechanisms, including fluidized bed reactors, air-agitated reactors (Le Corre et al., 2009; Rahman et al., 2014), and membrane separation processes (Xie et al., 2014). Struvite crystallization is influenced by the ion's supersaturation ratio, temperature, induction time, and surface area (Ali et al., 2005; Ch Bouropoulos et al., 2000; Hao et al., 2008).

As a result of ions solubility (i.e.,  $Mg^{2+}$ ,  $NH_4^+$ , and  $PO_4^{3-}$ ), struvite precipitation was observed to be favored at elevated pH (8-10) (Harrison et al., 2011; Nelson et al., 2003). At these conditions, struvite particles were also about 3-5 folds smaller than struvite, which precipitated at neutral pH values (Kozik et al., 2013). As smaller particles have elevated surface area (Matynia et al., 2006) and, therefore, higher nutrient availability, they are considered beneficial for agricultural application (Johnston A.E. and Richards, 2003). Overall, coupling struvite recovery with wastewater treatment may save phosphorus as a resource; for example, Jardin et al. (2001) claimed that about 640,000 \$/year could be saved

by recovering 20% of P from the sewage waste produced at the wastewater treatment plant (Jardin and Pöpel, 2001).

Electrochemical recovery of struvite is based on the electrochemical reduction of oxygen to establish a local pH gradient close to the electrode surface (Cusick et al., 2014; Wang et al., 2010), in contrast to commercial struvite recovery, which controls the pH either by chemical additions or by CO<sub>2</sub> stripping (Ben Moussa et al., 2011). This approach was shown to be efficient using metal and carbon-based electrodes (Chen et al., 2009; Cusick et al., 2014) when treating simulated wastewater after sludge treatment (155mg/L of P and 70 mg/L of N)(Wang and Hao, 2009), simulated supernatant from anaerobic digesters (46.5 mg/L of P and 21mg/L of N)(Wang et al., 2010), and real digestate from anaerobic wastewater (46 mg/L of P and 490 mg/L of N)(Cusick et al., 2014). At the same time, mass transport limits the electrochemical recovery of struvite based on electrodes (Ben Moussa et al., 2006; Doyle et al., 2002; Wang et al., 2006). Conventional ultrafiltration: The surface characteristics of membranes and the mass transport into and out of the membrane can be altered by an external electrical field or potential. Conventional ultrafiltration membranes have been shown to effectively reduce organic, inorganic, and biological fouling, as well as combining filtration with electro-oxidation, electro-reduction, and electro-Fenton processes (De Lannoy et al., 2013; Duan et al., 2017a, 2016, 2014a; Dudchenko et al., 2014; Ronen et al., 2015). Conductive Ultrafiltration Membranes offer an advantage over electrodes for struvite recovery applications because water movement (i.e., permeate) through the membrane improves mass transfer and lowers diffusion restrictions (Gao and Vecitis, 2012). Therefore, earlier studies on conductive ultrafiltration membranes shown a notable improvement in reaction rates and removal ratio of several pollutants, including

chromium(VI) by electrochemical reduction and methylene blue by electrochemical oxidation (Duan et al., 2017b, 2016; Ronen et al., 2015).

This work examines how well struvite may be recovered from livestock wastewater effluents after digestion and fermentation in an anaerobic bioreactor using conductive ultrafiltration membranes. Struvite recovery is investigated using synthetic solutions that simulated animal wastewater effluents from swine farms, which included N, P, and Mg at two typical amounts (O. Ichihashi and Hirooka, 2012).

No organic molecules or extra ions were introduced to the feed because this is just a proof-of-concept for the electrochemical recovery of conductive ultrafiltration membranes. The presence of ions and organic substances impacts struvite quality and induction times. However, problems have already been addressed in several research (Kabdaşlı et al., 2006; Le Corre et al., 2005; Saidou et al., 2015) and are not exclusive to the electrochemical recovery strategy. For instance, sodium and aluminum were shown to have shorter induction times, but carbonate ions did not affect this. Modified Struvite (k-Struvite, Ammonium Calcium Phosphate), also employed as a fertilizer, is created when calcium and potassium are present.

## **2.2. Materials & Methods**

### **2.2.1. Materials**

Flat sheet ultrafiltration (UF) polyethersulfone (PES) membranes with a molecular weight cut-off (MWCO) of 50 kDa were purchased from Synder Filtration, USA. Graphitized Multi-wall Carbon Nanotubes (G-Carbon nanotubes) functionalized with carboxylic

groups (Outer Diameter: 10-20nm, Inside Diameter: 3-5nm, purity >95 %) was purchased from CheapTubes Inc. Polyvinyl alcohol (MW 146000-168000), 50 wt% glutaraldehyde solution, hydrochloric acid 37%, and ammonium phosphate monohydrate were purchased from Sigma Aldrich and used without further modification. Magnesium sulfate was purchased from LabChem.

### ***2.2.2. Membrane Fabrication***

Conductive Ultrafiltration Membranes were created, as previously explained by (Ronen et al., 2015). After purification, sodium dodecylbenzenesulfonate (1:2.5) and carboxylic functionalized carbon nanotubes (0.1 % weight) were mixed to form a suspension in deionized water. A. V. Dudchenko et al. (2014) used a probe sonicator (750W, Fisher Scientific FB705) to sonicate carbon nanotube dispersions for 30 minutes at 100% intensity. A carbon nanotube layer with a total mass of 0.1 g was then pressure-deposited onto a polyethersulfone membrane (Dudchenko et al., 2014). The layer was then cross-linked using polyvinyl alcohol, glutaraldehyde, and hydrochloric acid in a 2:1 ratio and cured at 90°C for 60 minutes after the deposition. The membranes used in each experiment have a surface area of 0.0055 m<sup>2</sup>.

#### ***2.2.2.1. Feed Solutions***

After anaerobic digestion, synthetic feed solutions were used in recovery tests to mimic the P and N contents in swine effluent. Two solutions were tested, the first representing highly concentrated swine wastewater effluents with an average concentration of 10 mM, or 1150 mg/L of P and N (Kim and Kwon, 2010). Accordingly, we utilized an average of 1 mM, or 115 mg/L, P and N in the second assessed solutions, representing medium-concentrated swine wastewater effluents comprising 70-110 mg/L of ammonium and phosphorus

(Hasan, 2014; Terán et al., 2017). P, N, and Mg ions were in equal amounts in each solution.

As the capacity of Conductive Ultrafiltration Membranes to minimize biological fouling has already been demonstrated (Ronen et al., 2015), and this is outside the scope of this study, the feed solutions were not spiked with organic compounds or suspended particles. The compositions and recovery efficiency of struvite may be impacted by other ions, although they have already been well-studied in the literature and are not anticipated to change throughout the electrochemical recovery process (Kabdaşlı et al., 2006; Saidou et al., 2015).

#### ***2.2.2.2 Experimental Setup***

A crossflow filtration cell was used in the experiments to apply an electrical potential to the reactive electrochemical membrane surface. The flow cell had a stainless-steel counter electrode in the permeate reservoir and an Ag/AgCl reference electrode close to the reactive electrochemical membrane. An electrochemical workstation/potentiostat (CHI 600E) operating in bulk electrolysis mode was used to regulate the applied voltage. The counter electrode acted as an anode and the membrane as a cathode (i.e., negatively charged) throughout the filtering process (i.e., positively charged). After linear sweep voltammetry (LSV), the applied potential was chosen to ascertain the membrane and flow cell's oxygen reduction reaction (ORR) potential per tested solution. As a struvite formation indication, the change in permeate flow was observed throughout filtering cycles at a constant pressure of 10 psi (0.69 bar). Permeate flux was calculated according to Eq.1.

$$J = \frac{\Delta V}{A\Delta t} \quad \text{Eq 3}$$

Where  $J$  is the permeate flux expressed in  $L/m^2 \cdot h$ ,  $V$  is the volume of permeate (L).  $A$  is the membrane area ( $m^2$ ), and  $t$  is the time period (hr). Before each experiment, the membrane was compressed overnight at an elevated pressure of 15psi(1bar). Following each filtering cycle, struvite particles accumulated on the membrane's surface were eliminated by flushing the flow cell with deionized water while obstructing permeate passage. The reactive electrochemical membranes were neither backwashed nor chemically cleaned as the flux rapidly returned to initial values.

### ***2.2.2.3 Membrane And Struvite Characterization***

The surface of the Conductive Ultrafiltration Membranes and cross-sections before and after struvite production and deposition were imaged using scanning electron microscopy (FEI Quanta 450FEG SEM). The wetting contact angle (WCA) of Conductive Ultrafiltration Membranes was determined using a goniometer (Ossila) and DIW. The electrical conductivity of Conductive Ultrafiltration Membranes was assessed using a 4-point conductivity meter, and surface roughness was assessed using an atomic force microscope in QI mode on a JPK NanoWizard. X-ray powder diffraction was used to analyze particles collected on the Conductive Ultrafiltration Membranes' surface (without washing them first) (Bruker D8 Advance X-ray Powder Diffractometer). Fourier Transform Infrared Spectroscopy (FTIR) was used to measure the energy of particle bonds (Perkin-Elmer Spectrum 100). Hach Ammonium (TNT 832) and Phosphorus kits were used to measure the amounts of dissolved phosphorus and nitrogen in feed, permeate, and concentrate (TNT 845). We measured the permeate and concentrated volumes and concentrations and detected each component's N and P concentrations. Masses of nitrogen and phosphorus removed as struvite were calculated according to Eq. 2.

$$M_i = \sum C_{i,feed} \frac{\Delta V}{\Delta t} - \sum \frac{\Delta(C_{i,conc}V_{i,conc})}{\Delta t} - \sum \frac{\Delta(C_{i,perm}V_{i,perm})}{\Delta t} \quad Eq 4$$

where  $M_i$  is mass removed (mg),  $C_i$  (mg/L) is the concentration of each species at the feed, concentration, and permeate, and  $V_i$  is the volume collected (L) over a duration of time ( $\Delta t$ ).

In addition to directly measuring struvite formation and recovery, changes in  $PO_4^{3-}$  and  $NH_4^+$  concentration in the concentrate and permeate were addressed as indirect indicators for struvite formation.

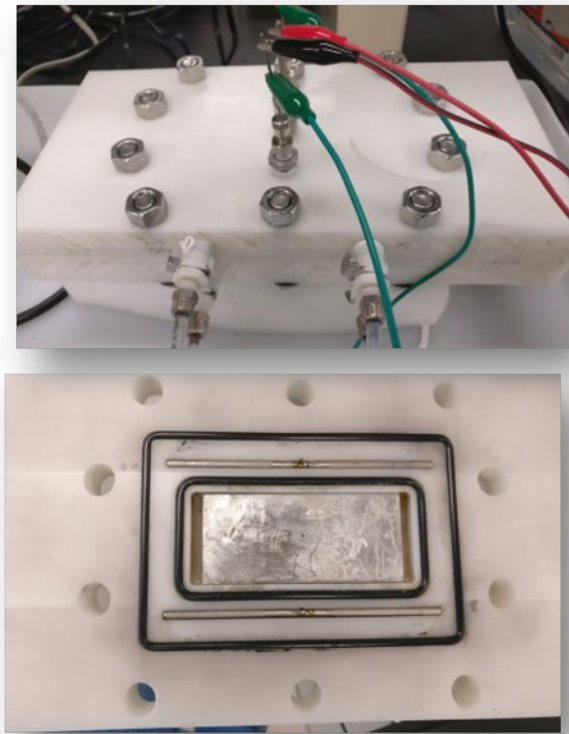


**Figure 1** Membrane Flow-cell design

## 2.3 Results And Discussion

### 2.3.1 Reactive Electrochemical Membrane Characterization

A layer of multiwall carbon nanotubes is seen on the support Polyethersulfone membrane in scanning electron microscopy pictures of the reactive electrochemical membranes after carbon nanotube deposition and cross-linking (Figure 2 a,b), as shown in our earlier work (Anvari et al., 2019; Ronen et al., 2015). According to Ronen et al. 2015, the deposited layer has substantial porosity with pore diameters between 100 and 200 nm (Ronen et al., 2015). Following freeze fracturing of the membrane, scanning electron microscopy imaging determined that the total thickness of the carbon nanotubes layer was in the region of 15 m (Fig. 2b). It should be mentioned that the quantity of carbon nanotubes put on the surface of the support polyethersulfone membrane can regulate the thickness of the electrically conducting layer. In order to maintain the mechanical stability and durability of the deposited layer while allowing excellent electrical conductivity, a specified layer thickness (15 m) was chosen. Permeate flux and selectivity for reactive electrochemical membranes coated with carbon nanotubes are controlled mainly by the PES support layer rather than the coated carbon nanotubes layer (Dudchenko et al., 2014). As a result, flux values obtained for the pristine PES membranes (permeability  $4.2 \times 10^9 \frac{L}{m^2 \cdot hr \cdot Pa}$ ) were comparable to those obtained for the reactive electrochemical membranes (permeability  $3 \times 10^9 \frac{L}{m^2 \cdot hr \cdot Pa}$ ). After the carbon nanotubes layer was cross-linked, its electrical conductivity was around 103 S/m and its electrical resistance ranged from 100 to 200 /sq. The reactive electrochemical membrane's hydrophilicity was further improved by the layer of carbon nanotubes and polyvinyl alcohol that was applied, resulting in a WCA of 29.52°, or nearly 40% less than the pristine PES support (Figure ). The Polyvinyl Alcohol layer,

which contains hydroxide groups and makes the reactive electrochemical membrane surface more hydrophilic, is responsible for the shift in contact angle. According to three  $1 \times 1 \text{ m}^2$  segments, the layer's roughness was 43.461.9 nm, which is consistent with roughness values for thin films made of carbon nanotubes that have been published (Dudchenko et al., 2014).

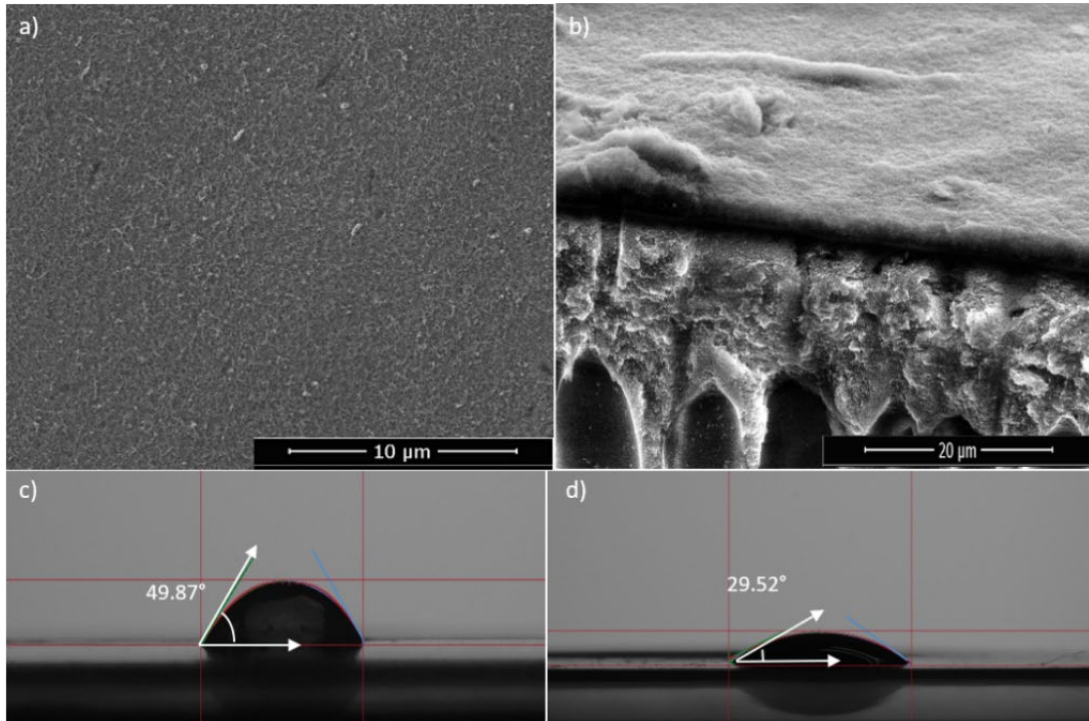


**Figure 2.** Characterization of fabricated Conductive Ultrafiltration Membranes based on Carbon nanotubes. a) SEM images of the REM top surface; b) Conductive Ultrafiltration Membranes cross-section following freeze-fracture, showing the deposited Carbon nanotubes layer; c) wetting contact angle for pristine PES; d) wetting contact angle for CNT-polyvinyl alcohol coated PES.

### 2.3.2 *Struvite Recovery Cycles*

Continuous filtering was used for the struvite generation and recovery tests, and the change in permeate flow served as an indirect signal for the deposition of struvite particles on the reactive electrochemical membrane surface. Three recovery cycles were included in the 7–8-hour trial. All experiments were conducted with an applied voltage of 3.5 V vs. an

Ag/AgCl reference electrode. The reactive electrochemical membrane was flushed with Deionized water without permeate flow after each recovery cycle, and the concentrate solution containing struvite particles was then collected, filtered, and dried for additional research. The studies were stopped after three filtration cycles, and the reactive electrochemical membranes were dissected to see if any struvite particles were still on the surface.

All filtering cycles generally followed the same pattern. However, due to the poised electrical potential, the pH rose, and struvite development and deposition caused a reduction in permeate flow (Figure 3). Therefore, for 150-minute recovery cycles, flux and pH measurements were made every 30 minutes (three cycles per experiment). At least three times, each of the tests was repeated.

The pH rose quickly from 6 to 8.75 in a 1 mM solution when the electrical potential on the REM surface was poised, and it remained relatively stable during the recovery cycle. Permeate flux decreased by roughly 10% during each recovery cycle (i.e.,  $10.01\% \pm 2$ ,  $8.88\% \pm 3.73$ , and  $8.47\% \pm 4.64$  for cycles 1-3), and it was completely restored to its previous value after being washed with deionized water. While pH levels in the 10 mM solution went from 6 to about 8, the permeate flow fall was quicker, with permeate decreases of  $57.8\% \pm 1.77$  after the first cycle,  $30.3\% \pm 4.62$  after the second cycle, and just  $12.6\% \pm 3.22$  decreases after the third recovery cycle. Due to the high ionic strength and buffering capacity, the detected pH was lower than the values obtained with a 1 mM solution. Still, the thicker layer of struvite particles that resulted from the elevated ion concentrations made inorganic fouling more challenging to remove by simply washing it with deionized water. The initial recovery cycle's abrupt fall in permeate flux shows that

struvite particles were still being created and deposited on the reactive electrochemical membrane, but subsequent recovery cycles showed a lesser decrease in permeate flux, indicating less struvite generation. This is thought to be because portions of the reactive electrochemical membranes already have inorganic struvite coatings, which stop new local struvite synthesis. The mechanism causing fouling in a 10 mM solution is anticipated depending on how far away the stoichiometrically balanced solution is from the charged reactive electrochemical membrane surface.

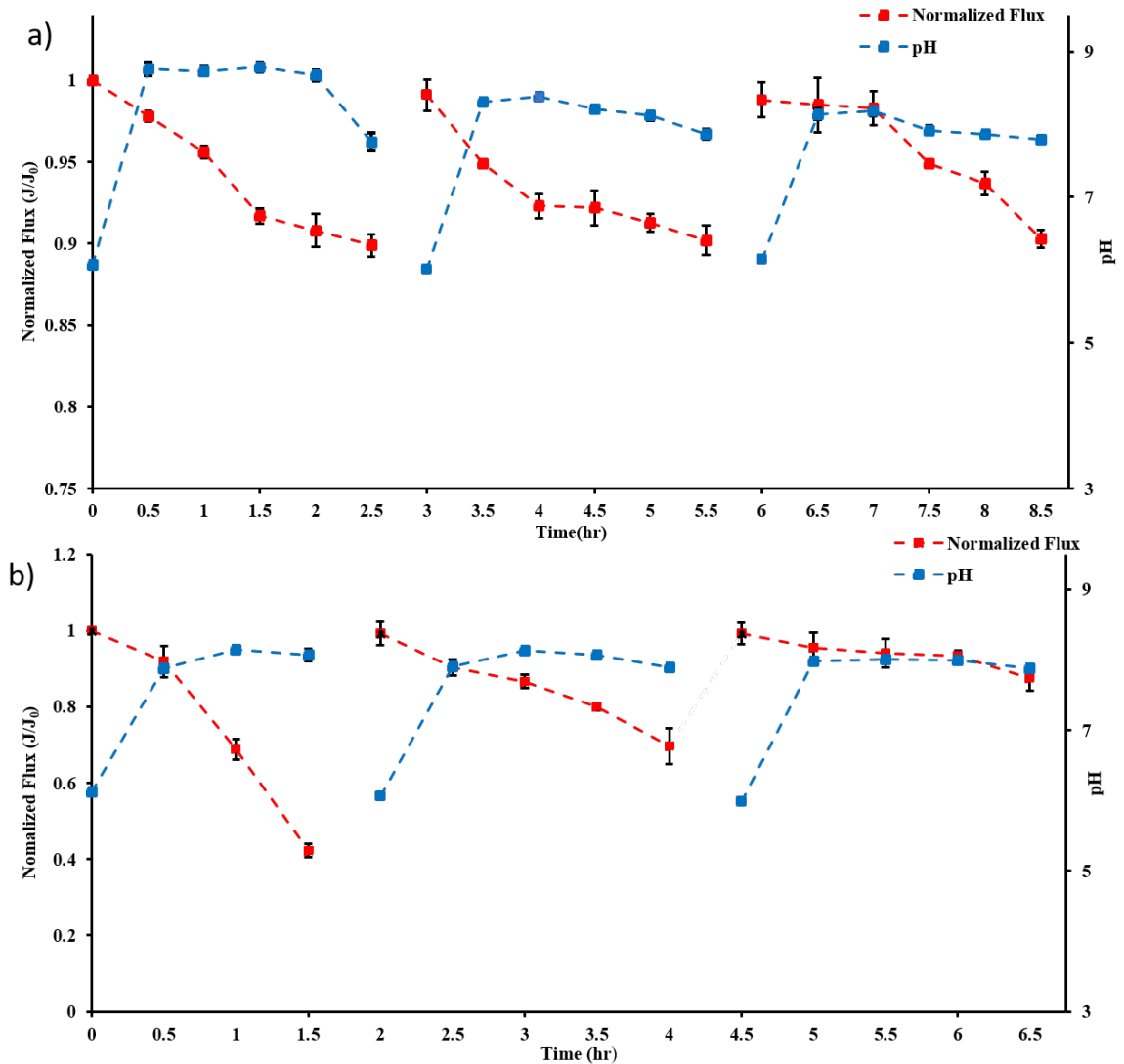
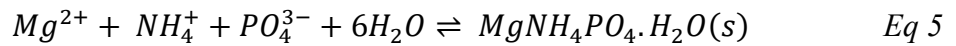


**Figure 3.** Recovery cycles of 1mM and 10mM solutions. (a) 1mM flux and pH profile as a function of time; (b) 10mM flux and pH profile as a function of time. Dotted lines

represent shutting the permeate flux and washing the reactive electrochemical membranes with Deionized water.

In addition to flux and pH, N and P recovery was evaluated by measuring the difference in orthophosphate ( $PO_4^{3-}$ -P) and ammonia ( $NH_4^+$ -N) concentrations of the feed, concentrate and permeate.

For 10mM solution, high  $PO_4$ -P removal of  $64.7\% \pm 1.03$  was detected in the first cycle, correlating to about  $123 \text{ g/h}\cdot\text{m}^2 \pm 1.56$  or  $310 \text{ g/ m}^2$  per recovery cycle. As a result of the deposited struvite layer, the subsequent recovery cycles had lower removal values ( $44.6\% \pm 1.16$  and  $27.9\% \pm 1.21$  for cycles 2 and 3).  $NH_3$ -N removal was higher, with  $64.3\% \pm 2.41$  removal in the first cycle and lower values in the following cycles, i.e.,  $36.4\% \pm 0.57$  and  $38.3\% \pm 1.76$  for cycles 2 and 3. For 1mM solution,  $PO_4$ -P removal was  $22.7\% \pm 2.98$ ,  $23.4\% \pm 2.17$ , and  $22.4\% \pm 5.41$  for recovery cycles 1-3, which correlates to about  $5.8 \text{ g/h}\cdot\text{m}^2 \pm 1.15$  or  $15 \text{ g/ m}^2$  per cycle.  $NH_4$ -N removal showed a similar trend with an average removal of  $20\% \pm 1.48$ , corresponding to  $8.9 \pm 1.6 \text{ g/h}\cdot\text{m}^2$  or about  $22 \text{ g/ m}^2$  per cycle. It is believed that two mechanisms connected to the high pH, namely struvite precipitation (Eq. 5) and ammonia volatilization (Eq. 6), are the causes of the increased ammonium removal compared to phosphorus removal in cycles 2-3 (Hou et al., 2018). Ammonia volatilization can be regarded as relatively small based on the elimination of each species.



A more significant concentration of ions in the feed solution accelerates the first precipitation rate since the supersaturation ratio value of struvite at  $pH = 9$  is 2.41 for 10 mM solutions and 0.137 for 1 mM solutions. Due to a decreasing concentration of

accessible ions, the rate of precipitation reduces as more struvite is generated (Rahaman et al., 2008). Additionally, we postulate that the reduced struvite generation results from the membrane's constrained surface area due to precipitation and struvite particle deposition. The precipitated struvite layer may hinder the electromigration and diffusion of electrochemically produced hydroxides towards the bulk, inhibiting further precipitation, as was shown in 10 mM solutions.

Due to the lower ion concentrations in 1 mM solutions, the precipitation rate was noticeably slower. However, because the precipitated and deposited particles did not completely cover the reactive electrochemical membrane's surface, the clearance rate was consistent when compared to the previously tested solution. Generally speaking, the recovery cycles demonstrate the possibility of struvite removal by reactive electrochemical membranes, with nearly 100% recovery of permeate flow occurring after removing the deposited struvite particles using a straightforward washing procedure.

### ***2.3.3. Membrane And Particles Analysis***

A further deposition stage was introduced without washing or removing the deposited particles in order to evaluate the generated and deposited particles. The deposited layer on the surface of the reactive electrochemical membrane was examined using light microscopy, scanning electron microscopy, Fourier transforms infrared spectroscopy, and X-ray diffraction. Particles were visible on the reactive electrochemical membrane's surface for both solutions; however, feed concentrations were shown to influence the deposited particles' mass substantially.

Needles-like structures were among the particles discovered after the electrochemical deposition with a 10 mM solution (Figure 3 c,d), which had a high

concentration of ions and is consistent with previously published information on struvite recovery (Hanhoun et al., 2013). The synthesis and deposition of struvite occurred quickly because the circumstances were conducive to crystal development due to the elevated ion concentration and pH. Due to the slightly weaker ionic strength of the 1 mM solution, smaller crystalline clusters were formed and deposited on the reactive electrochemical membrane surface. Lower amounts of struvite have been shown to produce similar precipitates (Cusick et al., 2014). Struvite particles were evenly dispersed throughout the surface of the reactive electrochemical membrane for both ionic strengths. By using X-ray diffraction and Fourier transform infrared spectroscopy to describe the particles and compare them to struvite of commercial quality, it was possible to determine the composition of the deposited layer. The sample taken off the surface of the reactive electrochemical membrane (Fig. 3f) exhibits X-ray diffraction patterns that had peaks that are comparable to those of commercial-grade struvite, proving that the powder that was deposited was in fact struvite. Assumed effects of the precipitation technique and post-treatment (i.e., water supply, pressure, and drying process) include negligible changes in peak location and intensity (Luft et al., 2011).

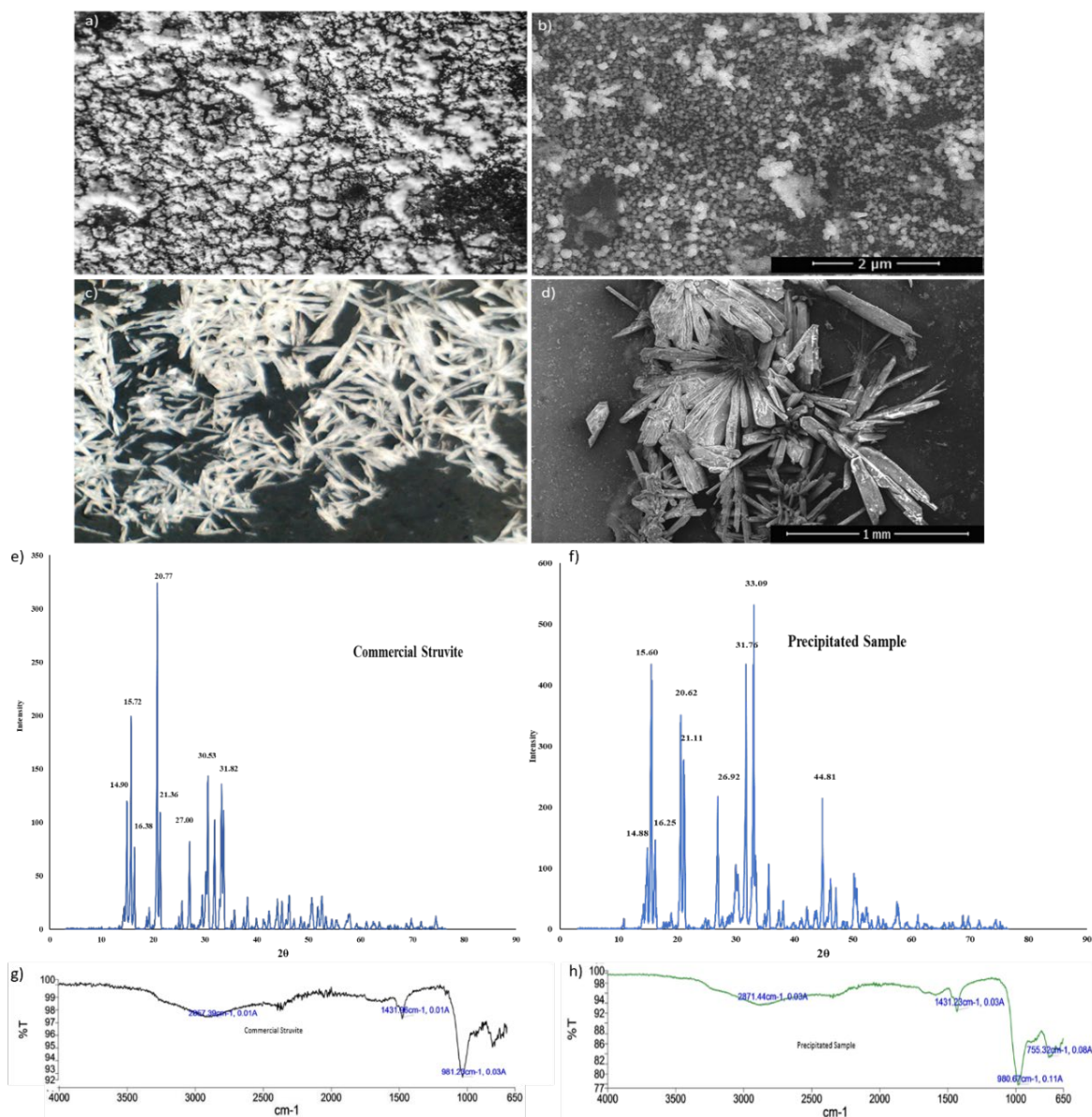


**Figure 4** Precipitated struvite by USB-microscopy at **(a)** 1mM solution and **(c)** 10mM solutions; **(b)** Scanning electron microscopy images of the precipitated particles at **(c)** 1mM solution and **(d)** 10mM solution; X-ray diffraction **(e)** commercial struvite and **(f)** precipitated sample ; Fourier transform infrared spectra for **(g)** commercial struvite **(h)** precipitated sample

According to the Fourier Transform Infrared Spectroscopy spectra (fig.3 (g)&(h)), the precipitated samples had phosphate and ammonium groups, as predicted for struvite. The precipitated sample's and commercial struvite's infrared spectra coincided at wavelengths of  $2850\text{ cm}^{-1}$ ,  $1431\text{ cm}^{-1}$ , and  $980\text{ cm}^{-1}$ , which correspond to the N-H bond

(2800–3000  $\text{cm}^{-1}$ ), the  $\text{NH}_4^+$  bending spectrum (1431  $\text{cm}^{-1}$ ), the  $\text{PO}_4^{3-}$  stretching spectrum (982  $\text{cm}^{-1}$ ), and water-based hydrogen-bonding peaks (Herald et al., 2017).

#### 2.3.4. Influence Of External Potential On pH Change

As explained in the preceding section, all flow tests used the reactive electrochemical membrane as a cathode and a potentiostat with an Ag/AgCl reference electrode to regulate the poised potential. As a result, the reactive electrochemical membrane surface is anticipated to undergo the following electrochemical reaction.



Eq. 7 predicts that hydroxides will form close to the reactive electrochemical membrane, causing a local pH to rise and the development of a thin hydroxide ion diffusion layer on the membrane's surface.

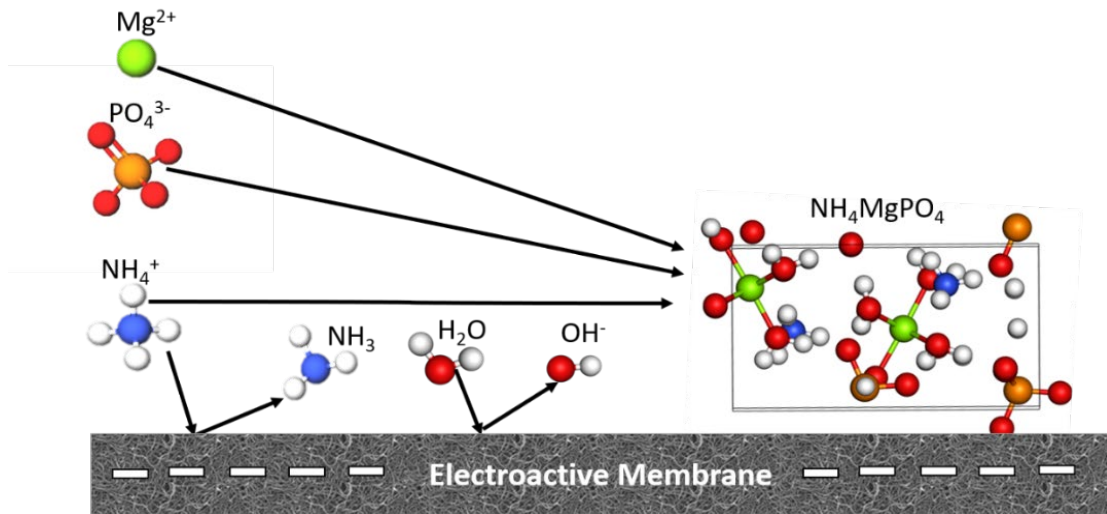


**Figure 5** Schematic representation of struvite recovery by charged membranes. Electrochemical production of hydroxide at the membrane surface catalysis struvite formation while excess ammonium is turned into ammonia.

Katsounaros et al. (2011) documented the establishment of a hydroxide diffusion layer and addressed it in experimental and analytical studies evaluating the local pH change as a function of applied electrical potential (Katsounaros et al., 2011). The hydroxide

formed by electrolysis and electromigration of the hydroxide ions raises the pH in the area close to the REM's surface (Duan et al., 2017a; Tang et al., 2017). Eq. 6 may be used to explain the diffusion flow of protons ( $H^+$ ) and hydroxides ( $OH^-$ ) within the diffusion layer (Katsounaros et al., 2011)

$$j_{H^+/OH^-} = F(D_{H^+}\nabla c_{H^+} - D_{OH^-}\nabla c_{OH^-}) \quad Eq 8$$

where  $j_{H^+/OH^-}$  is the current density as a result of  $OH^-$  and  $H^+$  diffusion,  $F$  is the Faraday constant,  $D_{H^+}$  and  $D_{OH^-}$  are the molecular diffusion constants associated with the  $H^+$  and  $OH^-$ , and  $\nabla c_{H^+}$  and  $\nabla c_{OH^-}$  are the concentration gradients associated with  $H^+$  and  $OH^-$ . The equation was modified to allow an analytical solution (Auinger et al., 2011).

$$j_{H^+/OH^-} = \frac{F}{\delta_{eff}} \left( D_{H^+} (c_{H^+}^{surface} - c_{H^+}^{solution}) - D_{OH^-} K_w \left( \frac{1}{c_{H^+}^{surface}} + \frac{1}{c_{H^+}^{solution}} \right) \right) \quad Eq 9$$

where  $\delta_{eff}$  is the effective thickness of the diffusion layer (defined as  $30\mu m$  according to (Auinger et al., 2011)), and  $K_w$  is the dissociation coefficient of water. When addressing synthetic LWW solutions at the expected pH range of 8-10, the buffering capacity is mainly a function of the phosphate and ammonium ions and can be determined according to eq.10 and eq.11 (Auinger et al., 2011)

$$j_{Buffer} = \left( \frac{C_{buffer}}{\delta_{eff}} F \right) \left( \frac{3D_1 + D_2 \frac{K_{S1}}{c_{s,H^+}} - D_3 \frac{K_{S1}K_{S2}}{c_{s,H^+}^2} - 3D_4 \frac{K_{S1}K_{S2}K_{S3}}{c_{s,H^+}^3}}{1 + \frac{K_{S1}}{c_{s,H^+}} + \frac{K_{S1}K_{S2}}{c_{s,H^+}^2} + \frac{K_{S1}K_{S2}K_{S3}}{c_{s,H^+}^3}} \right) \quad Eq 10$$

$$j_{Buffer} = \left( \frac{C_{buffer}}{\delta_{eff}} F \right) \left( \frac{D_{NH_4^+} c_{s,H^+} - D_{NH_3} - K_s}{K_s + c_{s,H^+}} - \frac{D_{NH_4^+} c_{sol,H^+} - D_{NH_3} - K_s}{K_s + c_{sol,H^+}} \right) \quad Eq 11$$

where  $D_1$ ,  $D_2$ ,  $D_3$ , and  $D_4$  are the coefficient of diffusion associated with phosphate species, i.e.,  $H_3PO_4$ ,  $H_2PO_4^-$ ,  $HPO_4^{2-}$ , and  $PO_4^{3-}$ , respectively.  $K_{S1}$ ,  $K_{S2}$ , and  $K_{S3}$  are the dissociation constants for the phosphate buffer system.  $c_{s,H^+}$  and  $c_{sol,H^+}$  are the concentration of  $H^+$  ions

on the surface of the REM and the concentration of  $H^+$  ions in the feed solution  $D_{NH_4^+}$  and  $D_{NH_3}$  are the coefficient of diffusion associated with ammonium species. Finally, the current density of the total system was calculated according to eq. 12, considering the buffer capacity of the system.

$$j = J_{H^+/OH^-} + J_{Buffer} \quad Eq\ 12$$

The experimental results show that for 10mM and 1mM LWW solutions, a constant potential of 3.5V was applied against an Ag/AgCl reference electrode, resulting in current densities of 4.54 A/m<sup>2</sup> and 2.91 A/m<sup>2</sup>, respectively. Theoretically, the  $H^+$  concentration was determined to be  $2.79 \times 10^{-13}$  M and  $2.81 \times 10^{-12}$  M, respectively, which translates to high pH values between 12.55 and 11.55. On the basis of the data collected, it can be concluded that, as anticipated, the application of increased current density increases the local pH close to the reactive electrochemical membrane. The experimental pH values were measured at the permeate stream rather than directly at the reactive electrochemical membrane surface to prevent altering the hydrodynamics close to the membrane surface. According to experimental findings, the applied voltage raises the pH value of both synthetic solutions.

The 10 mM solution attained pH values of 8.3 at a comparable applied potential; however, the total pH rise was more prominent for the 1 mM solution, reaching 9.2 against a 3.5V potential. The buffer capacity of the examined solutions should also be considered since, in addition to the carbonate system, they also include phosphorus and nitrogen (i.e., ammonium) species. These include the carbonate system (pKa,1=6.33, pKa,2=10.35), ammonium/ammonia system (pKa=9.24), and phosphoric system (pKa,2=7.2) at the appropriate pH range. All three species may have contributed to the studied solutions'

ability to act as buffers based on the experimental pH values that were determined to range from 5-9.75. The extra carbonate and ammonium systems, which were not taken into account in eqs. 9-10 can be used to explain the discrepancy between observed and theoretical pH values. As a result, estimated pH values are greater than the outcomes of experiments.

Additionally, when comparing the two solutions, the 10 mM solution's high ionic strength causes a higher rate of electrolysis, which results in the production of more hydroxide ions at the surface of the reactive electrochemical membrane, but because the solution's buffering capacity is also higher, the overall pH at the permeate stream is lower. Therefore, the poised potential should be observed to raise the permeate pH to levels that favor struvite production. The pH values at the water-reactive electrochemical membrane surface were also higher than predicted by the theoretical models. The pertinent literature states that struvite precipitates at a pH of more than 8.5 (Rahaman et al., 2008; Wang et al., 2005). In order to achieve pH levels suitable for struvite precipitations, an applied voltage of 3.5V vs. an Ag/AgCl reference electrode was sufficient.

### ***2.3.5. Modeling Ions Concentration Near The Electrically Charged Membrane***

The recommended model is based on the model developed by Duan et al. for scaling mitigation in the presence of charged membranes and is utilized to explain the recovery cycle findings that were obtained. According to the suggested model, the charged surfaces increased the concentration polarization layer's distance. On the carbon nanotube membrane, a precipitation process was proposed. According to reports, negatively charged ions form a barrier a few angstroms away from the membrane's surface when the carbon nanotube membrane is negatively charged (Duan et al., 2014a).

The Modified Poisson-Boltzmann (MPB) equation has been used to predict and explain the behavior of ions near electrically charged membranes in earlier studies (Duan et al., 2014b; Dudchenko et al., 2014). The MPB equation, in contrast to the conventional Poisson-Boltzmann equation, which assumes point charges, considers the volume of the hydrated ions when determining the number of counter ions attracted to the membrane surface. Based on the MPB, a potential profile can be obtained by Eq.11 and Eq.12 (López-García et al., 2011),

$$\varepsilon \frac{d\psi}{dx} = \frac{-eN_A \sum_{i=1}^m z_i c_i^\infty \exp\left(-\frac{z_i e \psi}{kT}\right)}{1 + \sum_{i=1}^m \frac{c_i^\infty}{c_i^{max}} \left[ \exp\left(-\frac{z_i e \psi}{kT}\right) - 1 \right]} \quad Eq 13$$

$$c_i^{max} = \frac{p}{\frac{4}{3}\pi R_i^3 N_A} \quad Eq 14$$

Next, based on the potential profile values, the ionic concentrations can be calculated as a function of distance from the charged membranes by Eq.13,

$$c_i = \frac{c_i^\infty \exp\left(-\frac{z_i e \psi}{kT}\right)}{1 + \sum_{i=1}^m \frac{c_i^\infty}{c_i^{max}} \left[ \exp\left(-\frac{z_i e \psi}{kT}\right) - 1 \right]} \quad Eq 15$$

where  $\psi$  is the electrical potential,  $z$  is the valence of ions,  $N_A$  is Avogadro's number,  $e$  is the elementary charge,  $c_i^{max}$  is the maximum ion concentration due to ionic steric effects,  $\varepsilon$  is the permittivity of the ionic solution,  $c_i^\infty$  is the bulk ion concentration,  $k$  is the Boltzmann's constant, and  $T$  is the temperature.

According to the model, 10mM and 1mM solutions, when under voltage circumstances, the concentration profiles of ammonium, phosphate, and magnesium ions were estimated as a distance from the charged membrane (Figure 6). According to earlier research, under zero voltage conditions, no changes were seen at the membrane surface

(Gao et al., 2020). Similarly, modeling under zero voltage showed that the ionic concentration did not change. Since there was no applied voltage in the simulation results, the charges on the ions did not cause particle movement, resulting in the overlapping lines on the graph for the ion concentrations. Negatively charged ions are electrostatically drawn to the membrane's surface by its negative charge (Figure 6 c). As a result, the concentration of negatively charged ions (such as phosphate) was low, while that of positively charged ions (such as ammonium and magnesium) showed larger quantities close to the membrane surface. The concentration of phosphate concentration rose with the extension of the distance from the charged membrane, and the change was demonstrated to be a function of ionic strength, around 50Å for 10 mM solutions and 150Å for 1 mM solutions until a rise in concentration was noticed. For 10 mM solutions 110Å and roughly 280Å for 1 mM solutions, the nucleation zone, defined as the distance in which the ions are present at stoichiometric levels, has been observed (Figure 6b). Since the nucleation zone is farther from the membranes in solutions with lower ionic strength, struvite forms in bulk, and the particles amass on the membrane's surface due to permeating drag force. This might account for the easier recovery of the deposited struvite after the recovery cycles with 1 mM solutions. A schematic model for the spatial ion dispersion away from the negatively charged membrane is shown in Figure 6c.

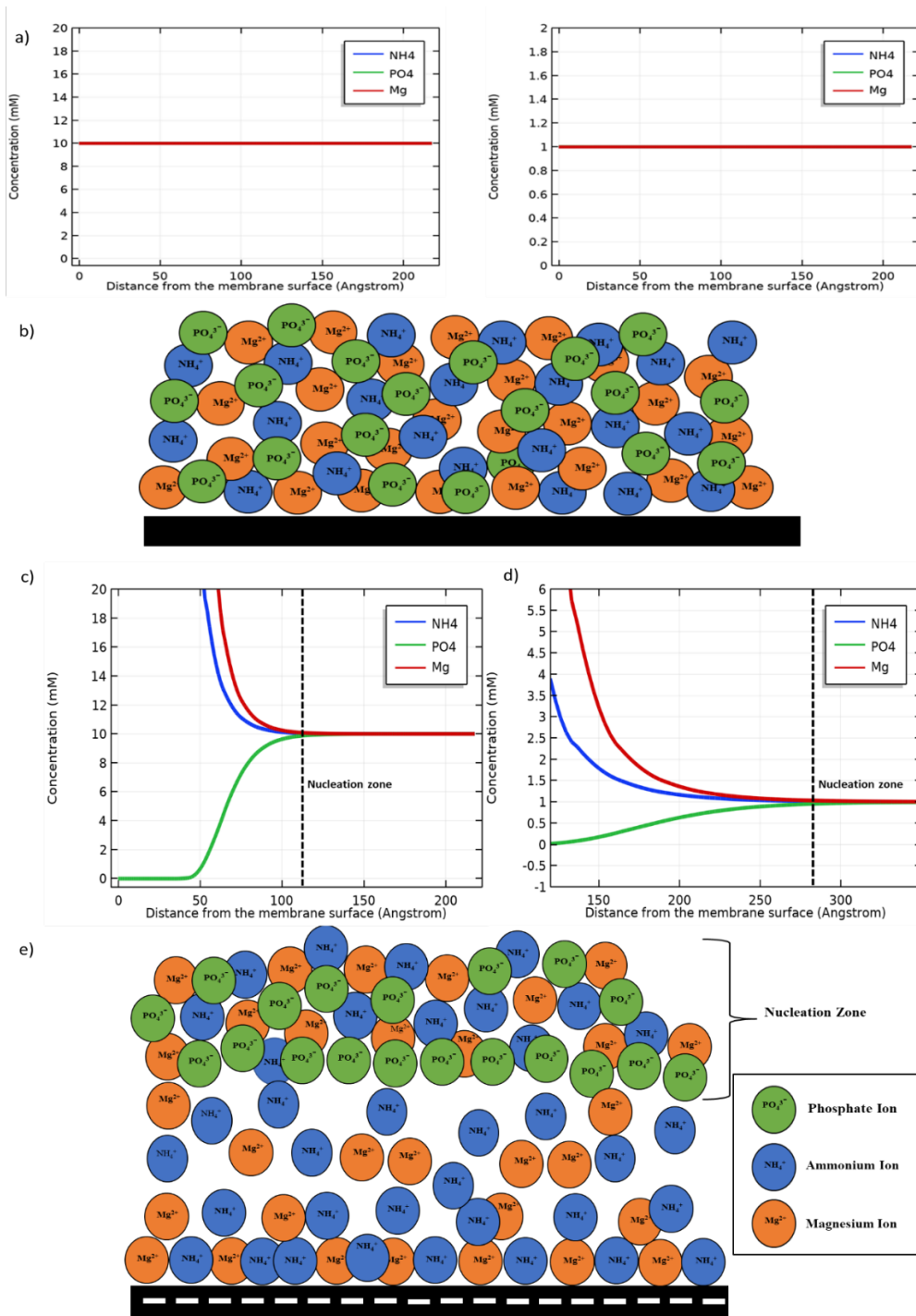


**Figure 6** a) Graphical description of concentration profile as a function of the membrane's surface charge: b) Ions concentration profile without voltage c) Ions concentration profile a function of distance from the charged membrane surface in 10mM solution d) Ions concentration profile as a function of distance from the charged membrane surface in 1mM solution e) schematic model describing the distribution of the ions in proximity to charged membranes. The nucleation zone is formed a few angstroms away from the membrane surface

### ***2.3.6. Estimated Cost Of Electrochemical Struvite Recovery***

The extra chemicals needed to keep the ideal conditions for struvite crystallization impact around 40% of the cost of struvite manufacturing (Parsons and Smith, 2008). According to the most recent research, the price of struvite precipitated can range from \$1,538 per ton to \$1538 per ton (Vaneeckhaute et al., 2017). The reason for the price variance is the technique, energy needs, and raw materials utilized for precipitation.

According to Quist-Jensen et al., phosphorus recovery in conventional membrane systems, the cost of struvite is reported to be \$420 per ton for nanofiltration and membrane crystallization and \$222 per ton for nanofiltration and membrane distillation(Quist-Jensen et al., 2016). However, these systems rely on the use of seawater to obtain magnesium sources, which can restrict the use of technology (Quist-Jensen et al., 2016). Adding sodium hydroxide accounts for around \$220 per ton (PHOSNIX) of the cost of struvite gathered using standard crystallization methods (Jaffer et al., 2002).

It should be noted that the extra chemicals needed to maintain ideal crystallization conditions impact the cost of producing struvite. For example, magnesium is still required and may account for up to 30% of the manufacturing cost, which may be as high as \$150 per ton of electrochemically generated hydroxides, although magnesium is still necessary and may prevent the need for chemical additions for pH correction (e.g., NaOH) (Kelting et al., 2010; Telzhensky et al., 2011).

Following our experimental findings, using just the electricity required to change the pH at the membrane's surface, the tested system consumed 0.125 Watts of power overall at 3.5 V vs. Ag/AgCl, or around 5 V whole-cell potential, and 25 mA of current. According to Philadelphia's power supply statistics, the system used 0.25 Wh of electricity

during 1.5-hour recovery cycles, or around \$8 per ton of recovered phosphorous (Philadelphia, Wilmington, Atlantic City). This does not include additional expenses for the membrane preparation, cleaning, pumping, etc., which are part of the recovery process and are also anticipated in other precipitation methods. The projected cost of energy and magnesium for recovery should result in a struvite price of between \$108 and \$158 per ton.

### **3. ENHANCED NUTRIENT RECOVERY FROM LIVESTOCK WASTEWATER WITH ELECTRICITY – ASSISTED FORWARD OSMOSIS**

*(This section has been published as Kekre, K. M., Tiburcio, D., Ronen, A., Suri, R., Andaluri, G., & Yuan, H. (2022). Electrically charged forward osmosis: Promoting reverse salt flux to enhance water recovery and struvite precipitation. Resources, Conservation and Recycling, 186, 106522. <https://doi.org/https://doi.org/10.1016/j.resconrec.2022.106522>)*

We observed in the previous section that ultrafiltration membranes get fouled, leading to the need for excess pressure. However, excess pressure leads to additional energy requirements, eventually leading to more irreversible fouling. Hence, forward osmosis could be an excellent alternative to the pressure-based ultrafiltration method. Furthermore, to have electrochemical activity, a stainless-steel mesh was kept near the membrane surface to provide optimum conditions for nutrient recovery.

### **3.1. Introduction**

The human population has been growing exponentially, and to keep up with demand, agricultural practices have adapted by using modern technology and optimized processes. These adaptations include the application of fertilizers and pesticides on crop fields and concentrated animal feeding operations to raise livestock. While these innovations have allowed farmers to cultivate more food, they have also caused several negative impacts on the environment. In order to support the growth in agriculture, the global manufacturing of nitrogen-based fertilizers has increased from less than 10 million metric tons per year in 1950 to more than 150 million t/yr. in 2013 (Glibert et al., 2014).

Nutrient pollution and harmful algal blooms are becoming a global concern as they damage the environment, cause economic strain, and endanger human health. Harmful algal blooms can cause severe disruptions to the aquatic food chain and disperse toxins through the ecosystem, which can end up being consumed by humans. Excessive algal growth can also lead to hypoxic conditions and acidification of the water system due to increased respiration because of the higher mortality of biomass. Lastly, the algal blooms lead to a loss of biodiversity due to the abnormal population growth of one species (Burkholder et al., 2018). Not only does the increase in nitrogen and phosphorous concentrations harm water systems, but it also harms terrestrial ecosystems, especially soil health. One response is that soils have nitrogen deposition changes in bacteria, mycorrhizal fungi, and non-mycorrhizal fungi populations and increased acidity. Furthermore, increased nitrogen concentrations in the environment can, directly and indirectly, affect human health (Clark et al., 2017).

As a result, several innovative solutions have been developed and researched to tackle this problem. For example, Ling Ren et al. Researched the implementation of nano zero-valent iron-modified biochar to absorb phosphorus from eutrophic water. This research paper even studied the effectiveness of utilizing phosphorus-laden biochar as a fertilizer (Ren et al., 2021). It was also determined that when the nano zero-valent iron was prepared at 700 degrees Celsius, it had the greatest phosphorus absorption capacity. Another solution is using aluminum pillar bentonite to absorb phosphorus from aquaculture discharge water. It was determined that the absorption capacity of bentonite layered with polyhydroxide aluminum increased with increasing temperature; however, the absorption capacity decreased in saline systems. There is also a plan to construct a biogas plant in Denmark that will anaerobically digest pectin wastes, carrageenan wastes, manure, and beach-cast seaweed to produce bioenergy. The plant is estimated to reduce the GHG emissions by 40,000 t CO<sub>2</sub> and reduce nitrogen and phosphorous loads to Køge Bay by approximately 63 t yr.<sup>-1</sup> and 9 t yr.<sup>-1</sup>, respectively (Kaspersen et al., 2016).

Another solution to nutrient pollution is nutrient recovery from swine wastewater and carbon-rich starch wastewater by using microalgae-bacteria consortia. The research found recovery efficiencies of ammonia nitrogen, total phosphorus, chemical oxygen demand, and total nitrogen of the mixture of microbial cultures. Currently, nutrient recovery and nutrient absorption are two highly researched forms of addressing this growing problem. Additionally, the current treatment of livestock wastewater include activated sludge and trickling filter systems and bioremediation, which has several shortcomings that allow the deterioration of nearby soil and groundwater properties (You et al., 2021).

Membrane-based technologies offer practical techniques for nutrient recovery and the treatment of animal effluent. For instance, it has been demonstrated that the ammonium in the feed solution may be converted to ammonia using membrane distillation, a thermally driven membrane process (Ahn et al., 2011; Qu et al., 2013), which can then be collected with acids in the form of ammonium salts (Ahn et al., 2011). However, high energy requirements and problems with temperature polarization are the primary problems with membrane distillation (Anvari et al., 2020a, 2020b). In addition, reduced ammonium recovery efficiency can also result from scaling and fouling of the membranes (Zhao et al., 2013). Another membrane-based technique that separates ions in the presence of an electrical field is electrodialysis. Phosphate and ammonium can be concentrated in the anode and cathode chambers during electrodialysis (Shi et al., 2018). For nutrient recovery, the higher current density is advantageous, but it consumes much energy and might harm the membrane (Tran et al., 2014; Wang and Ren, 2013a; Zhang et al., 2011). Ammonium and phosphorus have also been recovered using pressure-driven systems like reverse osmosis and nanofiltration (Gerardo et al., 2015). However, as with other membrane techniques, fouling is still a limiting issue that necessitates extra cleaning and maintenance procedures (Dadrasnia et al., 2021).

A potential membrane-based energy-efficient water and nutrient recovery method is forward osmosis (FO) (Lu et al., 2015; Yuan et al., 2016, 2015; Yuan and He, 2015). The osmotic pressure differential between a high-salinity solution (draw) and a low-salinity solution (feed) drives spontaneous water diffusion (osmosis) during FO (Yuan et al., 2015; Yuan and He, 2015). In earlier research (Van Der Bruggen and Luis, 2015), concentrated fertilizer was employed as the draw solution to recover water from municipal wastewater,

and the diluted fertilizer could be utilized immediately for irrigation (Federico Volpin et al., 2019). FO-based techniques have also successfully recovered nutrients and clean water from cattle effluent. For instance, struvite was extracted from a swine-based effluent feed solution using magnesium chloride as the draw solute, which resulted in a high phosphate removal rate of up to 99% (Wu et al., 2018). Furthermore, for treating landfill leachate, FO was combined with bioelectrochemical systems and could eliminate 60% of the ammonia (Qin and He, 2014).

Reverse salt flux is an inherent problem of FO, during which salt ions diffuse reversely from the draw solution to the treated water (Chun et al., 2017; Kahrizi et al., 2022). Controlling FO membrane surface charge (i.e., Zeta potential) may help increase ion selectivity and lower reverse salt flux. This can be achieved by functionalizing the membrane or applying an external voltage, which has been reported to impose additional repulsion effects, thereby enhancing ammonium rejection in FO systems (Jafarinejad et al., 2019; Li et al., 2017). Conductive FO membranes have been employed to suppress reverse salt flux and have shown efficient rejection of organic compounds by applying an external voltage of 2.5 V (Li et al., 2017). Furthermore, a recent study used conductive membranes to control the recovery of reversed salt based on reduced ion migration due to the electric field applied (Wang et al., 2021). In addition to suppressing reverse salt flux, electricity-driven forward osmosis systems show significantly higher water flux (Son et al., 2019).

Given that reverse salt flow will always occur throughout FO operations, we suggest taking advantage of this unwelcome occurrence and using it as a catalyst for nutrient and water recovery. The primary goal of this work is to create an electrically charged FO (eFO) system to recover struvite from animal effluent by encouraging reverse

salt flow. In order to do this, a stainless-steel mesh was put in conjugation with an FO membrane made of cellulose triacetate, which functioned as the cathodic electrode (Fig. 1). Magnesium sulfate was used as the draw, and synthetic animal effluent (simulating after anaerobic treatment) as the feed to assess the system.

## **3.2. Materials and Methods**

### ***3.2.1. Feed And Draw Solutions***

The FO system's feed solution was synthetic wastewater mimicking anaerobically digested animal wastewater effluent. According to the literature, the biochemical oxygen demand (BOD),  $\text{NH}_4^+$ , and  $\text{PO}_4^{3-}$  in livestock effluent after anaerobic digestion range from 1000 to 5000 mg/L. (Hooda et al., 2000). So, 24 mM phosphate buffer saline (9.4 mM  $\text{KH}_2\text{PO}_4$  and 14.6 mM  $\text{K}_2\text{HPO}_4$ , 2280 mg/L phosphate), 24 mM  $\text{NH}_4\text{Cl}$  (1280 mg/L ammonium), and 39 mM sodium acetate (2400 mg/L BOD) were used to generate synthetic wastewater. The synthetic wastewater was fortified with more phosphate to prevent any pH changes brought on by water electrolysis. The draw solution, unless otherwise specified, was 1 M magnesium sulfate ( $\text{MgSO}_4$ ).

### ***3.2.2. System Setup And Operation***

The eFO system has two identical compartments (each measuring 25 mL), separated by a 55 cm<sup>2</sup> cellulose triacetate FO membrane made by Sterlitech. The membrane's active layer was on the feed side. The cathodic electrode and spacer were inserted into the feed chamber using a stainless-steel mesh. A plastic spacer was inserted inside the draw chamber for physical support and to lessen concentration polarization. The anodic electrode was a stainless-steel plate inserted in the draw chamber. A DC generator source was used to link

the electrodes. The feed and draw reservoirs were mounted atop digital scales, and each compartment included a connection to an external 1000-mL reservoir for tracking weight changes over time. The feed and draw solutions were moved through the corresponding compartments using peristaltic pumps at 75 mL/min.

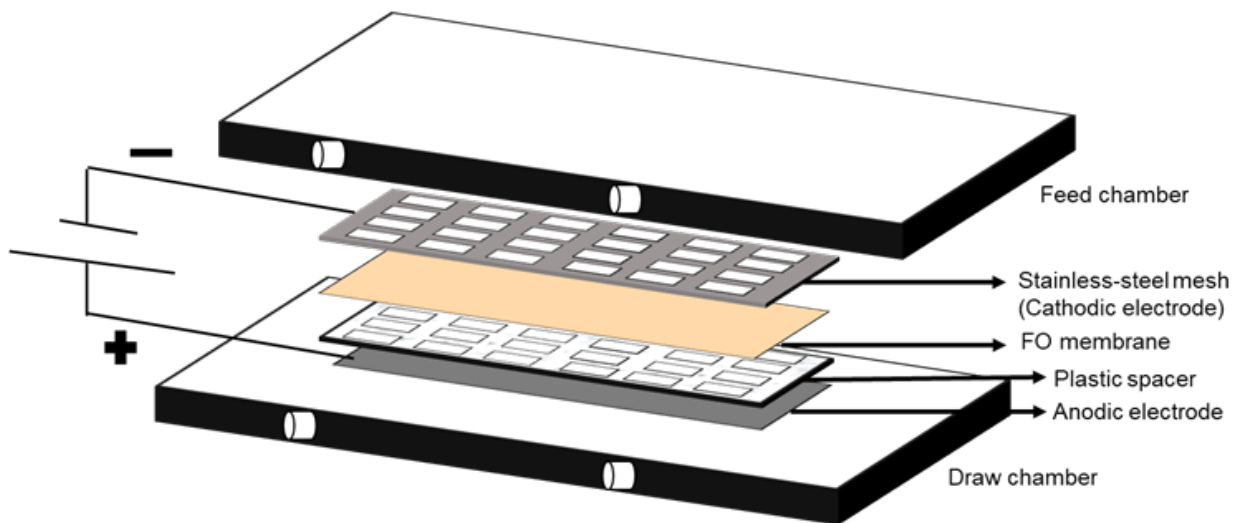


**Figure 7** Schematic of the eFO system

Using 1000 mL of synthetic livestock effluent as the feed solution and 300 mL of MgSO<sub>4</sub> as the draw solution, the eFO system was run in batch mode for 24 hours. The system's viability was evaluated using a 1.5 V external cell voltage during operation. Additionally, the system was used as a control group without any external voltage. According to the findings, the external voltage is one of the main factors influencing reverse salt flux (Wang et al., 2021; Zou and He, 2017). Furthermore, external voltage might also impact the ion concentration on the membrane surface and the water flow (Zou and He, 2017).

Furthermore, draw concentration is another distinguishing factor influencing reverse salt flow (Xu et al., 2010). Finally, the draw's pH might impact the ions' activity (Wang et al., 2014). We thus looked at how water flow and struvite recovery were affected

by external voltage (0.5 - 2.0 V), draw concentration (0.25 - 2.00 M), and draw pH (3.5 - 7.0). The detailed operating conditions are listed in Table 1.

**Table 1.** The operating parameters under different experimental conditions

<b>Investigated parameters</b>	<b>Voltage (V)</b>	<b>Draw concentration (mM)</b>	<b>Draw pH</b>
Voltage	0.5/1.0/1.5/2.0	1.00	9.3
Draw concentration	1.5	0.25/0.50/0.75/1.00/2.00	9.3
Draw pH	1.5	1.00	3.5/5.0/7.0

### 3.2.3. *Measurement And Analysis*

The weight change of the feed and draw reservoirs with electronic balances (Ohaus Scout) that were automatically registered at a time interval of 20 min was used to calculate the water flow (L/m<sup>2</sup>h), LMH). Five milliliters worth of samples were taken from the reservoirs for chemical analysis. A tabletop pH/conductivity meter was used to measure the pH and conductivity (Orion). The precipitates on the membrane surface were manually collected using a plastic spatula after each 24-hour operation. The eluent was mixed with the feed effluent and filtered through an ultrafiltration membrane to remove suspended struvite after being rinsed with deionized water. The collected precipitate was air-dried in a fume hood before being weighed and griddled for further examination.

Meanwhile, commercial kits and a spectrophotometer (Hach) based on accepted practices were used to assess the phosphate contents in the feed and draw effluents. Ion chromatography further investigated the effluent samples (Metrohm 930 Compact IC Flex). In order to verify struvite recovery, precipitate bulk and phosphate loss were compared. Membrane samples were taken at 3 and 24 hours to describe the shape and content of the precipitates. Scanning electron microscopy was used to see the morphology (SEM, FEI Quanta 450FEG SEM). Powder X-ray diffraction measurements (XRD, Bruker

D8 Advance X-ray Powder Diffractometer) and Fourier transform infrared radiation analysis was used to examine the chemical structure (FTIR, PerkinElmer Spectrum 100).

### 3.3. Results And Discussion

#### 3.3.1. Enhanced System Performance Under External Voltage

The eFO system was run in batch mode using a 1.5 V external voltage. Within the first hour, a maximum water flow of 3.5 LMH was noticed (Figure 7). Following that, the water flow steadily decreased to 2.1 LMH at 12 hours and 1.4 LMH at 24 hours. The control membrane, in contrast, had a maximum water flow of 1.3 LMH by the conclusion of the operation after peaking at 2.7 LMH early on (Figure 7). The eFO system recovered 39% more water than the control due to the considerably increased water flow during the first 15 h (t-test,  $p < 0.5$ ).

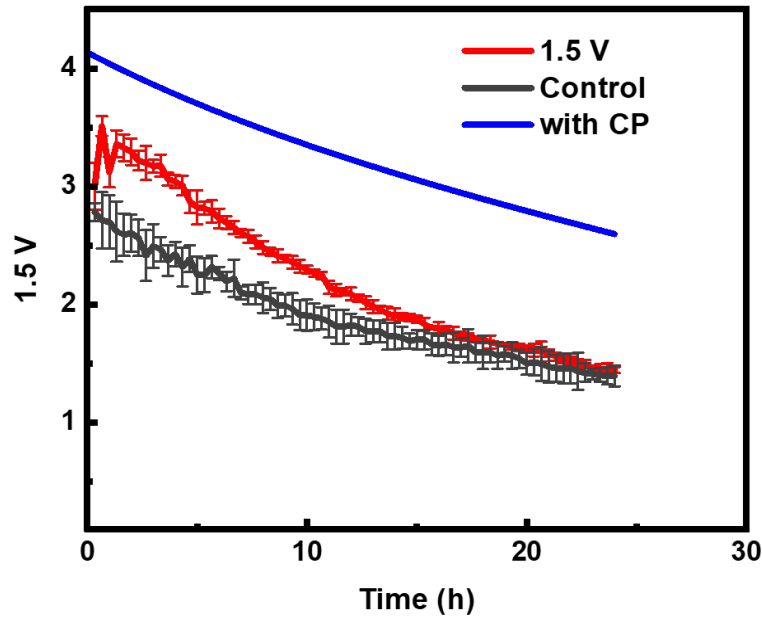


**Figure 8** Water flux in the eFO and control systems.

Based on the pure water permeability coefficient [ $0.09 \text{ L}/(\text{m}^2\text{hbar})$ ] and the osmotic pressures of the feed ( $9.2 \text{ mS/cm}$ ) and draw ( $1 \text{ MgSO}_4$ ,  $54.3 \text{ mS/cm}$ ) solutions, the theoretical maximum water flow in the current system was predicted to be  $4.1 \text{ LMH}$ . According to Lee et al. (2020), concentrative external polarization and dilutive internal concentration, which are constant in FO systems when the active layer of the membrane faces the feed side, are to blame for the disparity between the experimental and theoretical water flux. In addition, struvite precipitation may impact water flow in the eFO system (Lee et al., 2020). The precipitates fouled the membrane as  $\text{Mg}^{2+}$  was transported into the feed side during reverse salt flux and interacted with the  $\text{NH}_4^+$  and  $\text{PO}_4^{3-}$  accumulated on the membrane surface. This might have reduced water diffusion (Lee et al., 2010; Liu et al., 2019; She et al., 2016).

At the conclusion of the 24-hour operation, the bulk of the precipitates was recovered from the FO membrane surface, with the quantity from the feed effluent and the stainless-steel mesh in the feed being insignificant. In contrast to the control system, which only generated  $0.17 \pm 0.01 \text{ g}$  of precipitate, the eFO system produced  $0.62 \pm 0.02 \text{ g}$ . Meanwhile, 27% and 8% of the total phosphate were removed by the eFO and control systems, respectively. Consequently, the control recovered somewhat less precipitate from the removed phosphate than the eFO system (39% vs. 32% in molar ratio). Given that no phosphate was found in the draw effluent, the precipitation in the tubing, the presence of uncollectable crystals on the membrane, and precipitate loss during collection might all be responsible for the phosphate loss.

It is interesting to note that throughout the batch experiments, the maximum water flux of the eFO system was higher than that of the control and closer to the theoretical

calculation even though it produced more precipitate on the membrane surface and should, in theory, experience more severe fouling. In recent research, higher water flow in electro-FO has been discovered. It was hypothesized that this was due to ion buildup in the draw solution, which reduced dilutive polarization (Son et al., 2019). A similar reaction may occur when  $Mg^{2+}$  travels toward the negatively charged feed and accumulates on the draw side of the membrane in the current eFO system. Additionally, substrate production may have lessened concentrative polarization, which ate up the  $NH_4^+$  and  $PO_4^{3-}$  accumulated on the feed side. The results showed improved water flow and struvite recovery by charging the FO system, albeit the actions and interactions of various ions still need more study.

### ***3.3.2. Struvite characterization***

Spectroscopic techniques were used to characterize the precipitates collected from the membrane surface (Figure x). Peaks in the FTIR data can be seen at  $2892.41\text{ cm}^{-1}$ , which is predominantly due to the energy of N-H bond stretching,  $1432.13\text{ cm}^{-1}$ , which is connected to  $NH_4^+$  v4 asymmetric bending,  $983.05\text{ cm}^{-1}$ , which is related to phosphate bond stretching, and  $752.54\text{ cm}^{-1}$  (water hydrogen bond stretching). It follows that the precipitates have N-H, phosphate, and water-based H bonds (Herald et al., 2017). The precipitate samples were further analyzed using powder XRD, which revealed a spectrum very similar to commercial struvite, demonstrating that struvite was the precipitate's primary constituent. The sources of the crystals and crystal formation circumstances, such as pressure, drying temperature, and water availability, might cause the slight variances in the XRD spectrum (Luft et al., 2011). Furthermore, the color of the struvite produced in the eFO system looks more uniform, whereas impurities in the control sample are brown and black.

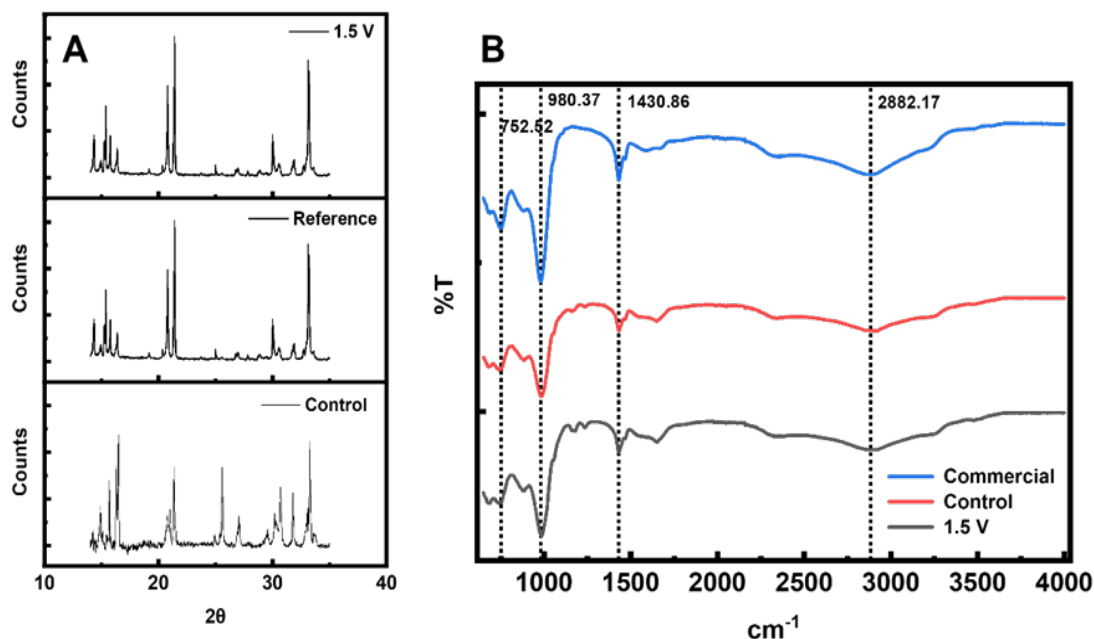


**Figure 9** (A) The XRD spectra for samples collected from the eFO system (black) and commercial struvite (red). (B) The FTIR spectrum for samples collected from the eFO system.

The FO membranes from the charged system were observed after 3 and 24 hours of operation to better understand the mechanism of struvite crystallization and development. Tiny orthorhombic crystals arranged haphazardly on the membrane surface collected after 3 hours (Hanhoun et al., 2013). Tiny crystals evolved into enormous clusters encircled by orthorhombic crystals after 24 hours. Also looked into was the reversibility of fouling. The FO membrane was removed from the precipitates, rinsed with deionized water, and reused without additional purification. The water flow was constant in three subsequent studies using a used membrane. The findings imply that removing struvite from the eFO system is simple without sacrificing water recovery.

Fouling is unavoidable, even though FO systems are renowned for having a low fouling propensity, especially in the current system that is intended to produce precipitates (Cruz-Tato et al., 2019). The struvite precipitates, however, are distinct from the typical inorganic foulant seen in FO systems. Our earlier research found that the nucleation of struvite during electrochemical treatment begins many angstroms distant from the electrode, principally because  $\text{PO}_4^{3-}$  is attracted to the negative charge. Given how the eFO system is set up, nucleation between the stainless-steel mesh electrode and FO membrane is possible. Crystals accumulate mass over time and land on the membrane surface (Kekre et al., 2021). In contrast to other inorganic foulants brought on by water flow, this might result in struvite precipitates with a loose structure that is simple to remove.

### **3.4. Effects Of Operating Conditions On System Performance**

#### **3.4.1. External Voltage**

Ion migration is significantly influenced by the external voltage, which may impact water flow and struvite recovery (Duan et al., 2017c, 2014a; Kekre et al., 2021). The applied voltage was changed from 0.5 to 2.0 V to understand its effect on the system's performance. It was found that high voltage encourages water recovery (Figure 9a). Under 2.0 V, the highest water flux was 3.9 LMH, which is not far from the predicted water flux. The water flow at 2.0 V was higher than the control throughout the operation, in contrast to the water flux at 1.5 V, which decreased to the same level as the control after 15 hours. The eFO system recovered 43% more water than the control while operating at 2.0 V. At low voltages (i.e., 0.5 and 1.0 V), the water flow was comparable to the control. Struvite

recovery is also favored by high voltage (Figure.9b). At 2.0 V, the eFO system produced 0.92 g of struvite, 52% more than it did at 1.5 V.

**Table 2** Struvite recovery and P removal in different units.

	<b>Struvite Obtained (mg)</b>	<b>Struvite Obtained (mmol)</b>	<b>P Removed (mmol)</b>	<b>%P Removed</b>
<b>Control</b>	143	0.6	1.8	7.7
<b>0.5 V</b>	172	0.7	2.4	9.9
<b>1.0 V</b>	434	1.8	4.9	20.4
<b>1.5 V</b>	616	2.5	6.4	26.7
<b>2.0 V</b>	916	3.7	9.1	37.8
<b>0.25 M</b>	212	0.9	2.1	8.9
<b>0.50 M</b>	324	1.3	3.6	14.8
<b>0.75 M</b>	440	1.8	4.4	18.4
<b>1.00 M</b>	620	2.5	6.4	26.7
<b>2.00 M</b>	810	3.3	8.7	36.1
<b>pH 3.5</b>	230	0.9	2.1	8.9
<b>pH 5.0</b>	310	1.3	3.5	14.5
<b>pH 7.0</b>	445	1.8	4.7	19.4
<b>pH 9.3</b>	616	2.5	6.4	26.7

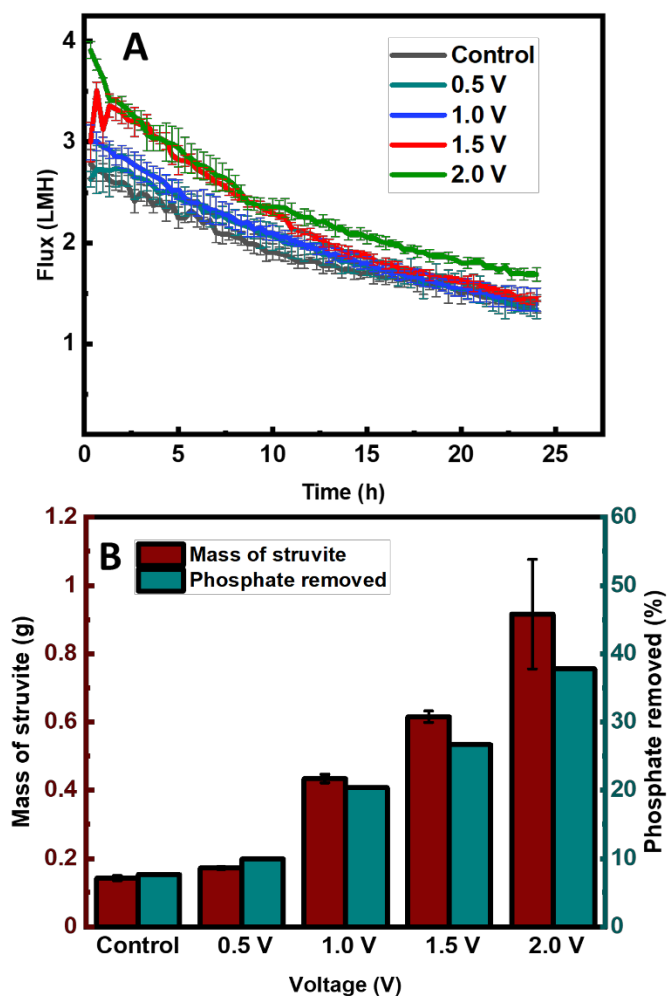


**Figure 10** (A) Water flux under different voltages. (B) Mass of struvite recovered and percentage of phosphate removed under different voltages.

There are various causes for the improved system performance at high voltages. First, the reverse flow of  $Mg^{2+}$  toward the negatively charged stainless-steel mesh in the feed will rise in a greater electrostatic field. Magnesium buildup on the membrane surface may even lead to a local  $Mg^{2+}$  concentration that is greater in the support layer than in the bulk solution, compensating for dilutive polarization. Second, the formation of struvite consumes more  $NH_4^+$  and  $PO_4^{3-}$  as the reverse flow of  $Mg^{2+}$  increases, balancing off concentrative polarization. Third, a hydroxide diffusion layer forms at the membrane

surface in the feed when water electrolysis is conducted at voltages greater than 1.23 V (Auinger et al., 2011; Katsounaros et al., 2011). Fourth, the alkaline microenvironment favors struvite precipitation. Finally, a stable hydroxide diffusion layer that is continually applied voltage can prevent the re-dissolution of struvite precipitates (Kekre et al., 2021).

#### ***3.4.2. Draw Concentration***

MgSO<sub>4</sub> concentrations ranging from 0.25 M to 2 M were used to investigate the impact of draw concentration on the functionality of the eFO system. Figure 5A illustrates that the average water flows with 0.25 M during the experiment was less than 1 LMH. With 0.50 and 0.75 MgSO<sub>4</sub>, respectively, it increased marginally to 1.2 and 1.6 LMH. The average water flow was much more prominent at higher draw concentrations (i.e., 1 and 2 M) than at lower draw concentrations, but it declined more quickly within the first 10 hours, perhaps due to more severe concentration polarization and struvite-induced membrane fouling. Similar patterns were seen in the recovery of struvite (Figure 10B). Only 0.21 g of struvite was recovered at 0.25 M of draw solution concentration, and the amount rapidly rose to over 0.44 g at 0.75 M and 0.81 g at 2 M. These outcomes were anticipated since reverse salt flux and water flux are tightly connected (Cath et al., 2013). Although water flow was comparable for 1 M and 2 M, 2 M retrieved 24% more struvite. The cause needs more research since it is unclear.

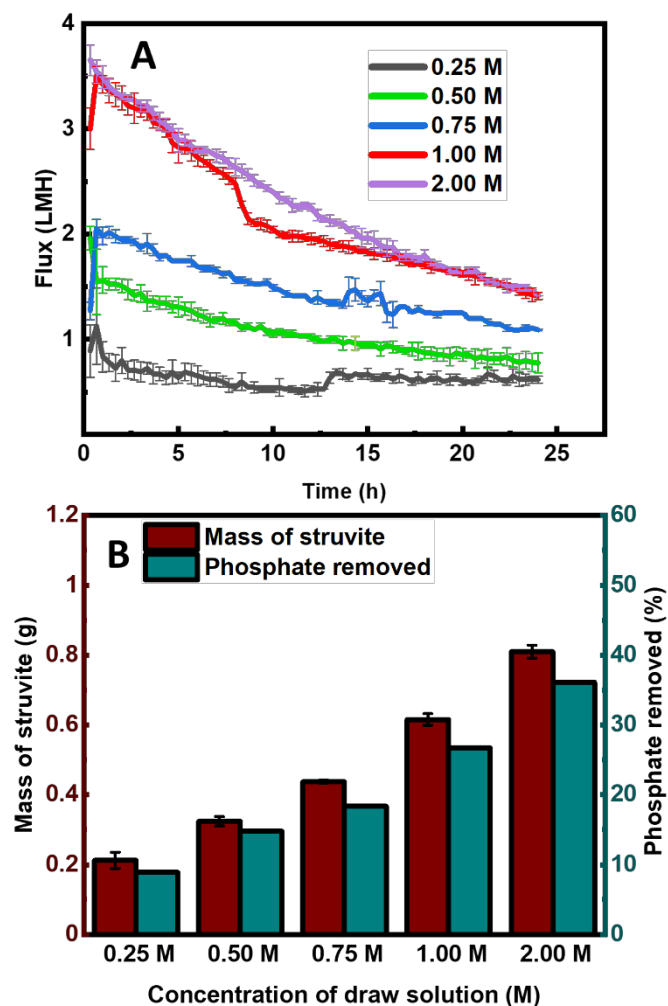


**Figure 11** (A) Water flux under different draw concentrations. (B) Mass of struvite recovered and percentage of phosphate removed under different draw concentrations

### 3.4.3. Draw pH

After 24 hours of operation, the draw pH in the eFO system at 1.5 V decreased from 9.3 to 6.5. This was anticipated, given that hydroxide was used up in the draw's anodic reaction.

In addition, the availability of free  $Mg^{2+}$  may increase in an acidic environment, which might be advantageous for reverse salt flow and struvite recovery. As a result, the draw pH was changed to neutral and acidic settings to test how they affected system performance.

As seen in Figure 11A, water flow exhibited similar behavior for pH values of 5 and 7;

however, within the first 15 hours, it rapidly decreased below 3.5. At pH 7, 0.45 g more struvite was found than under acidic circumstances (0.2 g) (Figure 11B). These findings suggested a complex interaction between the draw pH and the availability of free  $Mg^{2+}$ , with a high hydroxide concentration potentially favoring struvite precipitation (Rosrucker et al., 2015).

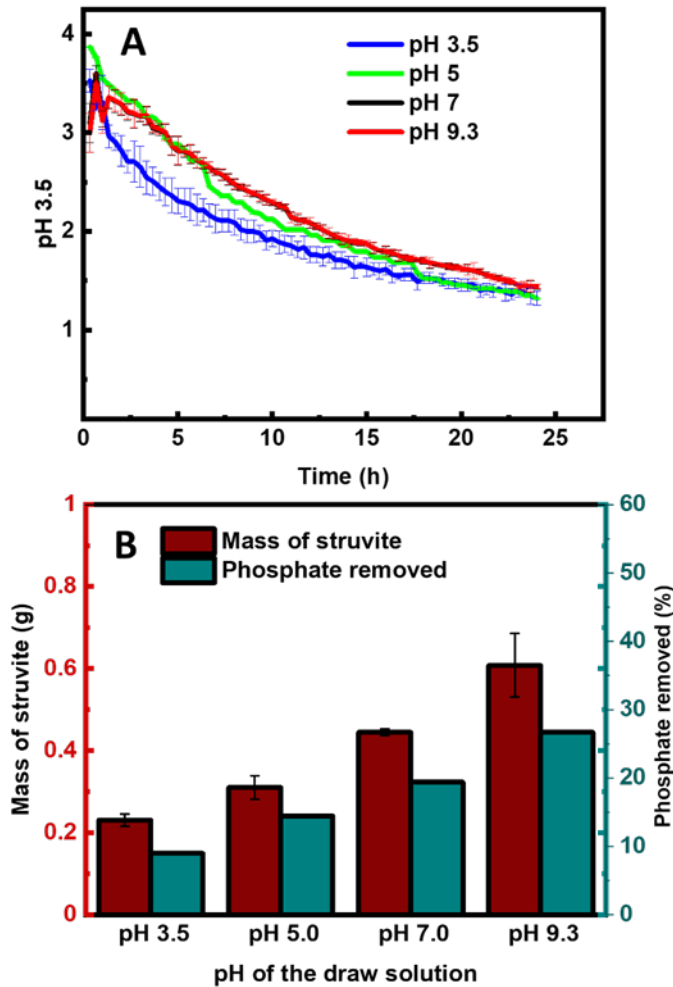


**Figure 12.** (A) Water flux under different draw pH conditions. (B) Mass of struvite recovered and percentage of phosphate removed under different draw pH conditions.

### 3.5. Perspective

Reverse salt flow is an issue that exists in all FO processes (Cath et al., 2006; Qiu et al., 2015; Shaffer et al., 2015). The feed effluent can deteriorate as a result of the salts from the draw solution, which can seep into the feed solution at a rate of up to 0.68 g/(m<sup>2</sup>h) (Van Der Bruggen and Luis, 2015). The issue may be solved by designing the procedure to use the salt that has been carried in reverse. For instance, to reduce fouling, oxidative conditions might cause the radicalization of chloride ions diffusing into the feed (Wang et al., 2022). Making value-added goods like struvite is another possible use for reverse salt flux. In a traditional FO procedure for treating digested swine wastewater, the precipitation of this beneficial fertilizer through the reverse flow of Mg<sup>2+</sup> has been shown (Wu et al., 2018). Struvite crystallized in the bulk solution on the feed side with 0.5 M MgCl<sub>2</sub> acting as the draw solution. Despite having a high phosphate and ammonia removal efficiency, MgCl<sub>2</sub> contamination reduced the quality of the struvite that was produced. In contrast, the struvite produced in the eFO system displayed a high purity, most likely due to undesired anions (sulfate ions) migrating toward the positively charged counter and being trapped in the draw chamber. A localized alkaline environment for more effective struvite precipitation may be created by applying voltages greater than 1.23 V, which also causes water to electrolyze (Kekre et al., 2021).

The results obtained under various voltages suggest that charge-induced reverse salt flow may also increase water flux (Figure 9). Similar outcomes were obtained using graphene oxide membranes, which may have ionized water molecules in the presence of a strong electric field and regulated water flow via the membranes' graphene capillaries (Zhou et al., 2018). However, reduced dilutive polarization is a more pertinent explanation

for the increased upper water flow. In addition,  $Mg^{2+}$  began to move and concentrate on the draw side of the FO membrane because of the electrode (stain-steel mesh) in the feed was negatively charged. This localized concentration helped maintain a high osmotic pressure across the membrane.

Furthermore, by reducing concentrative polarization, struvite precipitation can result in a larger water flow. This occurred due to the ions ( $NH_4^+$  in particular) precipitating out of the feed side of the FO membrane, which also contributed to maintaining a high osmotic pressure across the membrane. These findings offer helpful information for improving the water flow of FO by electrical means.

It should be highlighted that the eFO system cannot fully clean animal effluent on its own. Combining the eFO system with other biological and membrane-based technologies for organic eradication and water recovery is a potential approach. To treat wastewater, recover energy, and desalinate water simultaneously, FO has been hydraulically connected with bioelectrochemical systems (Lu et al., 2015; Sevda et al., 2017; Yuan et al., 2015; Yuan and He, 2015). By using the energy recovered by bioelectrochemical systems to build the eFO system described in this paper, the synergy between those two processes may be increased. In order to recover potable water and reconcentrate the draw solution, the eFO system can also be connected to membrane distillation. A closed-loop zero-discharge system may be created by applying the latter back to eFO. These viewpoints emphasize the crucial part that eFO plays in recovering resources for the future from nutrient-rich wastewater.

While eFO can be used with other technologies to complete the treatment process, several issues still need significant developments in engineering and membrane science.

First, the eFO system requires more energy for voltage application than traditional FO methods, increasing production costs and negatively impacting the environment. The total energy consumption is estimated at  $1.26 \times 10^{-5}$  kWh for a 24-hour operation with a voltage of 1.5 V and an average current of 0.35 mA. The cost of the struvite generated using this method (0.6 g) is around \$2 per ton based on the average energy tariff in the U.S. (10 cents/kWh). Even if the price is significantly less than the struvite market price (Wu et al., 2018), fossil fuel use is not considered sustainable. Second, struvite collection from the eFO system has to be improved for use in large-scale applications. The phosphate mass balance showed that over 60% of the struvite was lost in the tubing and during the collecting procedure. Reversible fouling and regeneration of the water flow were also noted, although long-term usage may cause the membrane to suffer from continuous precipitate removal and washing. This is especially troublesome given that FO membranes have a high initial cost and that care must be taken when collecting struvite to protect the membrane.

## **4. ENHANCED NUTRIENT RECOVERY FROM LIVESTOCK WASTEWATER BY COUPLING ELECTRICITY – ASSISTED FORWARD OSMOSIS & MEMBRANE DISTILLATION**

Preface – The following section details the combination of eFO with the MD system to enhance the eFO flux. The long-term use of the draw solution eventually leads to its dilution and then a drop in FO water flux. Combining a membrane distillation unit makes it possible to reconcentrate the draw solution, thus improving flux. The impact of heated draw solution on precipitates has also been researched.

#### **4.1. Introduction**

Desalination and distillation procedures have been created to recover water from salty or polluted water sources such as seawater, brackish groundwater, and hypersaline solutions (Giwa et al., 2017; Salih and Dastgheib, 2017). These new technologies for delivering freshwater have been developed to alleviate water stress. In general, desalination technologies may be split into two categories according to their separation techniques: membranes (also known as pressure-driven separation) and heat procedures. About one-third of the overall desalination capacity comes from thermal procedures (Deshmukh et al., 2018; Ghaffour et al., 2013), including multi-effect distillation and multi-stage flash. The remaining capacity comes from membrane methods.

In comparison to thermal distillation, membrane-based desalination offers several advantages. These include a reduced requirement for the provision of thermal energy, low environmental impacts associated with the generation of thermal energy through fuel consumption, a reduction in the amount of pumping that is necessary, and the absence of the significant ecological footprints that are required in many thermal distillation plants (Jevons and Awe, 2010; Mezher et al., 2011; Suárez et al., 2015). On the other hand, reverse osmosis (RO) systems that use high pressure to separate saltwater suffer from limitations that are caused by the nature of their separation mechanism. These limitations include membrane fouling, the requirement for high pressure and energy when desalinating hypersaline feed, and pre-treatment of the feed solution, all of which contribute to an increased cost of treatment (Akther et al., 2015; Jamaly et al., 2014; Kimura et al., 2003; Sutzkover-Gutman and Hasson, 2010).

The membrane distillation (MD) method is a hybrid technique that incorporates the benefits of both membrane separation and thermal distillation (Al-Obaidani et al., 2008; Curcio and Drioli, 2005; Lawson and Lloyd, 1997). Membrane distillation is abbreviated as MD. The separation is achieved by the use of transmembrane partial vapor pressure, which results in the passage of only molecules of water vapor across a hydrophobic microfiltration membrane. Continuous heating of the feed solution is performed in order to meet the requirements for both an effective driving force and a reasonably high distillate flux. In spite of the fact that the volatile vapors are able to pass through the membrane to the distillate side, the liquid is unable to enter the membrane pores owing to the surface tension of the membrane and its hydrophobic character. A variety of operating designs, including direct contact membrane distillation (DCMD), air gap membrane distillation (AGMD), sweeping gas membrane distillation (SGMD), and vacuum membrane distillation (VMD), are used to collect and condense water vapor at the distillate side (Alkudhiri et al., 2012; Alklaibi and Lior, 2005; El-Bourawi et al., 2006). When compared to other methods of desalination, membrane distillation (MD) has a number of distinct advantages. These advantages include a high rejection of non-volatile compounds, a low concentration polarization (CP), limited fouling, and low operating pressure and temperature even when distilling hypersaline solutions (Adham et al., 2013; Bush et al., 2016; Cath et al., 2004).

FO is dependent on the differential in osmotic pressures that exist on opposing sides of a semi-permeable membrane as a result of the varying concentrations of the solutions that are being used. This process moves water molecules from a solution that is less concentrated, called the feed solution, to a solution that is called the draw solution, which

is more concentrated. As water passes over the membrane, the feed solution loses volume and gets more concentrated, while the draw solution becomes more diluted and experiences a reduction in its osmotic pressure (Song et al., 2018). When combined with MD, FO often performs the function of a pre-treatment step, which allows MD to reduce the amount of impact caused by fouling and wetness. In MD, the diluted draw solution is continuously re-concentrated and recovered while, at the same time, pure water is produced on the permeate side of the membrane (Xie et al., 2016). For the sake of simplicity, these settings are referred to as hybrid MD-FO. The hybrid MD-FO and FO-MD systems enable the double-barrier purification of complex wastewater, such as wastewater that contains oil, surfactants, and organic and inorganic pollutants.

Desalination of salt water, the concentration of juices and protein solutions, and reclamation of wastewater from home wastewater, brine, urine, dairy effluent, and industrial wastewater are some of the many uses for hybrid MD-FO (Song et al., 2018). The hybrid MD-FO system is capable, in point of fact, of concurrently extracting nutrients such as phosphorus, nitrogen, or potassium from wastewater or urine as well as producing fresh water for human use. Because of this, the hybrid system is a desirable method for the production of sustainable water as well as the recovery of nutrients.

Both FO and MD can be used on their own as potential processes for extracting fresh water from non-traditional sources such as hypersaline solution, wastewater, urine, and so on. However, when combined, these two processes have the potential to increase the amount of freshwater that can be extracted significantly. Nevertheless, when employed independently, each of them has inherent restrictions that must be considered. For example, although it has been established that FO can effectively extract water from the feed solution

since the extracted water mixes with the draw solution, it is not possible to utilize it directly for many different uses. Although specific methods, such as fertilizer-drawn forward osmosis, make it possible for the draw solution to be used directly as a fertilizer (Phuntsho et al., 2011), in most situations, the draw solution has to be further processed before the extracted water can be used for the intended purposes.

On the other hand, MD has the ability to provide a steady flux that is not reliant on the concentration of the input salt and has the potential to enable the total rejection of non-volatile components (Tijing et al., 2015). However, if the hydrophobic MD membrane is subjected to complex wastewater in the presence of foulants, it is possible for the membrane to get wet. This results in liquid water being able to flow through the membrane, which in turn contaminates the MD permeate (Woo et al., 2018; Yao et al., 2018). Due to the fact that hybrid MD-FO utilizes the complementary functions of both processes, it is capable of producing permeate water of high quality (Xie et al., 2013). This helps alleviate some of the problems caused by the limits of both situations.

When using FO, the extracted clean water is mixed with the draw solution, necessitating the need for an additional procedure to separate, but when using MD, the combination of oil and surfactants makes it very prone to fouling and wetting (Al-Furaiji et al., 2019). No matter what sort of draw solution was used, MD was able to accomplish approximately one hundred percent rejection and high-purity water recovery thanks to the utilization of FO as a pre-treatment. In order to have a hybrid operation that is both stable and continuous, the best functional design required was one with a water extraction rate comparable for both the FO and the MD (Li et al., 2014). This assures that the draw solution, which is also the feed of the MD, will substantially retain its osmotic efficiency,

avoiding either the quick dilution caused by the FO or the fast concentration caused by the MD (Zhang et al., 2014).

Using hybrid MD-FO, it was recently shown that it is possible to produce freshwater while also recovering phosphorus in the form of struvite ( $\text{MgNH}_4\text{PO}_4 \cdot 6\text{H}_2\text{O}$ ) from anaerobically digested sludge (Xie et al., 2014). This was one of the more recent breakthroughs in the field of hybrid MD-FO. In their hybrid system, the FO was used to concentrate the orthophosphate and ammonium by removing fresh water from the feed solution (digested sludge centrate), and the MD was used to recover and recycle the draw solution in addition to producing fresh water. The FO was responsible for extracting fresh water from the feed solution (digested sludge centrate). The use of  $\text{MgCl}_2$  as the draw solution was a new approach that made use of the bidirectional diffusion of ions and made it possible for magnesium to penetrate into the digested sludge centrate. This was one of the innovative aspects.

By making use of the bidirectional diffusion of ions (reverse solute flow) and by allowing the magnesium to diffuse to the digested sludge centrate, the process of removing magnesium from the digested sludge may speed up. This, in conjunction with the movement of protons toward the draw solution, creates an environment that is conducive to the precipitation of struvite on the feed side. FO served both as a pretreatment for MD and as a barrier that prevented contaminants from reaching the draw solution. It did this by acting as a barrier.

The hybrid MD-FO system provides complementary tasks, such as the recovery of phosphate and nitrogen from urine while simultaneously creating freshwater. Because of this assumption, Volpin et al. (F Volpin et al., 2019) decided to study whether or not it

would be possible to use a hybrid system to recover nitrogen and water from source-separated urine. After determining that this hybrid system has a high propensity to accumulate nitrogen compounds at the draw solution, the researchers decided to concentrate first on nitrogen recovery and then on the optimization of FO and MD operating parameters in order to improve nitrogen rejection and prevent MD membrane wetting. It is undesirable if nitrogen is allowed to escape into the MD permeate as a result of nitrogen that has accumulated in the draw solution. The use of FO as a pre-treatment for MD effectively mitigated the adverse effects of wetness on MD, which were caused by the presence of surfactants and organic pollutants in the urine. Furthermore, the concentrated urine that is produced on the FO feed side presents an opportunity for the recovery of nutrients since water is removed during the operation of the FO.

Because of the way that MD processes work, the water that is generated is of better quality, and it may be easily recycled for indirect potable uses, such as flushing toilets or serving as cooling water (Leaper et al., 2019). In the meanwhile, the solution that was rejected is very concentrated, and it has the potential to be used in the process of recovering valuable items (El-Abbassi et al., 2009; Zhao et al., 2013). Furthermore, due to the concentrating effect of the membrane distillation process on the feed solution makes it an ideal candidate for combination with electricity-assisted forward osmosis. In addition, the draw solution can be reconcentrated in order to maintain the FO flux characteristics and prevent excess wastage of the draw salt solution.

## 4.2. System Setup

### 4.2.1. Forward Osmosis Setup

As explained previously, the eFO system was made up of two compartments that were precisely the same in size (each holding 25 mL), and they were separated by a cellulose triacetate FO membrane from Sterlitech that had a surface area of 55 cm<sup>2</sup>. The feed side of the membrane was in contact with the active layer. A stainless-steel mesh served both as the cathodic electrode and the spacer in the feed chamber once it was put there. The draw chamber was outfitted with a polyethylene spacer to lower concentration polarization and provide additional support. A plate made of stainless steel was mounted to serve as the anodic electrode in the draw chamber. A power supply was used to make the connection between the electrodes.

Each compartment was linked to an external reservoir with a capacity of 1000 mL, and both the feed and draw reservoirs were put on digital scales so that the rate of change in their weight could be tracked. Peristaltic pumps were used to move feed and draw solutions at a rate of 75 milliliters per minute through each of the various compartments of the apparatus.

The eFO system was run in batch mode for twenty-four hours with a feed solution of one thousand milliliters of synthetic livestock wastewater and a draw solution of three hundred milliliters of magnesium sulfate. In order to determine whether or not the system is practicable, an external cell voltage of 1.5 V was applied during the operation.

As part of the control group's operations, the system was also run without any external voltage. According to the findings, it was determined that one of the primary driving mechanisms of reverse salt flow is external voltage (Wang et al., 2021; Zou and

He, 2017). According to Zou and He (2017), external voltage has the potential to influence both the concentration of ions on the membrane surface and, as a result, the water flow. Furthermore, draw concentration is an additional factor that often contributes to reverse salt flow (Xu et al., 2010). In conclusion, the pH of the draw may influence the activity of the ions (Wang et al., 2014).

#### ***4.2.2. Vacuum Membrane Distillation***

The vacuum permeate collector, the heating system, and the membrane module are the three primary components that comprise the VMD experimental system. The membrane module can contain a flat sheet membrane that has an effective area of 32 cm<sup>2</sup> and was made by a CNC machine using a Nylon sheet from McMaster Carr. The feed solution was heated and supplied to the membrane module through a feed reservoir that was heated using a stirring hotplate. A peristaltic pump was used to supply the membrane module with feed solution (FO draw Solution) with MgSO<sub>4</sub> concentrations in a continuous manner (Masterflex 77201–60). Using a peristaltic pump, the concentrate kept moving in a loop back to the feed tank, which served as the brane module (Masterflex 77201–60). To maintain a consistent feed concentration, the concentrate was continually recirculated back into the feed tank, which was continuously monitored for salinity variations by electrical conductivity (EC, Thermo Scientific- Orion Star A329) measurements. A vacuum pump and a condenser were used in order to collect the permeate. In addition, the temperature of the feed tank was checked repeatedly at regular intervals. The draw solution or the feed solution for VMD consists of 0.8 M and 1.0 M concentrations for the initial testing of the synergistic effects of the system. Permeate flow was determined by using the equation, and the results were as follows:

$$J = \frac{M}{A \cdot \Delta t} \quad \text{Eq 16}$$

Where M (kg) denotes the total quantity of condensate that was collected, A denotes the effective membrane area that was used (32 cm<sup>2</sup>), and t (hr) represents the length of time that the MD operation was carried out.

#### ***4.2.3. Measurement And Analysis***

The weight change of the feed and draw reservoirs using electronic balances (Ohaus Scout) that were automatically registered at a time interval of 20 minutes was used to calculate the water flow (in liters per square meter per hour, or LMH), which was the same for both FO and VMD. For the purpose of conducting chemical analysis, samples were taken from the reservoirs. A tabletop pH/conductivity meter was used in order to get readings for both the pH and conductivity (Orion). The precipitates that formed on the surface of the membrane were scraped off by hand after every 24 hours of operation using a plastic spatula. After washing with deionized water, the membrane, and the stainless-steel mesh, the effluent was mixed with the effluent from the feed and filtered through an ultrafiltration membrane to recover the suspended struvite. After collecting the precipitate, it was subjected to air drying in a fume hood before being weighed and ground for further examination. To verify the struvite recovery, the mass of the precipitate was compared to the amount of phosphate lost. At three hours and twenty-four hours after the precipitation began, samples of the membrane were taken so that the shape and composition of the precipitates could be characterized. Powder X-ray diffraction measurements (conducted using a Bruker D8 Advance X-ray Powder Diffractometer) and Fourier transform infrared radiation analysis were used to investigate the chemical structure (FTIR, PerkinElmer Spectrum 100).

### **4.3. Results and Discussion**

#### ***4.3.1. MD Setup Testing***

The initial MD setup aimed to look at the efficiency of the total system yield of permeate based on draw solution concentration to make decisions and changes concerning combining the VMD with eFO. The initial testing was done with a feed solution of 0.5 M MgSO<sub>4</sub>, the approximate concentration of the draw solution after 24-hour eFO treatment. The initial testing was done in order to gauge the correct vacuum pressure and permeate volume without too much rise in the conductivity of the permeate. Based on previous studies, the increased vacuum pressure increases the volume of permeate but also decreases the quality of the permeate. Hence, applying higher vacuum pressure of 65 KPa saw an increased flux value of 1.81 LMH but with permeate conductivity of 10 mS/cm. On further testing, when the vacuum pressure dropped down to 10 KPa, the water flux dropped to 0.75 LMH, with a total permeate volume dropping down to 53 mL positively. The average conductivity of the permeate was recorded at 0.83 mS/cm. The following testing experiments were conducted at 80 °C to provide maximum temperature characteristics and obtain maximum permeate. In order to test the ability of both systems together, a common draw reservoir was utilized and heated. The heated draw solution was then supplied to the FO and the MD systems.

#### ***4.3.2. Hybrid FO-MD Operation***

The Hybrid FO-MD operation was first tested under unelectrified conditions, which was done to have baseline values for further treatment conditions. The Draw solution concentration was selected to be 0.8 M, and the feed solution characteristics were explained

previously. It was observed that the maximum flux observed was lower compared to previous FO experiments due to the reduction in osmotic pressure between the feed and the draw. The flux characteristics of the VMD system seem to be unstable initially. This could be due to the presence of air in the system initially. But over time, the flux behavior became homogenous and constant. The maximum FO flux in FO-MD was observed to be 2.06 LMH, and that of MD was observed to be 0.25 LMH. During this process, precipitates were collected to a value of 0.11g.

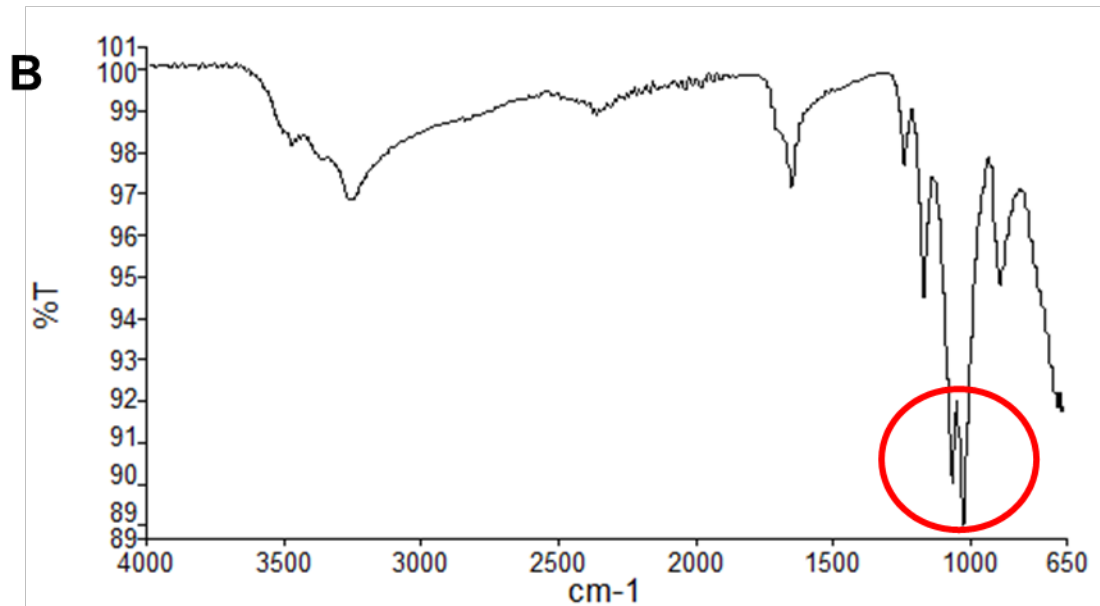
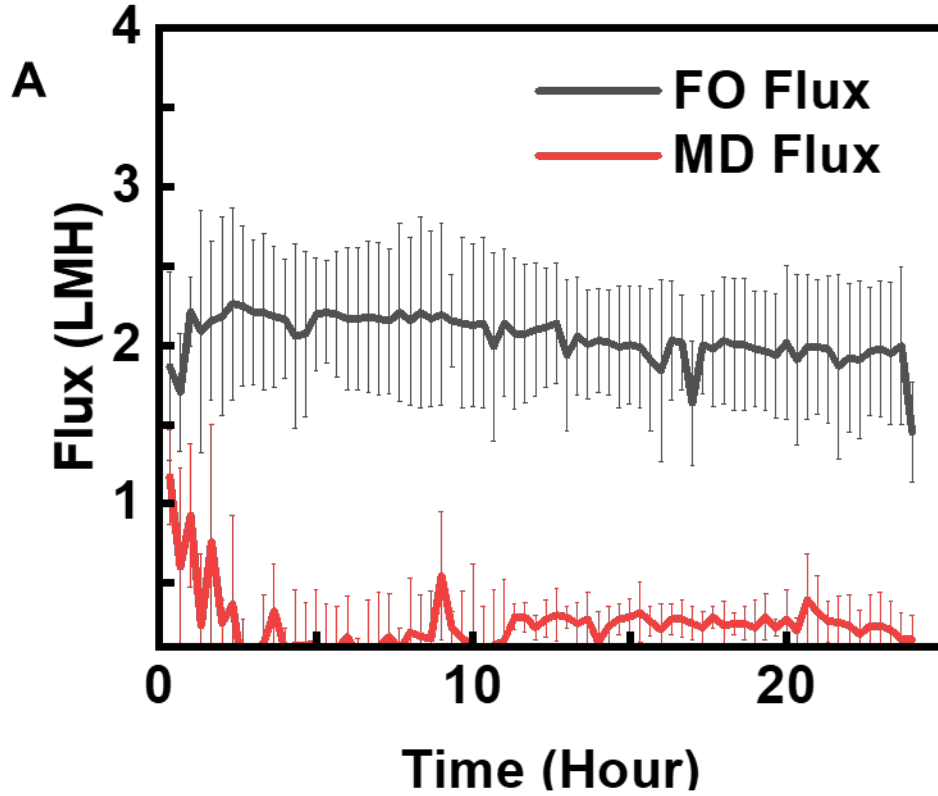


**Figure 13** A. FO flux and MD Flux characteristics at 80 C and 10KPa B. FTIR spectra of precipitates obtained in FO-MD processes.

It was observed that the heated draw solution had no negative impact on the flux of the system. The previous section shows that a draw concentration near 0.8M with eFO had

a flux of 1.6 LMH this was comparable to the 2.06 LMH of FO with the heated draw. This could be because thermal energy increases the kinetic energy near the membrane surface, potentially favoring better flux. It has been previously reported that a higher temperature of draw solution is favorable for flux efficiency in the forward osmosis process (Feng et al., 2018). The high number of fluctuations observed is due to the unpredictable nature of high heat. The higher temperature also impacts the membrane structural parameters (S-Value) (Feng et al., 2018), leading to fluctuations. Even though the flux characteristics seem to improve under hot draw solution conditions, the precipitate formation is lower. The analysis of precipitates revealed the formation of magnesium phosphate rather than struvite. Due to the hotter temperatures of the feed (40-45°C), the ammonia present in the feed water has the potential to vaporize along with water vapors. Therefore, magnesium phosphate precipitation is favored over struvite due to the higher temperatures. This is also evidenced by the FTIR analysis of the precipitates, which are a match for magnesium phosphate. Based on the Flux values, it can be concluded that using more than one MD module would be beneficial to purify most of the FO-recovered water in the draw solution. Also, an additional process to cool the feed solution would benefit the struvite precipitation process. It will enhance the favorable conditions on the draw side and prevent contamination due to the formation of other compounds.

#### **4.4. Perspectives**

Further Investigation is needed in order to see the enhancement of the FO process when electricity is applied to the membrane surface. Previous studies show the increase in flux and struvite precipitation, but the impact of higher temperature draw solution is unknown

on the system. One of the critical challenges in this process would be maintaining favorable conditions for struvite precipitation voltage application and the maintenance of feed solution temperature. Much research has been done to enhance FO membranes' capabilities by fabrication and modifications with carbon-based nanomaterials to MXene (Kekre et al., 2021; Rastgar et al., 2019; Xu et al., 2022). Similarly, MD membranes have also seen modifications in order to reduce thermal loss, scaling, and temperature polarization in order to conserve energy and maintain the efficiency of the system (Anvari et al., 2020b, 2020a, 2019; Bhadra et al., 2014; Thomas et al., 2018). Though these processes have been studied to be promising for the treatment of livestock-based anaerobically digested sludge, they do require pretreatment for organic carbon present, which can lead to fouling issues. Therefore, coupling of MECs with these membrane systems could be vital. MECs could utilize the organic carbon present in these systems and provide energy for the membrane processes. This could lead to a reduction in production costs and also prevent operational costs by reducing biofouling. There are already technologies and studies that look at combinations of FO-MD or FO-MEC. But there is a lack of a complete treatment option that could be potentially reached through hybridizing these technologies. A combination of MEC-eFO-MD could provide the possibility of zero waste discharge in the treatment of highly nutrient-rich lines.

**5. FUTURE PERSPECTIVES: COUPLING MICROBIAL  
ELECTROLYSIS CELL, ELECTRICITY – ASSISTED  
FORWARD OSMOSIS & MEMBRANE DISTILLATION FOR  
ZERO-CHARGE NUTRIENT RECOVERY**

The following section provides a perspective on the potential of combining MECs with eFO -MD processes. The eFO and MD system when operating together could consume huge amounts of energy in the form of electrical energy needed for nutrient precipitation and then heat energy to heat the draw solution. In order to reduce the energy needs of these technologies they could be coupled to a microbial electrolytic cell in order to treat the organic carbon and produce energy that could power the membrane systems.

## 5.1. Introduction

Due to industrial nutrient supply constraints, which is especially worrying given the world's expanding population, there has recently been a substantial demand for ammonium and phosphate, which are used in the production of fertilizer (Yan et al., 2018). In addition, it has been shown that wastewater sources contain high quantities of nutrients, including not just wastewater but also wastewater sludge, which is now regarded as a valuable source of nutrients. As a result, nitrogen recovery from wastewater may increase the number of fertilizers available for food production, reduce the cost of nutrient removal (e.g., by reducing the formation of excess sludge), and improve the sustainability of wastewater treatment (Chen et al., 2017).

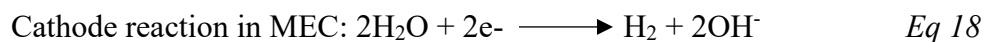
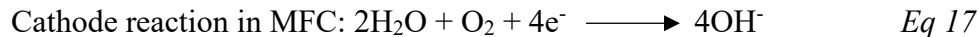
Numerous technologies have been studied for their effectiveness in nutrient recovery, including traditional techniques like chemical precipitation and adsorption and more advanced methods like bioelectrochemical systems and osmotic membrane bioreactors (OMBRs) (Li et al., 2019). Additionally, throughout the liquid phase of treatment, such as anaerobic digestion supernatant, sludge dewatering filtrate, and the sludge phase, i.e., dry surplus sludge and sewage sludge ash, nutrients from the wastewater may be recovered (Ye et al., 2019). Although wet-chemical and thermochemical treatments can remove phosphate from the sludge phase and interact with other recovery processes, most nutrient recovery methods are used in the liquid phase. Although wet-chemical and thermochemical treatments can remove phosphate from the sludge phase and then interact with other recovery processes, the majority of nutrient recovery methods are used in the liquid phase. In addition, phosphate can be moved biologically from the liquid phase to the sludge phase for recovery (Rasouli et al., 2018). For example, bioelectrical systems convert

waste to energy by utilizing microbes as a biocatalyst to convert organic materials in waste streams into electrical output through electrochemical processes (Jadhav et al., 2020).

Researchers studying renewable energy are becoming more and more interested in BESs. BES technology operates without external power sources and generates clean electricity by turning wastewater contaminants into CO<sub>2</sub> and water. BES has been employed in various industries to remove organic and inorganic contaminants from wastewater, but they still have issues with large-scale use, poor performance, cost-effectiveness, and appropriate design materials (Apollon et al., 2022).

The anode chamber and cathode chamber of the BES are typically divided by a cation-exchange membrane (Logan et al., 2006). Through biological and electrochemical processes in a multitude of wastewater, the BES can recover the chemical energy contained in the organic matter as well as various essential resources, such as nutrients (Patrick T. Kelly and He, 2014). In addition, the carbon impact can also be reduced in this circumstance. The most researched BESs are microbial electrolysis cells (MEC) and microbial fuel cells (MFC).

In an MFC, protons and biogas are produced by the anaerobic oxidation of organic substances through microbial action. Microbes degrade organic compounds in these conditions, generating electrons released to the anode (Logan et al., 2006). Electricity is created due to the electrons flowing from the anode to the cathode with a resistor connected to the circuit, and protons transfer through the cation exchange membrane (Marcus et al., 2011). Application of an external voltage between the anode and cathode electrode in the MFC, the system is called MEC. The anodic reactions in the MEC and MFC are the same. The cathode reactions are (Logan et al., 2008)



Electrons are oxidized in an MFC through the interaction with O<sub>2</sub>, the terminal electron acceptor. In the case of MEC, the protons are reduced for H<sub>2</sub> formation. This happens as the thermodynamic barrier for proton reduction is overcome by the voltage applied (Zhang and Angelidaki, 2014).

## 5.2. Nutrient Recovery In Bioelectrical Systems

In bioelectrical systems, the ammonium passes through the cation exchange membrane from the anodic chamber to the cathodic chamber due to electricity-based migration and diffusive transport due to the ammonium concentration gradient between two cell compartments (Kuntke et al., 2011). The declining ammonium concentration gradient causes ammonium diffusion between the anode and cathode chambers to establish an equilibrium, whereas electricity-driven ammonium migration from anolyte to catholyte goes against the concentration gradient (Cheng et al., 2013). In the cathodic chamber, concentrated ammonium could be volatilized ammonia gas due to the cathodic chamber being at high pH due to the production of a hydroxyl group, which is further stripped or obtained by aeration (Patrick T Kelly and He, 2014). The stripped ammonia can be directly adsorbed by reacting with acids to form ammonium salts (Zhao et al., 2006). Ammonia can also be obtained as ammonium bicarbonate by reacting it with carbon dioxide and water (Qin and He, 2014).

Unlike MFC, the MEC has an imposed voltage to reduce the cathodic potential, allowing reduced products such as H<sub>2</sub> and CH<sub>4</sub> to be created at considerably lower voltages than the top stability limit of water (Wang and Ren, 2013b). Anodic biofilm is used in MEC to oxidize organic or inorganic substrates, releasing electrons and protons to the cathode; an enforced voltage makes the electrons more reductive, reducing the electron acceptors to a more reduced state. As a result, the MEC leads to ammonium-rich catholyte (Villano et al., 2013). The application of external power enhances the ammonium migration and pH elevation leading to further ammonia recovery (Wu and Modin, 2013). Studies show that the removal of ammonia in BES is about 94% and 79% in synthetic and real wastewater. The volatile ammonia was precipitated by stripping with the help of HCl. The real wastewater was observed to have lower removal efficiency because real wastewater has a higher buffering capacity (Wu and Modin, 2013).

For P removal through BES has been studied to varying degrees. Studies have been conducted where BES-based treatment systems are used to extract FePO<sub>4</sub>-based phosphate from digested sewage sludge. The phosphate-rich supernatant was dosed with magnesium and ammonia for struvite formation (Fischer et al., 2011). Single chamber configuration BES has been reported to remove phosphate as struvite in about 70-82%. These precipitates are obtained on the cathode surface. One probable reason is that the reduction in oxygen on the cathode raises the localized pH, which contributes to struvite precipitation (O Ichihashi and Hirooka, 2012). Other authors have used single-chamber MFC to recycle P from landfill leachate and urine, respectively, and both achieve excellent efficiency in P recovery with phosphate-based precipitates on the cathode electrode surface (Damiano et al., 2014; Zang et al., 2012). The struvite precipitation on the cathode can potentially affect

the mass transfer of ions and oxygen and the electricity generation, but this can be rectified by removing precipitates from the cathode (Hirooka and Ichihashi, 2013).

Wastewater feed solutions used in these systems contain many cations like  $Mg^{2+}$ ,  $Ca^{2+}$ , and  $K^+$ , which also diffuse and migrate between anode and cathode chambers affecting nutrient accumulation and recovery (Rozendal et al., 2006). Furthermore, transferring such mineral salts is necessary to preserve the system's charge neutrality (Logan et al., 2006; Qin et al., 2016). The cations' forward and backward diffusion will achieve equilibrium (Rozendal et al., 2006; Sleutels et al., 2009), but the cation transport caused by the electrical field will not be impacted by the concentration gradient between the anolyte and catholyte (Rozendal et al., 2006). Transferring mineral salts to the cathode chamber may raise the salinity of the catholyte, lowering catholyte resistance and increasing power output (Qin et al., 2016).

### **5.3. Combining BES With Forward Osmosis Processes**

FO processes can be engineered to finish a variety of water quality processes such as the production of potable water from natural waters (Cath et al., 2006), recycling water from complex wastewater streams (Holloway et al., 2007), and dewatering of activated sludge (Zhang et al., 2014). But FO processes are limited to concentrating the feed rather than treatment of contaminants present in the feed. The concentrated feed from a FO process requires post-processing, and energy is lost in these processes. It must be acknowledged that pure water cannot be obtained from FO processes because the water recovered as the diluted draw solution needs to be separated from the draw constituents and the draw

solution itself needs regeneration. BES and FO are very different technologies, but both have properties that could provide a positive effect on their treatment capabilities.

The synergy between these technologies provides the increased advantage of effective water extraction. In order to increase the sustainability of the entire system, BES can degrade pollutants in wastewater, offer a supply of treated wastewater for recovery, and collect valuable products. Some significant problems in each process, like the availability of draw solute, reverse solute leakage in the FO, and the energy needed to carry out specific reactions in the BES, may be resolved with the correct combination of the two. The treatment of contaminants in water and wastewater can be improved with the use of BES. The FO procedures produce diluted draw solution (saline water) and concentrated feed solution (wastewater), both of which require further treatment to be suitable for discharge and reuse. By using electricity to remove salt from the anode, BES can achieve organic degradation. The draw solution is a crucial component of the FO process, and the optimal draw solution has high osmotic pressure, simple regeneration, non-toxicity, and cheap cost (Ge et al., 2013). Due to reverse salt flow, the typically utilized draw solution based on inorganic salts requires an external supply as well as energy-consuming regeneration procedures. Since draw solution dilution/feed solution concentration and reverse salt flux result in a drop in osmotic pressure, water flux is a crucial performance parameter for FO—decreases with FO operation (Lutchmiah et al., 2014).

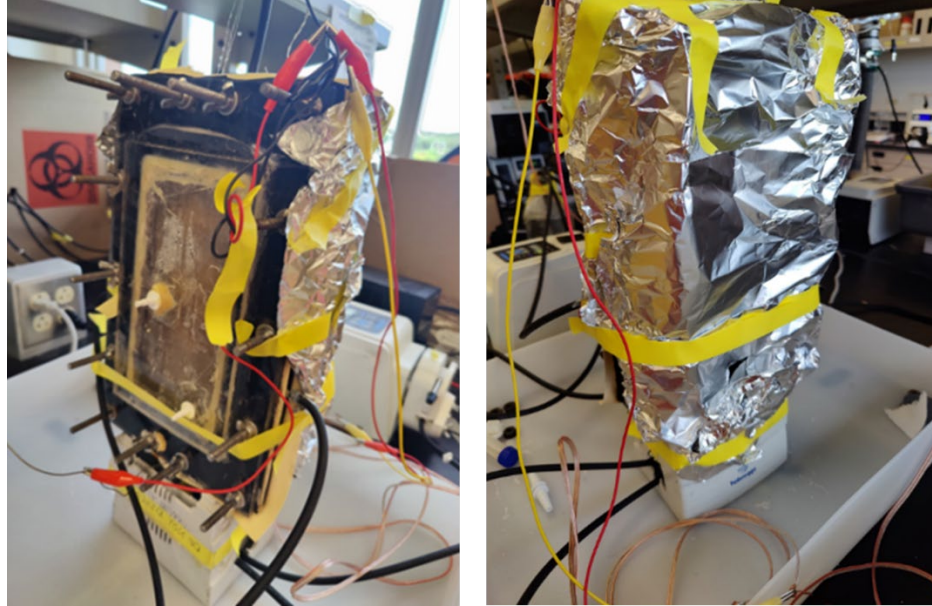


**Figure 14** MEC-FO system for livestock wastewater treatment and biofilm development

## **5.4. Methods**

### ***5.4.1 Fabrication Of MEC***

The MEC was constructed using acrylic cubes (McMaster, Inc). The MEC system consisted of two compartments, an anode, and a cathode, separated by a cation exchange membrane. The anodic chamber has dimensions of 8 x 4 x 1.5 and consists of carbon brushes to promote biofilm growth. The cathodic side had dimensions 8 x 4 x 0.3 inches. The cathodic side consisted of a stainless-steel mesh as an electron collector. The cathodic chamber acts as the feed chamber for the electricity FO system and consists of the cellulose triacetate membrane. Beyond the membrane is the draw chamber that allows MgSO<sub>4</sub> in the chamber to have osmotic pressure difference-based water flux from the reactor's cathodic chamber.

### 5.4.2. System Operation

The supernatant from the sludge obtained at the wastewater treatment plant was inoculated in a synthetic wastewater solution circulated in the anode chamber. The MEC system's anode solution was made of synthetic wastewater mimicked anaerobically digested animal wastewater effluent. According to the available research, cattle wastewater after anaerobic digestion generally contains 1000–5000 mg/L of biochemical oxygen demand (BOD), 520–1300 mg/L of  $\text{NH}_4^+$ , and 600–1400 mg/L of  $\text{PO}_4^{3-}$  (Hooda et al., 2000). As a result, synthetic wastewater was created using 24 mM phosphate buffer saline (9.4 mM  $\text{KH}_2\text{PO}_4$  and 14.6 mM  $\text{K}_2\text{HPO}_4$ , for a total phosphate concentration of 2280 mg/L), 24 mM  $\text{NH}_4\text{Cl}$  (1280 mg/L ammonium), and 39 mM sodium acetate (2400 mg/L BOD). The feed solution consisted of 50mM of phosphate buffer for the initial startup, and the anodic side of the MEC was inoculated with sludge supernatant from the wastewater sludge sample.

### 5.4.3. Analytical Measurements

The voltage of the MEC was measured by a digital data collector (Keithly Instruments, Inc., OH, USA) every 2 minutes. The concentration of soluble COD was measured through a colorimeter (DR300, Hach, CO, USA). Since the initial maturation process of the biofilm is based on batch operation, the coulombic efficiency was calculated based on (Bruce E. Logan, Bert Hamelers, René Rozendal, Uwe Shroder, Jurg Keller, Stefano Freguia, Peter Aelterman, 2006)

$$\epsilon_{Cb} = \frac{M \int_0^{t_b} I dt}{F b v_{An} \Delta COD} \quad \text{Eq 19}$$

Where  $M = 32$  is the molecular weight of oxygen,  $F$  is the Faraday constant,  $b = 4$  is the number of electrons exchanged per mole of oxygen,  $v_{An}$  is the volume of liquid in the anodic compartment of the MEC, and  $\Delta\text{COD}$  signifies the change in the COD over time  $t_b$ .

#### 5.4.4. System Perspective

During biofilm development on the carbon brushes, the electricity generation from the reactor acts as an indicator of microbial activity. Therefore, the external resistance is dropped successively over time to provide controlled biofilm growth on the carbon brushes. For the initial operation, the reactor showed promise. We were able to drop the external resistance of the system to about 100 ohms producing about 500 mV. This progress was carried over with the system switching to MEC operation and application of about 0.8 V with 100 ohms external resistance. But eventually, there was a fall in microbial activity, and the microbial community could not continue growing; this cycle was repeated about 3-4 times, resulting in similar results. The following section discusses the possible reasons for the drop-in microbial activity and the eventual failure of the reactor. This has been rectified by changing the reactor design, and instead of using a big reactor, the current approach is being tried with multiple smaller MECs.

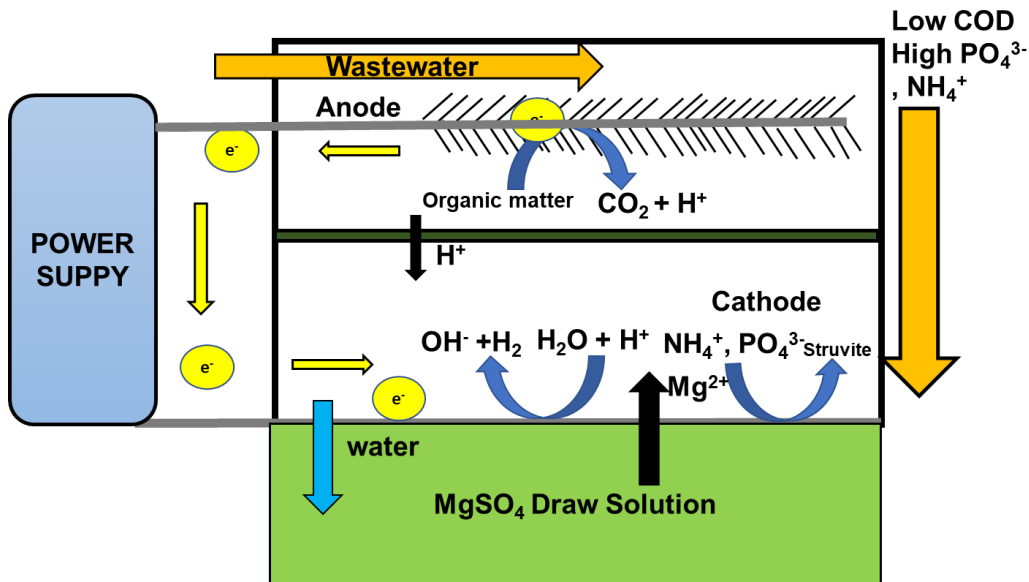


Figure 15 Schematic of microbial electrolysis system

### **5.5. Potential Reasons For MEC Failure**

The microbial fuel cell (MFC), which transforms organic materials into energy, and the microbial electrolysis cell (MEC), which transforms organic materials into hydrogen, are the BESs that are most often explored. Failure is conceivable in either type of BES. The biological components of BESs complicate failure investigations further since the anode contains a microbial ecosystem that is constantly changing due to microbial regrowth, mortality, mutation, and adaptability. In contrast to abiotic systems, biology may rebound after being subjected to circumstances that cause failure. Helder et al. exposed a plant-based MFC to weather patterns and were the first to precisely measure BES resistance and resilience (Helder et al., 2013). The scientists found that the reactor's current output was permanently reduced by the subfreezing temperatures.

The anode community can also suffer from several other situations besides temperature. On MFCs (Oh et al., 2009; Quan et al., 2012) and MECs (Ajayi et al., 2010), oxygen introduction is frequently used, and complete recovery is frequently seen. Acidification is another shock that frequently causes anode microbiological failure. BESs can withstand both acidic and alkaline environments (Badia-Fabregat et al., 2019; Borole et al., 2008), while acidic circumstances can permanently harm MFC function (Lesnik et al., 2020). Osmotic shock and sudden variations in applied voltage are a few other failure mechanisms that haven't been considered. Operator mistakes or changes in waste streams, which can include high quantities of salts, might result in the unintentional introduction of salts. Abrupt voltage changes may be brought by power surges, blackouts, or bad connections in the standard 3-electrode assemblies used in BESs. MFCs coupled in series are susceptible to adverse voltage fluctuations (Oh and Logan, 2007). While additional

negative potentials are feasible and might potentially harm performance, positive whole-cell voltage has been reported to be deleterious to the performance of MFCs (Ding et al., 2015).

#### ***5.5.1. Acidification***

Due to pH drops, previous acidification studies show the most significant impact of anodic microbial communities. According to the authors, even if the microbial communities recovered, the coulombic efficiency of the system dropped significantly. This drop in coulombic efficiency was attributed to dead biomass that prevented the conversion of organic material to electrons. These efficiency parameters could not make a full recovery even after prolonged recovery attempts (Satinover et al., 2020). Additionally, entrapped inactive microorganisms in the biofilm are not likely to transmit electrons as efficiently as active bacteria do. Losses in anode Coulombic efficiency are likely if there aren't effective means to transmit electrons to the anode. Even though the regenerated microorganisms were more successful at breaking down organic materials, they did not transport electrons to the anode as efficiently. The microorganisms appear to have stabilized, but they may have continued to adapt and thrive following the recovery operations.

#### ***5.5.2. Osmotic Shock***

Osmotic Shock was reported to have an intermediate impact on the operational efficiency of the MFC and MECs. But these impacts were overcome with recovery periods on the reactors. The inability to break down as much of the carbon supply was the main reason for the reduced current density brought on by osmotic shock. The coulombic efficiency measured before the osmotic shock remained almost unchanged. The buildup of organic acid following osmotic shock was one of the signs of performance decline. This suggests

that osmotically shocked MECs were less effective at converting organic acid following exposure. Despite having identical communities, it was also shown that the type of organic acid that accumulated altered the MEC systems' efficiency recovery (Hari et al., 2017). The osmotic shock impacted MEC's performance, although the losses were soon repaired. Osmotic shock exposure that lasts longer might be harmful to the neighborhood.

In the air, oxygen is the primary oxidizing agent. Due to its high redox potential (+1.23 V vs. RHE), it is the primary final electron acceptor used to finish the circuit at the cathode (Vélez-Pérez et al., 2020). However, the performance of the MFC is adversely impacted by the presence of oxygen in the anodic chamber (Watson et al., 2011). First, it poisons the anaerobic bacteria that act as biocatalysts in the anode chamber when it is present. Additionally, it is the primary electron acceptor in terms of thermodynamics. Therefore, dissolved oxygen will be the first option for an electron acceptor in the case of facultative bacteria, another type of biocatalyst found in the anode.

After failure, aeration barely reduced the current density or hydrogen productivity, and long-term recovery was only necessary for two days. BESs may be inhibited by dissolved oxygen, although employing anaerobic replacement of the anode liquid medium immediately restored performance to typical operating conditions. If MEC production is the main issue, repairs intended to minimize oxygen infiltration should concentrate more on stopping leaks than replanting the community. After aeration, more COD was used, and greater current density was produced. Following long-term recovery, losses resulting from aeration may be brought on by a combination of electron diversion and inefficient electron production. Accumulated bubbles at the anode membrane are a real threat that might result in losses in electrical efficiency. An insoluble gas phase is directly introduced by aeration

and has the potential to be trapped in the anode chamber. When gases are unintentionally or intentionally introduced into the cell, it will be crucial to properly purge them from MECs to ensure electrical efficiency and encourage mass transfer. All BES designs continue to be seriously concerned with mass transfer. Aerated cells generated current and hydrogen at rates almost identical to those before the application of the failure condition. Even if aeration wouldn't help MECs, this failure condition seems like it might be readily fixed.

### ***5.5.3. Voltage Issues***

Voltage reversal caused performance and efficiency changes, although they were not as severe as other failure circumstances. Bubbles may have been created at the anode as a result of water electrolysis under reductive circumstances, and they may have included hydrogen, which exoelectrogens may utilize as an electron donor (Lovley et al., 2004). It was found that cleaning the anode sufficiently rectified any potential losses to electrical efficiency and that there were no substantial changes to the materials or community. Voltage reversal had a negligible impact on the electrochemical behavior that resulted and should be simple to fix.

A reduction in COD elimination was seen when the current density dropped. The two situations where losses were seen, acidification and osmotic shock, may have damaged exoelectrogens, fermenters, or a mix of both types of bacteria. According to these investigations, osmotic shock negatively impacted fermenters more than acidification did, whereas the latter had a greater negative impact on exoelectrogenic activity. Overall, it seems that fermenters were less impacted in both instances than exoelectrogens. Most Studies conducted in order to study the failure of MECs did not consider using a spectrum

of parameter ranges but rather the extremes. Hence further studies will be required to study the range of efficiency changes and statistics involved. MECs will gain more traction as a viable green technology and consolidate their position in the future bioeconomy if they can demonstrate their resilience in the face of further failure scenarios.

#### ***5.5.4. Impact Of Separating Membrane***

Operationally, the type of ion exchange membrane used could also cause MEC efficiency and microbial community development issues. The nature and thickness of the membrane can contribute to the internal resistance, thus affecting the efficiency of MEC. It was also observed that nonporous thinner membranes have higher electroactive species permeability. Thinner membranes also have comparatively lower mechanical strength, thus preventing overall reactor performance (Ghasemi et al., 2012). Furthermore, using a porous membrane increases the possibility of high oxygen and substrate crossover. Nonporous membranes that have been completely hydrated provide the greatest ion-exchange functionality. Therefore, maintaining membrane hydration is related to oxygen diffusion. The oxygen diffusion process is the method by which oxygen diffuses simultaneously through the membrane and water toward the anode, where the oxygen content is lower (Leong et al., 2013; Malekmohammadi and Mirbagheri, 2021). In general, porous membranes have a more significant tendency to facilitate the flow of oxygen from the cathode to the anode due to the existence of pores compared to nonporous membranes. It will be challenging to create a membrane that completely avoids oxygen diffusion, though, because IEMs must be hydrated in order to operate.

If a membrane possesses the following qualities, it may be considered ideal for use in MFCs: high, low water and substrate loss, low thickness, impermeability to oxygen and

cations like  $\text{NH}_4^+$ ,  $\text{Na}^+$ ,  $\text{K}^+$ ,  $\text{Mg}^{2+}$ , and  $\text{Ca}^{2+}$ , good mechanical properties, chemical stability, low internal resistance values, impermeability to gases like  $\text{H}_2$ ,  $\text{N}_2$ , and, unquestionably, a low price. Meeting all of these demands at once is challenging. However, the goal of this search is to identify membranes with the greatest number of advantageous properties and, most importantly, whose use demonstrates good MFC performance in terms of low average internal resistance, prolonged stability or durability over time and under various operating conditions, biofouling resistance, nonbiodegradability, low cost, and high coulombic efficiency. Unfortunately, the perfect membrane does not exist.

Membrane filtration can be implemented into BES as a separator between the electrodes, an internal filtering component in the anode/cathode compartment, or an external treatment procedure before or after BES. This type of integration has several benefits, including high-quality effluent, high energy efficiency, lower capital costs, less fouling, and sustainable desalination. The challenges lie in gaining a better knowledge of the coupled system's energy output and consumption, membrane fouling, identifying appropriate application niches, and scaling up the system. Nevertheless, BES combined with membrane filtration has the potential to be developed as energy-efficient technology for wastewater treatment and water reclamation.

## 6. EXECUTIVE SUMMARY, CONCLUSIONS, AND FUTURE

In this dissertation, the modified membrane-based processes, their optimization for various conditions, their potential for conjunction with other advantageous technologies, and the obstacles connected with the recovery of water and nutrients are investigated.

Chapter 1 looks at the current issues due to increased dependence on fertilizers and CAFOs for food production demands due to the growing population. It highlights the conventional methods for livestock wastewater treatment. It details the struvite and favorable conditions required for precipitation in the treatment system. It highlights the research's hypothesis and objective and the goals required to achieve it. It also illuminates the significance of dissertation research work.

Chapter 2 highlights the conductive ultrafiltration membrane. Conductive ultrafiltration membranes were fabricated by depositing functionalized carbon nanotubes on the commercial membrane surface. The conductive membrane overcame the buffering capacity of the synthetic wastewater solution and produced alkaline pH. The flux of the system reduced with time during the treatment process due to the deposition of the struvite crystals on the membrane surface, whereas the pH was maintained at the optimum alkaline levels. The precipitates obtained were analyzed with powder X-ray diffraction and FTIR and identified as struvite. Rapid struvite precipitation and phosphate removal were observed. With successive cycles, phosphate removal dropped due to decreased precipitation cycles. Ionic behavior was modeled under conductive conditions, and it was observed that the nucleation of struvite takes place away from the membrane surface and is then eventually deposited on the membrane surface.

Chapter 3 looks at the electricity-assisted forward osmosis process. The forward osmosis system removes the need for hydraulic pressure and utilizes osmotic pressure to recover water. A stainless-steel mesh was used as the conductive surface and placed near the membrane's active side. Increased voltage application resulted in higher flux values and higher struvite precipitation. The lower draw pH did not impact water flux but reduced the struvite precipitation. Higher draw concentration increased the water flux and increased the struvite precipitation. Further it was observed that nutrients precipitated in the absence of electricity produced a mixture of salts, whereas, under voltage conditions, struvite was obtained. The precipitate analysis was carried out through powder X-ray diffraction and FTIR. On analysis of magnesium values, it was observed that increased voltage increased magnesium values on the feed side, i.e., increasing voltage increases the reverse salt flux. The charge on the membrane surface also increases the concentration of magnesium ions near the membrane surface, leading to an increase in water flux.

Chapter 4 examines the enhancement of eFO efficiency when combined with the membrane distillation process. The system consists of a heated draw solution reservoir that is supplied to the eFO and the membrane distillation system. The flux value for the eFO dropped due to the changes in the membrane structural parameters due to excess heat of the draw solution but overtime the water flux was maintained due to draw reconcentration. The precipitates formed were identified as magnesium phosphate due to the higher temperature of the feed solution.

Chapter 5 offers a perspective on combining microbial electrolysis cells with eFO and the membrane distillation process. It details the engineering challenges and issues with

long-term MEC coupling with EFO. It also outlines the challenges and requirements for combining all these technologies.

Treatment of livestock-based wastewater is not efficient through conventional wastewater treatment methods. However, applying an electric field in combination with membrane treatment was shown to be effective in recovering nutrients and wastewater treatment. In this research, conductive ultrafiltration, eFO, and eFO -MD systems with the ability to precipitate nutrients and treat wastewater were discussed and presented.

Overall, voltage application was observed to be favorable for struvite precipitation and water treatment. The conductive ultrafiltration membranes highlighted the need for high voltage to overcome phosphate buffering capacity in wastewater. It further consolidates the idea of proper membrane cleanup in order to maintain the precipitate recovery rates. The electricity-assisted forward osmosis helped in removing the dependence on pressure. It was further made efficient by coupling with a membrane distillation system which stabilized the water flux obtained over time.

Though applying electricity and combining different treatment strategies looked positive, challenges still need to be considered to understand these processes better. First and foremost, additional systems could help trap the precipitates and provide a better collection methodology. Though favorable for struvite production, eFO processes saw extensive struvite deposition on the tubing, potentially reducing the total yield and quality. Potentially combining conductive UF with forward osmosis processes could alleviate these issues, but that remains to be investigated.

Secondly, Further investigation is needed on the behavior of magnesium ions during the process. Though we could detect high amounts of dissolved magnesium in the

feed side, it is still unclear how much takes part in the struvite precipitation process and how the application of electricity and, later on, heat impact the kinetics of these ions. A better understanding would be vital for mathematical modeling and predictive analysis of these processes to scale up in the future.

Lastly, developing advanced FO and MD membranes could be the answer to better energy utilization and increasing efficiency. For example, highly conductive materials like N-doped CNTs, MXene, etc., could be studied for eFO treatment processes. In addition, photothermal coatings and MD systems materials could be studied to decrease energy needs and temperature polarization.

## REFERENCES

- Adham, S., Hussain, A., Matar, J.M., Dores, R., Janson, A., 2013. Application of Membrane Distillation for desalting brines from thermal desalination plants. *Desalination* 314, 101–108. <https://doi.org/10.1016/j.desal.2013.01.003>
- Adham, S., Hussain, A., Minier-Matar, J., Janson, A., Sharma, R., 2018. Membrane applications and opportunities for water management in the oil & gas industry. *Desalination* 440, 2–17. <https://doi.org/10.1016/j.desal.2018.01.030>
- Ahn, Y.T., Hwang, Y.H., Shin, H.S., 2011. Application of PTFE membrane for ammonia removal in a membrane contactor. *Water Sci. Technol.* 63, 2944–2948. <https://doi.org/10.2166/wst.2011.141>
- Ajayi, F.F., Kim, K.-Y., Chae, K.-J., Choi, M.-J., Kim, I.S., 2010. Effect of hydrodynamic force and prolonged oxygen exposure on the performance of anodic biofilm in microbial electrolysis cells. *Int. J. Hydrogen Energy* 35, 3206–3213. <https://doi.org/https://doi.org/10.1016/j.ijhydene.2010.01.057>
- Akther, N., Sodiq, A., Giwa, A., Daer, S., Arafat, H.A., Hasan, S.W., 2015. Recent advancements in forward osmosis desalination: A review. *Chem. Eng. J.* 281, 502–522. <https://doi.org/10.1016/j.cej.2015.05.080>
- Al-Furaiji, M., Benes, N., Nijmeijer, A., McCutcheon, J.R., 2019. Use of a Forward Osmosis–Membrane Distillation Integrated Process in the Treatment of High-Salinity Oily Wastewater. *Ind. Eng. Chem. Res.* 58, 956–962. <https://doi.org/10.1021/acs.iecr.8b04875>

- Al-Obaidani, S., Curcio, E., Macedonio, F., Di Profio, G., Al-Hinai, H., Drioli, E., 2008. Potential of membrane distillation in seawater desalination: Thermal efficiency, sensitivity study and cost estimation. *J. Memb. Sci.* 323, 85–98. <https://doi.org/10.1016/j.memsci.2008.06.006>
- Ali, M.I., Schneider, P.A., Hudson, N., 2005. Thermodynamics and solution chemistry of struvite. *J. Indian Inst. Sci.* 85, 141–149.
- Alkhudhiri, A., Darwish, N., Hilal, N., 2012. Membrane distillation: A comprehensive review. *Desalination*. <https://doi.org/10.1016/j.desal.2011.08.027>
- Alklaibi, A.M., Lior, N., 2005. Membrane-distillation desalination: Status and potential. *Desalination* 171, 111–131. <https://doi.org/10.1016/j.desal.2004.03.024>
- Anvari, A., Azimi, A., Kekre, K.M., Ronen, A., 2020a. State-of-the-art methods for overcoming temperature polarization in membrane distillation process : A review. *J. Memb. Sci.* 616, 118413. <https://doi.org/10.1016/j.memsci.2020.118413>
- Anvari, A., Kekre, K.M., Azimi Yancheshme, A., Yao, Y., Ronen, A., 2019. Membrane distillation of high salinity water by induction heated thermally conducting membranes. *J. Memb. Sci.* 589. <https://doi.org/10.1016/j.memsci.2019.117253>
- Anvari, A., Kekre, K.M., Ronen, A., 2020b. Scaling mitigation in radio-frequency induction heated membrane distillation. *J. Memb. Sci.* 600. <https://doi.org/10.1016/j.memsci.2020.117859>
- Apollon, W., Rusyn, I., González-Gamboa, N., Kuleshova, T., Luna-Maldonado, A.I., Vidales-Contreras, J.A., Kamaraj, S.-K., 2022. Improvement of zero waste

sustainable recovery using microbial energy generation systems: A comprehensive review. *Sci. Total Environ.* 817, 153055.

<https://doi.org/https://doi.org/10.1016/j.scitotenv.2022.153055>

Auinger, M., Katsounaros, I., Meier, J.C., Klemm, S.O., Biedermann, P.U., Topalov, A.A., Rohwerder, M., Mayrhofer, K.J.J., 2011. Near-surface ion distribution and buffer effects during electrochemical reactions. *Phys. Chem. Chem. Phys.* 13, 16384–16394. <https://doi.org/10.1039/c1cp21717h>

Badia-Fabregat, M., Rago, L., Baeza, J.A., Guisasola, A., 2019. Hydrogen production from crude glycerol in an alkaline microbial electrolysis cell. *Int. J. Hydrogen Energy* 44, 17204–17213. <https://doi.org/10.1016/j.ijhydene.2019.03.193>

Ben Moussa, S., Maurin, G., Gabrielli, C., Ben Amor, M., 2006. Electrochemical precipitation of struvite. *Electrochem. Solid-State Lett.* 9, C97. <https://doi.org/10.1149/1.2189222>

Ben Moussa, S., Tlili, M.M., Batis, N., Amor, M. Ben, 2011. Influence of temperature on Struvite precipitation by CO<sub>2</sub>-deagassing method. *Cryst. Res. Technol.* 46, 255–260. <https://doi.org/10.1002/crat.201000571>

Bhadra, M., Roy, S., Mitra, S., 2014. Nanodiamond immobilized membranes for enhanced desalination via membrane distillation. *Desalination* 341, 115–119. <https://doi.org/10.1016/j.desal.2014.02.036>

Borole, A.P., O'Neill, H., Tsouris, C., Cesar, S., 2008. A microbial fuel cell operating at low pH using the acidophile *Acidiphilium cryptum*. *Biotechnol. Lett.* 30, 1367–1372. <https://doi.org/10.1007/s10529-008-9700-y>

- Bruce E. Logan, Bert Hamelers, René Rozendal, Uwe Shroder, Jurg Keller, Stefano Freguia, Peter Aelterman, W.V. and K.R., 2006. Critical Review Microbial Fuel Cells : Methodology and Technology. *Environ. Sci. Technol.* 40, 5181–5192.
- Burkholder, J.M., Shumway, S.E., Glibert, P.M., 2018. Food Web and Ecosystem Impacts of Harmful Algae. *Harmful Algal Bloom.*, Wiley Online Books.  
<https://doi.org/https://doi.org/10.1002/9781118994672.ch7>
- Bush, J.A., Vanneste, J., Cath, T.Y., 2016. Membrane distillation for concentration of hypersaline brines from the Great Salt Lake: Effects of scaling and fouling on performance, efficiency, and salt rejection. *Sep. Purif. Technol.* 170, 78–91.  
<https://doi.org/10.1016/j.seppur.2016.06.028>
- Cath, T.Y., Adams, V.D., Childress, A.E., 2004. Experimental study of desalination using direct contact membrane distillation: A new approach to flux enhancement. *J. Memb. Sci.* 228, 5–16. <https://doi.org/10.1016/j.memsci.2003.09.006>
- Cath, T.Y., Childress, A.E., Elimelech, M., 2006. Forward osmosis : Principles , applications , and recent developments 281, 70–87.  
<https://doi.org/10.1016/j.memsci.2006.05.048>
- Cath, T.Y., Elimelech, M., McCutcheon, J.R., McGinnis, R.L., Achilli, A., Anastasio, D., Brady, A.R., Childress, A.E., Farr, I. V., Hancock, N.T., Lampi, J., Nghiem, L.D., Xie, M., Yip, N.Y., 2013. Standard Methodology for Evaluating Membrane Performance in Osmotically Driven Membrane Processes. *Desalination* 312, 31–38.  
<https://doi.org/10.1016/j.desal.2012.07.005>
- Ch Bouropoulos, N., Koutsoukos, P.G., Schieber, M., 2000. Spontaneous precipitation of

- struvite from aqueous solutions. *J. Cryst. Growth* 213, 381–388.  
[https://doi.org/10.1016/S0022-0248\(00\)00351-1](https://doi.org/10.1016/S0022-0248(00)00351-1)
- Chen, C., Hu, J., Shao, D., Li, J., Wang, X., 2009. Adsorption behavior of multiwall carbon nanotube/iron oxide magnetic composites for Ni(II) and Sr(II). *J. Hazard. Mater.* 164, 923–928. <https://doi.org/10.1016/j.jhazmat.2008.08.089>
- Chen, W., Gu, Z., Ran, G., Li, Q., 2021. Application of membrane separation technology in the treatment of leachate in China: A review. *Waste Manag.* 121, 127–140.  
<https://doi.org/10.1016/j.wasman.2020.12.002>
- Chen, X., Zhou, H., Zuo, K., Zhou, Y., Wang, Q., Sun, D., Gao, Y., 2017. Self-sustaining advanced wastewater purification and simultaneous in situ nutrient recovery in a novel bioelectrochemical system. *Chem. Eng. J.* 330, 692–697.  
<https://doi.org/10.1016/j.cej.2017.07.130>
- Cheng, K.Y., Kaksonen, A.H., Cord-Ruwisch, R., 2013. Ammonia recycling enables sustainable operation of bioelectrochemical systems. *Bioresour. Technol.* 143, 25–31. <https://doi.org/10.1016/j.biortech.2013.05.108>
- Childers, D.L., Corman, J., Edwards, M., Elser, J.J., 2011. Sustainability Challenges of Phosphorus and Food: Solutions from Closing the Human Phosphorus Cycle. *Bioscience* 61, 117–124. <https://doi.org/10.1525/bio.2011.61.2.6>
- Clark, C.M., Bell, M.D., Boyd, J.W., Compton, J.E., Davidson, E.A., Davis, C., Fenn, M.E., Geiser, L., Jones, L., Blett, T.F., 2017. Nitrogen-induced terrestrial eutrophication: Cascading effects and impacts on ecosystem services. *Ecosphere* 8. <https://doi.org/10.1002/ecs2.1877>

- Cordell, D., White, S., 2013. Sustainable Phosphorus Measures: Strategies and Technologies for Achieving Phosphorus Security. *Agronomy* 3, 86–116.  
<https://doi.org/10.3390/agronomy3010086>
- Cruz-Tato, P., Rivera-Fuentes, N., Flynn, M., Nicolau, E., 2019. Anti-Fouling Electroconductive Forward Osmosis Membranes: Electrochemical and Chemical Properties. *ACS Appl. Polym. Mater.* 1, 1061–1070.  
<https://doi.org/10.1021/acsapm.9b00087>
- Curcio, E., Drioli, E., 2005. Membrane distillation and related operations - A review. *Sep. Purif. Rev.* <https://doi.org/10.1081/SPM-200054951>
- Cusick, R.D., Ullery, M.L., Dempsey, B.A., Logan, B.E., 2014. Electrochemical struvite precipitation from digestate with a fluidized bed cathode microbial electrolysis cell. *Water Res.* 54, 297–306. <https://doi.org/10.1016/j.watres.2014.01.051>
- Dadrasnia, A., de Bona Muñoz, I., Yáñez, E.H., Lamkaddam, I.U., Mora, M., Ponsá, S., Ahmed, M., Argelaguet, L.L., Williams, P.M., Oatley-Radcliffe, D.L., 2021. Sustainable nutrient recovery from animal manure: A review of current best practice technology and the potential for freeze concentration. *J. Clean. Prod.* 315.  
<https://doi.org/10.1016/j.jclepro.2021.128106>
- Damiano, L., Jambeck, J.R., Ringelberg, D.B., 2014. Municipal Solid Waste Landfill Leachate Treatment and Electricity Production Using Microbial Fuel Cells 472–485.  
<https://doi.org/10.1007/s12010-014-0854-x>
- De Lannoy, C.F., Jassby, D., Gloe, K., Gordon, A.D., Wiesner, M.R., 2013. Aquatic biofouling prevention by electrically charged nanocomposite polymer thin film

membranes. *Environ. Sci. Technol.* 47, 2760–2768.

<https://doi.org/10.1021/es3045168>

De Paepe, J., De Pryck, L., Verliefde, A.R.D., Rabaey, K., Clauwaert, P., 2020.

Electrochemically Induced Precipitation Enables Fresh Urine Stabilization and Facilitates Source Separation. *Environ. Sci. Technol.*

<https://doi.org/10.1021/acs.est.9b06804>

Deshmukh, A., Boo, C., Karanikola, V., Lin, S., Straub, A.P., Tong, T., Warsinger, D.M.,

Elimelech, M., 2018. Membrane distillation at the water-energy nexus: Limits, opportunities, and challenges. *Energy Environ. Sci.*

<https://doi.org/10.1039/c8ee00291f>

Ding, A., Yang, Y., Sun, G., Wu, D., 2015. Impact of applied voltage on methane generation and microbial activities in an anaerobic microbial electrolysis cell

(MEC). *Chem. Eng. J.* 283, 260–265. <https://doi.org/10.1016/j.cej.2015.07.054>

Doyle, J.D., Oldring, K., Churchley, J., Parsons, S.A., 2002. Struvite formation and the fouling propensity of different materials. *Water Res.* 36, 3971–3978.

[https://doi.org/10.1016/S0043-1354\(02\)00127-6](https://doi.org/10.1016/S0043-1354(02)00127-6)

Driver, J., Lijmbach, D., Steen, I., 2010. Why Recover Phosphorus for Recycling, and

How? *Environ. Technol.* 20, 651–662. <https://doi.org/10.1080/09593332008616861>

Duan, W., Chen, G., Chen, C., Sanghvi, R., Iddya, A., Walker, S., Liu, H., Ronen, A.,

Jassby, D., 2017a. Electrochemical removal of hexavalent chromium using electrically conducting carbon nanotube/polymer composite ultrafiltration

membranes. *J. Memb. Sci.* 531, 160–171.

<https://doi.org/10.1016/j.memsci.2017.02.050>

Duan, W., Chen, G., Chen, C., Sanghvi, R., Iddya, A., Walker, S., Liu, H., Ronen, A., Jassby, D., 2017b. Electrochemical removal of hexavalent chromium using electrically conducting carbon nanotube/polymer composite ultrafiltration membranes. *J. Memb. Sci.* 531, 160–171.

<https://doi.org/10.1016/j.memsci.2017.02.050>

Duan, W., Dudchenko, A., Mende, E., Flyer, C., Zhu, X., Jassby, D., 2014a.

Electrochemical mineral scale prevention and removal on electrically conducting carbon nanotube-polyamide reverse osmosis membranes. *Environ. Sci. Process. Impacts* 16, 1300–1308. <https://doi.org/10.1039/c3em00635b>

Duan, W., Dudchenko, A., Mende, E., Flyer, C., Zhu, X., Jassby, D., 2014b.

Electrochemical mineral scale prevention and removal on electrically conducting carbon nanotube-polyamide reverse osmosis membranes. *Environ. Sci. Process. Impacts* 16, 1300–1308. <https://doi.org/10.1039/c3em00635b>

Duan, W., Ronen, A., Chen, G., Chen, C., Sanghvi, R., Walker, S., Liu, H., Jassby, D., 2017c. In-Situ Hexavalent Chromium Removal via Composite Carbon Nanotubes Electrically Conductive Ultrafiltration Membranes. *preparation Environ. Sci. Technol.*

Duan, W., Ronen, A., Walker, S., Jassby, D., 2016. Polyaniline-Coated Carbon Nanotube Ultrafiltration Membranes: Enhanced Anodic Stability for in Situ Cleaning and Electro-Oxidation Processes. *ACS Appl. Mater. Interfaces* 8, 22574–22584.

<https://doi.org/10.1021/acsami.6b07196>

- Dudchenko, A. V., Rolf, J., Russell, K., Duan, W., Jassby, D., 2014. Organic fouling inhibition on electrically conducting carbon nanotube-polyvinyl alcohol composite ultrafiltration membranes. *J. Memb. Sci.* 468, 1–10.  
<https://doi.org/10.1016/j.memsci.2014.05.041>
- El-Abbassi, A., Hafidi, A., García-Payo, M.C., Khayet, M., 2009. Concentration of olive mill wastewater by membrane distillation for polyphenols recovery. *Desalination* 245, 670–674. <https://doi.org/https://doi.org/10.1016/j.desal.2009.02.035>
- El-Bourawi, M.S., Ding, Z., Ma, R., Khayet, M., 2006. A framework for better understanding membrane distillation separation process. *J. Memb. Sci.*  
<https://doi.org/10.1016/j.memsci.2006.08.002>
- Feng, L., Xie, L., Suo, G., Shao, X., Dong, T., 2018. Influence of Temperature on the Performance of Forward Osmosis Using Ammonium Bicarbonate as Draw Solute. *Trans. Tianjin Univ.* 24, 571–579. <https://doi.org/10.1007/s12209-018-0159-1>
- Fischer, F., Bastian, C., Happe, M., Mabillard, E., Schmidt, N., 2011. Microbial fuel cell enables phosphate recovery from digested sewage sludge as struvite. *Bioresour. Technol.* 102, 5824–5830.  
<https://doi.org/https://doi.org/10.1016/j.biortech.2011.02.089>
- Gao, F., Wang, L., Wang, J., Zhang, H., Lin, S., 2020. Nutrient recovery from treated wastewater by a hybrid electrochemical sequence integrating bipolar membrane electrodialysis and membrane capacitive deionization. *Environ. Sci. Water Res. Technol.* 6, 383–391. <https://doi.org/10.1039/c9ew00981g>
- Gao, G., Vecitis, C.D., 2012. Reactive depth and performance of an electrochemical

- carbon nanotube network as a function of mass transport. *ACS Appl. Mater. Interfaces* 4, 6096–6103. <https://doi.org/10.1021/am301724n>
- Ge, Q., Ling, M., Chung, T.S., 2013. Draw solutions for forward osmosis processes: Developments, challenges, and prospects for the future. *J. Memb. Sci.* 442, 225–237. <https://doi.org/10.1016/j.memsci.2013.03.046>
- Gerardo, M.L., Aljohani, N.H.M., Oatley-Radcliffe, D.L., Lovitt, R.W., 2015. Moving towards sustainable resources: Recovery and fractionation of nutrients from dairy manure digestate using membranes. *Water Res.* 80, 80–89. <https://doi.org/10.1016/j.watres.2015.05.016>
- Gerardo, M.L., Zacharof, M.P., Lovitt, R.W., 2013. Strategies for the recovery of nutrients and metals from anaerobically digested dairy farm sludge using cross-flow microfiltration. *Water Res.* 47, 4833–4842. <https://doi.org/10.1016/j.watres.2013.04.019>
- Ghaffour, N., Missimer, T.M., Amy, G.L., 2013. Technical review and evaluation of the economics of water desalination: Current and future challenges for better water supply sustainability. *Desalination* 309, 197–207. <https://doi.org/10.1016/j.desal.2012.10.015>
- Ghasemi, M., Shahgaldi, S., Ismail, M., Yaakob, Z., Daud, W.R.W., 2012. New generation of carbon nanocomposite proton exchange membranes in microbial fuel cell systems. *Chem. Eng. J.* 184, 82–89. <https://doi.org/https://doi.org/10.1016/j.cej.2012.01.001>
- Giwa, A., Dufour, V., Al Marzooqi, F., Al Kaabi, M., Hasan, S.W., 2017. Brine

management methods: Recent innovations and current status. *Desalination*.

<https://doi.org/10.1016/j.desal.2016.12.008>

Glibert, P.M., Maranger, R., Sobota, D.J., Bouwman, L., 2014. The Haber Bosch-harmful algal bloom (HB-HAB) link. *Environ. Res. Lett.* 9. <https://doi.org/10.1088/1748-9326/9/10/105001>

Gong, H., Wang, Z., Zhang, X., Jin, Z., Wang, C., Zhang, L., Wang, K., 2017. Organics and nitrogen recovery from sewage via membrane-based pre-concentration combined with ion exchange process. *Chem. Eng. J.* 311, 13–19.

<https://doi.org/10.1016/j.cej.2016.11.068>

González, C., García, P.A., Muñoz, R., 2009. Effect of feed characteristics on the organic matter, nitrogen and phosphorus removal in an activated sludge system treating piggery slurry. *Water Sci. Technol.* 60, 2145–2152.

<https://doi.org/10.2166/wst.2009.579>

Guignard, M.S., Leitch, A.R., Acquisti, C., Eizaguirre, C., Elser, J.J., Hessen, D.O., Jeyasingh, P.D., Neiman, M., Richardson, A.E., Soltis, P.S., Soltis, D.E., Stevens, C.J., Trimmer, M., Weider, L.J., Woodward, G., Leitch, I.J., 2017. Impacts of nitrogen and phosphorus: From genomes to natural ecosystems and agriculture.

*Front. Ecol. Evol.* 5. <https://doi.org/10.3389/fevo.2017.00070>

Hanhoun, M., Montastruc, L., Azzaro-Pantel, C., Biscans, B., Frèche, M., Pibouleau, L., 2013. Simultaneous determination of nucleation and crystal growth kinetics of struvite using a thermodynamic modeling approach. *Chem. Eng. J.* 215–216, 903–

912. <https://doi.org/10.1016/j.cej.2012.10.038>

- Hao, X.D., Wang, C.C., Lan, L., Van Loosdrecht, M.C.M., 2008. Struvite formation, analytical methods and effects of pH and Ca<sup>2+</sup>. *Water Sci. Technol.* 58, 1687–1692. <https://doi.org/10.2166/wst.2008.557>
- Hari, A.R., Venkidusamy, K., Katuri, K.P., Bagchi, S., Saikaly, P.E., 2017. Temporal microbial community dynamics in microbial electrolysis cells - Influence of acetate and propionate concentration. *Front. Microbiol.* 8, 1–14. <https://doi.org/10.3389/fmicb.2017.01371>
- Harrison, M.L.L., Johns, M.L.R., White, E.D.T., Mehta, C.G.M., 2011. Growth rate kinetics for struvite crystallisation, in: *Chemical Engineering Transactions*. pp. 309–314. <https://doi.org/10.3303/CET1125052>
- Hasan, R., 2014. Bioremediation of Swine Wastewater and Biofuel Potential by using *Chlorella vulgaris*, *Chlamydomonas reinhardtii*, and *Chlamydomonas debaryana*. *J. Pet. Environ. Biotechnol.* 05, 3–7. <https://doi.org/10.4172/2157-7463.1000175>
- Heffer, P., Prud'homme, M., 2014. Fertilizer Outlook 2014-2018. 82nd IFA Annu. Conf. Sydney 1–7.
- Helder, M., Strik, D.P.B.T.B., Timmers, R.A., Raes, S.M.T., Hamelers, H.V.M., Buisman, C.J.N., 2013. Resilience of roof-top Plant-Microbial Fuel Cells during Dutch winter. *Biomass and Bioenergy* 51, 1–7. <https://doi.org/https://doi.org/10.1016/j.biombioe.2012.10.011>
- Herald, E., Rahmawati, F., Heriyanto, Putra, D.P., 2017. Preparation of struvite from desalination waste. *J. Environ. Chem. Eng.* 5, 1666–1675. <https://doi.org/10.1016/j.jece.2017.03.005>

- Hirooka, K., Ichihashi, O., 2013. Phosphorus recovery from artificial wastewater by microbial fuel cell and its effect on power generation. *Bioresour. Technol.* 137, 368–375. [https://doi.org/https://doi.org/10.1016/j.biortech.2013.03.067](https://doi.org/10.1016/j.biortech.2013.03.067)
- Holloway, R.W., Childress, A.E., Dennett, K.E., Cath, T.Y., 2007. Forward osmosis for concentration of anaerobic digester centrate. *Water Res.* 41, 4005–4014. <https://doi.org/10.1016/j.watres.2007.05.054>
- Hooda, P.S., Edwards, A.C., Anderson, H.A., Miller, A., 2000. A review of water quality concerns in livestock farming areas. *Sci. Total Environ.* 250, 143–167. [https://doi.org/10.1016/S0048-9697\(00\)00373-9](https://doi.org/10.1016/S0048-9697(00)00373-9)
- Hou, D., Iddya, A., Chen, X., Wang, M., Zhang, W., Ding, Y., Jassby, D., Ren, Z.J., 2018. Nickel-Based Membrane Electrodes Enable High-Rate Electrochemical Ammonia Recovery. *Environ. Sci. Technol.* 52, 8930–8938. <https://doi.org/10.1021/acs.est.8b01349>
- Ichihashi, O., Hirooka, K., 2012. Removal and recovery of phosphorus as struvite from swine wastewater using microbial fuel cell. *Bioresour. Technol.* 114, 303–307. <https://doi.org/10.1016/j.biortech.2012.02.124>
- Ichihashi, O., Hirooka, K., 2012. Removal and recovery of phosphorus as struvite from swine wastewater using microbial fuel cell. *Bioresour. Technol.* 114, 303–307. <https://doi.org/10.1016/j.biortech.2012.02.124>
- Jadhav, D.A., Das, I., Ghangrekar, M.M., Pant, D., 2020. Moving towards practical applications of microbial fuel cells for sanitation and resource recovery. *J. Water Process Eng.* 38, 101566. [https://doi.org/https://doi.org/10.1016/j.jwpe.2020.101566](https://doi.org/10.1016/j.jwpe.2020.101566)

- Jaffer, Y., Clark, T.A., Pearce, P., Parsons, S.A., 2002. Potential phosphorus recovery by struvite formation. *Water Res.* 36, 1834–1842. [https://doi.org/10.1016/S0043-1354\(01\)00391-8](https://doi.org/10.1016/S0043-1354(01)00391-8)
- Jamaly, S., Darwish, N.N., Ahmed, I., Hasan, S.W., 2014. A short review on reverse osmosis pretreatment technologies. *Desalination*.  
<https://doi.org/10.1016/j.desal.2014.09.017>
- Jardin, N., Pöpel, H.J., 2001. Refixation of phosphates released during bio-p sludge handling as struvite or aluminium phosphate. *Environ. Technol. (United Kingdom)* 22, 1253–1262. <https://doi.org/10.1080/09593332208618193>
- Jevons, K., Awe, M., 2010. Economic benefits of membrane technology vs. evaporator. *Desalination* 250, 961–963. <https://doi.org/10.1016/j.desal.2009.09.081>
- Johnston A.E., Richards, I.R., 2003. Effectiveness of different precipitated phosphates as phosphorus sources for plants. *Soil Use Manag.* 19, 45–49.  
<https://doi.org/10.1079/sum2002162>
- Kabdaşlı, I., Parsons, S. a, Tunay, O., 2006. Effect of major ions on induction time of struvite precipitation. *Croat. Chem. Acta* 79, 243–251.
- Kaspersen, B.S., Christensen, T.B., Fredenslund, A.M., Møller, H.B., Butts, M.B., Jensen, N.H., Kjaer, T., 2016. Linking climate change mitigation and coastal eutrophication management through biogas technology: Evidence from a new Danish bioenergy concept. *Sci. Total Environ.* 541, 1124–1131.  
<https://doi.org/10.1016/j.scitotenv.2015.10.015>

- Katsounaros, I., Meier, J.C., Klemm, S.O., Topalov, A.A., Biedermann, P.U., Auinger, M., Mayrhofer, K.J.J., 2011. The effective surface pH during reactions at the solid-liquid interface. *Electrochem. commun.* 13, 634–637.  
<https://doi.org/10.1016/j.elecom.2011.03.032>
- Katz, I., Dosoretz, C.G., 2008. Desalination of domestic wastewater effluents: phosphate removal as pretreatment. *Desalination* 222, 230–242.  
<https://doi.org/10.1016/j.desal.2007.01.160>
- Kekre, K.M., Anvari, A., Kahn, K., Yao, Y., Ronen, A., 2021. Reactive electrically conducting membranes for phosphorus recovery from livestock wastewater effluents. *J. Environ. Manage.* 282, 111432.  
<https://doi.org/10.1016/j.jenvman.2020.111432>
- Kelly, Patrick T., He, Z., 2014. Nutrients removal and recovery in bioelectrochemical systems: A review. *Bioresour. Technol.* 153, 351–360.  
<https://doi.org/10.1016/j.biortech.2013.12.046>
- Kelly, Patrick T, He, Z., 2014. Nutrients removal and recovery in bioelectrochemical systems: A review. *Bioresour. Technol.* 153, 351–360.  
<https://doi.org/https://doi.org/10.1016/j.biortech.2013.12.046>
- Kelting, D.L., Laxson, C.L., Smiths, P., 2010. Review of Effects and Costs of Road De-icing with Recommendations for Winter Road Management in the Adirondack Park.
- Kim, A.H., Chan, D., Yu, A.C., Abbadi, H. El, Lu, K., 2021. More than a fertilizer: wastewater-derived struvite as a high value, sustainable fire retardant. *Green Chem.* 23, 4510–4523. <https://doi.org/10.1039/d1gc00826a>

- Kim, B.U., Kwon, J.H., 2010. Treatment of High-Concentration Swine Wastewater By Anaerobic Digestion and an Aquatic Plant System. *Environ. Eng. Res.* 11, 134–142.  
<https://doi.org/10.4491/eer.2006.11.3.134>
- Kimura, K., Amy, G., Drewes, J.E., Heberer, T., Kim, T.U., Watanabe, Y., 2003. Rejection of organic micropollutants (disinfection by-products, endocrine disrupting compounds, and pharmaceutically active compounds) by NF/RO membranes. *J. Memb. Sci.* 227, 113–121. <https://doi.org/10.1016/j.memsci.2003.09.005>
- Kozik, A., Hutnik, N., Piotrowski, K., Mazienczuk, A., Matynia, A., 2013. Precipitation and Crystallization of Struvite from Synthetic Wastewater under Stoichiometric Conditions. *Adv. Chem. Eng. Sci.* 03, 20–26.  
<https://doi.org/10.4236/aces.2013.34b004>
- Kuntke, P., Geleji, M., Bruning, H., Zeeman, G., Hamelers, H.V.M., Buisman, C.J.N., 2011. Effects of ammonium concentration and charge exchange on ammonium recovery from high strength wastewater using a microbial fuel cell. *Bioresour. Technol.* 102, 4376–4382.  
<https://doi.org/https://doi.org/10.1016/j.biortech.2010.12.085>
- Lawson, K.W., Lloyd, D.R., 1997. Membrane distillation. *J. Memb. Sci.*  
[https://doi.org/10.1016/S0376-7388\(96\)00236-0](https://doi.org/10.1016/S0376-7388(96)00236-0)
- Le Corre, K.S., Valsami-Jones, E., Hobbs, P., Parsons, S. a., 2009. Phosphorus Recovery from Wastewater by Struvite Crystallization: A Review, *Critical Reviews in Environmental Science and Technology.*  
<https://doi.org/10.1080/10643380701640573>

- Le Corre, K.S., Valsami-Jones, E., Hobbs, P., Parsons, S.A., 2005. Impact of calcium on struvite crystal size, shape and purity. *J. Cryst. Growth* 283, 514–522.  
<https://doi.org/10.1016/j.jcrysgro.2005.06.012>
- Leaper, S., Abdel-Karim, A., Gad-Allah, T.A., Gorgojo, P., 2019. Air-gap membrane distillation as a one-step process for textile wastewater treatment. *Chem. Eng. J.* 360, 1330–1340. <https://doi.org/https://doi.org/10.1016/j.cej.2018.10.209>
- Lee, S., Boo, C., Elimelech, M., Hong, S., 2010. Comparison of fouling behavior in forward osmosis (FO) and reverse osmosis (RO). *J. Memb. Sci.* 365, 34–39.  
<https://doi.org/10.1016/j.memsci.2010.08.036>
- Lee, W.J., Ng, Z.C., Hubadillah, S.K., Goh, P.S., Lau, W.J., Othman, M.H.D., Ismail, A.F., Hilal, N., 2020. Fouling mitigation in forward osmosis and membrane distillation for desalination. *Desalination*.  
<https://doi.org/10.1016/j.desal.2020.114338>
- Leong, J.X., Daud, W.R.W., Ghasemi, M., Liew, K. Ben, Ismail, M., 2013. Ion exchange membranes as separators in microbial fuel cells for bioenergy conversion: A comprehensive review. *Renew. Sustain. Energy Rev.* 28, 575–587.  
<https://doi.org/https://doi.org/10.1016/j.rser.2013.08.052>
- Lesnik, K.L., Cai, W., Liu, H., 2020. Microbial Community Predicts Functional Stability of Microbial Fuel Cells. *Environ. Sci. Technol.* 54, 427–436.  
<https://doi.org/10.1021/acs.est.9b03667>
- Li, K., Liu, Q., Fang, F., Luo, R., Lu, Q., Zhou, W., Huo, S., Cheng, P., Liu, J., Addy, M., Chen, P., Chen, D., Ruan, R., 2019. *Bioresource Technology* Microalgae-based

- wastewater treatment for nutrients recovery : A review. *Bioresour. Technol.* 291, 121934. <https://doi.org/10.1016/j.biortech.2019.121934>
- Li, X.-M., Zhao, B., Wang, Z., Xie, M., Song, J., Nghiem, L.D., He, T., Yang, C., Li, C., Chen, G., 2014. Water reclamation from shale gas drilling flow-back fluid using a novel forward osmosis–vacuum membrane distillation hybrid system. *Water Sci. Technol.* 69, 1036–1044. <https://doi.org/10.2166/wst.2014.003>
- Liu, X., Wu, J., Hou, L. an, Wang, J., 2019. Removal of Co, Sr and Cs ions from simulated radioactive wastewater by forward osmosis. *Chemosphere* 232, 87–95. <https://doi.org/10.1016/j.chemosphere.2019.05.210>
- Logan, B.E., Call, D., Cheng, S., Hamelers, H.V.M., Sleutels, T.H.J.A., Jeremiase, A.W., Rozendal, R.A., 2008. Microbial Electrolysis Cells for High Yield Hydrogen Gas Production from Organic Matter. *Environ. Sci. Technol.* 42, 8630–8640. <https://doi.org/10.1021/es801553z>
- Logan, B.E., Hamelers, B., Rozendal, R., Schröder, U., Keller, J., Freguia, S., Aelterman, P., Verstraete, W., Rabaey, K., 2006. Microbial Fuel Cells: Methodology and Technology. *Environ. Sci. Technol.* 40, 5181–5192. <https://doi.org/10.1021/es0605016>
- López-García, J.J., Horno, J., Grosse, C., 2011. Poisson-Boltzmann description of the electrical double layer including ion size effects. *Langmuir* 27, 13970–13974. <https://doi.org/10.1021/la2025445>
- Lovley, D.R., Holmes, D.E., Nevin, K.P., 2004. Dissimilatory Fe(III) and Mn(IV) Reduction, in: *Advances in Microbial Physiology*. Academic Press, pp. 219–286.

[https://doi.org/https://doi.org/10.1016/S0065-2911\(04\)49005-5](https://doi.org/https://doi.org/10.1016/S0065-2911(04)49005-5)

- Lu, Y., Qin, M., Yuan, H., Abu-Reesh, I.M., He, Z., 2015. When bioelectrochemical systems meet forward osmosis: Accomplishing wastewater treatment and reuse through synergy. *Water (Switzerland)* 7, 38–50. <https://doi.org/10.3390/w7010038>
- Luft, J.R., Wolfley, J.R., Snell, E.H., 2011. What's in a drop? Correlating observations and outcomes to guide macromolecular crystallization experiments. *Cryst. Growth Des.* 11, 651–663. <https://doi.org/10.1021/cg1013945>
- Luo, Y., Li, H., Huang, Y.R., Zhao, T.L., Yao, Q.Z., Fu, S.Q., Zhou, G.T., 2018. Bacterial mineralization of struvite using MgO as magnesium source and its potential for nutrient recovery. *Chem. Eng. J.* 351, 195–202. <https://doi.org/10.1016/j.cej.2018.06.106>
- Lutchmiah, K., Verliefde, A.R.D., Roest, K., Rietveld, L.C., Cornelissen, E.R., 2014. Forward osmosis for application in wastewater treatment: A review. *Water Res.* 58, 179–197. <https://doi.org/10.1016/j.watres.2014.03.045>
- Malekmohammadi, S., Mirbagheri, S.A., 2021. A review of the operating parameters on the microbial fuel cell for wastewater treatment and electricity generation. *Water Sci. Technol.* 84, 1309–1323. <https://doi.org/10.2166/wst.2021.333>
- Marcus, A.K., Torres, C.I., Rittmann, B.E., 2011. Analysis of a microbial electrochemical cell using the proton condition in biofilm (PCBIOFILM) model. *Bioresour. Technol.* 102, 253–262. <https://doi.org/https://doi.org/10.1016/j.biortech.2010.03.100>
- Matynia, A., Koralewska, J., Wierzbowska, B., Piotrowski, K., 2006. The Influence of

- Process Parameters on Struvite Continuous Crystallization Kinetics. *Chem. Eng. Commun.* 6445, 37–41. <https://doi.org/10.1080/009864490949008>
- Metson, G.S., MacDonald, G.K., Haberman, D., Nesme, T., Bennett, E.M., 2016. Feeding the Corn Belt: Opportunities for phosphorus recycling in U.S. agriculture. *Sci. Total Environ.* 542, 1117–1126. <https://doi.org/10.1016/j.scitotenv.2015.08.047>
- Mezher, T., Fath, H., Abbas, Z., Khaled, A., 2011. Techno-economic assessment and environmental impacts of desalination technologies. *Desalination* 266, 263–273. <https://doi.org/10.1016/j.desal.2010.08.035>
- Mohammad, M.J., Mazahreh, N., 2003. Changes in soil fertility parameters in response to irrigation of forage crops with secondary treated wastewater. *Commun. Soil Sci. Plant Anal.* 34, 1281–1294. <https://doi.org/10.1081/CSS-120020444>
- Mu, E. V., 2012. 2000\_ Controlled Struvite Crystallisation for Removing Phosphorus From Anaerobic Digestion Sidestreams 35, 1–9.
- Nazir, A., Khan, K., Maan, A., Zia, R., Giorno, L., Schroën, K., 2019. Membrane separation technology for the recovery of nutraceuticals from food industrial streams. *Trends Food Sci. Technol.* 86, 426–438. <https://doi.org/https://doi.org/10.1016/j.tifs.2019.02.049>
- Nelson, N.O., Mikkelsen, R.L., Hesterberg, D.L., 2003. Struvite precipitation in anaerobic swine lagoon liquid: Effect of pH and Mg:P ratio and determination of rate constant. *Bioresour. Technol.* 89, 229–236. [https://doi.org/10.1016/S0960-8524\(03\)00076-2](https://doi.org/10.1016/S0960-8524(03)00076-2)

- Ng, L.Y., Ng, C.Y., Mahmoudi, E., Ong, C.B., Mohammad, A.W., 2018. A review of the management of inflow water, wastewater and water reuse by membrane technology for a sustainable production in shrimp farming. *J. Water Process Eng.* 23, 27–44. <https://doi.org/https://doi.org/10.1016/j.jwpe.2018.02.020>
- OECD, 2012. OECD Environmental Outlook to 2050.
- Oh, S.E., Kim, J.R., Joo, J.-H., Logan, B.E., 2009. Effects of applied voltages and dissolved oxygen on sustained power generation by microbial fuel cells. *Water Sci. Technol.* 60, 1311–1317. <https://doi.org/10.2166/wst.2009.444>
- Oh, S.E., Logan, B.E., 2007. Voltage reversal during microbial fuel cell stack operation. *J. Power Sources* 167, 11–17. <https://doi.org/10.1016/j.jpowsour.2007.02.016>
- Okamoto, Y., Lienhard, J.H., 2019. How RO membrane permeability and other performance factors affect process cost and energy use: A review. *Desalination* 470, 114064. <https://doi.org/10.1016/j.desal.2019.07.004>
- Osada, T., Haga, K., Harada, Y., 1991. Removal of nitrogen and phosphorus from swine wastewater by the activated sludge units with the intermittent aeration process. *Water Res.* 25, 1377–1388. [https://doi.org/10.1016/0043-1354\(91\)90116-8](https://doi.org/10.1016/0043-1354(91)90116-8)
- Parsons, S.A., Smith, J.A., 2008. Phosphorus removal and recovery from municipal wastewaters. *Elements* 4, 109–112. <https://doi.org/10.2113/GSELEMENTS.4.2.109>
- Perera, M.K., Englehardt, J.D., Dvorak, A.C., 2019. Technologies for Recovering Nutrients from Wastewater: A Critical Review. *Environ. Eng. Sci.* 36, 511–529. <https://doi.org/10.1089/ees.2018.0436>

- Phuntsho, S., Shon, H.K., Hong, S., Lee, S., Vigneswaran, S., 2011. A novel low energy fertilizer driven forward osmosis desalination for direct fertigation: Evaluating the performance of fertilizer draw solutions. *J. Memb. Sci.* 375, 172–181.  
<https://doi.org/https://doi.org/10.1016/j.memsci.2011.03.038>
- Qin, M., He, Z., 2014. Self-Supplied Ammonium Bicarbonate Draw Solute for Achieving Wastewater Treatment and Recovery in a Microbial Electrolysis Cell-Forward Osmosis-Coupled System. *Environ. Sci. Technol. Lett.* 1, 437–441.  
<https://doi.org/10.1021/ez500280c>
- Qin, M., Molitor, H., Brazil, B., Novak, J.T., He, Z., 2016. *Bioresource Technology* Recovery of nitrogen and water from landfill leachate by a microbial electrolysis cell – forward osmosis system 200, 485–492.  
<https://doi.org/10.1016/j.biortech.2015.10.066>
- Qin, Y., Mueller, N.D., Siebert, S., Jackson, R.B., AghaKouchak, A., Zimmerman, J.B., Tong, D., Hong, C., Davis, S.J., 2019. Flexibility and intensity of global water use. *Nat. Sustain.* 2, 515–523. <https://doi.org/10.1038/s41893-019-0294-2>
- Qiu, G., Law, Y.M., Das, S., Ting, Y.P., 2015. Direct and complete phosphorus recovery from municipal wastewater using a hybrid microfiltration-forward osmosis membrane bioreactor process with seawater brine as draw solution. *Environ. Sci. Technol.* 49, 6156–6163. <https://doi.org/10.1021/es504554f>
- Qiu, G., Ting, Y.-P., 2014. Direct phosphorus recovery from municipal wastewater via osmotic membrane bioreactor (OMBR) for wastewater treatment. *Bioresour. Technol.* 170, 221–229.

<https://doi.org/https://doi.org/10.1016/j.biortech.2014.07.103>

Qu, D., Sun, D., Wang, H., Yun, Y., 2013. Experimental study of ammonia removal from water by modified direct contact membrane distillation. *Desalination* 326, 135–140.

<https://doi.org/10.1016/j.desal.2013.07.021>

Quan, X., Quan, Y., Tao, K., 2012. Effect of anode aeration on the performance and microbial community of an air–cathode microbial fuel cell. *Chem. Eng. J.* 210, 150–

156. <https://doi.org/https://doi.org/10.1016/j.cej.2012.09.009>

Quist-Jensen, C.A., Jørgensen, M.K., Christensen, M.L., 2016. Treated seawater as a magnesium source for phosphorous recovery from wastewater—A feasibility and cost analysis. *Membranes (Basel)*. 6. <https://doi.org/10.3390/membranes6040054>

Rahaman, M.S., Ellis, N., Mavinic, D.S., 2008. Effects of Various Process Parameters on Struvite Precipitation. *Water Sci. Technol.* 57, 647–654.

<https://doi.org/10.2166/wst.2008.022>

Rahman, M.M., Salleh, M.A.M., Rashid, U., Ahsan, A., Hossain, M.M., Ra, C.S., 2014. Production of slow release crystal fertilizer from wastewaters through struvite crystallization - A review. *Arab. J. Chem.* 7, 139–155.

<https://doi.org/10.1016/j.arabjc.2013.10.007>

Rasouli, Z., Valverde-Pérez, B., D'Este, M., De Francisci, D., Angelidaki, I., 2018.

Nutrient recovery from industrial wastewater as single cell protein by a co-culture of green microalgae and methanotrophs. *Biochem. Eng. J.* 134, 129–135.

<https://doi.org/https://doi.org/10.1016/j.bej.2018.03.010>

- Rastgar, M., Bozorg, A., Shakeri, A., Sadrzadeh, M., 2019. Substantially improved antifouling properties in electro-oxidative graphene laminate forward osmosis membrane. *Chem. Eng. Res. Des.* 141, 413–424.  
<https://doi.org/10.1016/j.cherd.2018.11.010>
- Ren, L., Li, Y., Wang, K., Ding, K., Sha, M., Cao, Y., Kong, F., Wang, S., 2021. Recovery of phosphorus from eutrophic water using nano zero-valent iron-modified biochar and its utilization. *Chemosphere* 284, 131391.  
<https://doi.org/10.1016/j.chemosphere.2021.131391>
- Ronen, A., Duan, W., Wheeldon, I., Walker, S., Jassby, D., 2015. Microbial Attachment Inhibition through Low-Voltage Electrochemical Reactions on Electrically Conducting Membranes. *Environ. Sci. Technol.* 49, 12741–12750.  
<https://doi.org/10.1021/acs.est.5b01281>
- Rossrucker, L., Samaniego, A., Grote, J.-P., Mingers, A.M., Laska, C.A., Birbilis, N., Frankel, G.S., Mayrhofer, K.J.J., 2015. The pH Dependence of Magnesium Dissolution and Hydrogen Evolution during Anodic Polarization. *J. Electrochem. Soc.* 162, C333–C339. <https://doi.org/10.1149/2.0621507jes>
- Rozendal, R.A., Hamelers, H.V.M., Buisman, C.J.N., 2006. Effects of Membrane Cation Transport on pH and Microbial Fuel Cell Performance. *Environ. Sci. Technol.* 40, 5206–5211. <https://doi.org/10.1021/es060387r>
- Ruan, H., Yang, Z., Lin, J., Shen, J., Ji, J., Gao, C., Bruggen, B. Van Der, 2015. Biogas slurry concentration hybrid membrane process : Pilot-testing and RO membrane cleaning. *DES* 368, 171–180. <https://doi.org/10.1016/j.desal.2015.04.015>

- S.A, L.-E., 2006. Support to DG Environment for the development of the Mediterranean De-pollution Initiative “ Horizon 2020 ” 84–96.
- Saidou, H., Korchef, A., Moussa, S.B., Amor, M.B., 2015. Study of Cd<sup>2+</sup>, Al<sup>3+</sup>, and SO<sub>4</sub><sup>2-</sup> Ions Influence on Struvite Precipitation from Synthetic Water by Dissolved CO<sub>2</sub> Degasification Technique. *Open J. Inorg. Chem.* 5, 51–54.  
<https://doi.org/10.4236/ojic.2015.53006>
- Salih, H.H., Dastgheib, S.A., 2017. Treatment of a hypersaline brine, extracted from a potential CO<sub>2</sub> sequestration site, and an industrial wastewater by membrane distillation and forward osmosis. *Chem. Eng. J.* 325, 415–423.  
<https://doi.org/10.1016/j.cej.2017.05.075>
- Satinover, S.J., Rodriguez, M., Borole, A.P., 2020. Microbial electrolysis cell recovery after inducing operational failure conditions. *Biochem. Eng. J.* 164, 107800.  
<https://doi.org/10.1016/j.bej.2020.107800>
- Sevda, S., Abu-Reesh, I.M., Yuan, H., He, Z., 2017. Bioelectricity generation from treatment of petroleum refinery wastewater with simultaneous seawater desalination in microbial desalination cells. *Energy Convers. Manag.* 141, 101–107.  
<https://doi.org/10.1016/j.enconman.2016.05.050>
- Shaffer, D.L., Werber, J.R., Jaramillo, H., Lin, S., Elimelech, M., 2015. Forward osmosis : Where are we now ? *DES* 356, 271–284.  
<https://doi.org/10.1016/j.desal.2014.10.031>
- She, Q., Wang, R., Fane, A.G., Tang, C.Y., 2016. Membrane fouling in osmotically driven membrane processes: A review. *J. Memb. Sci.* 499, 201–233.

<https://doi.org/10.1016/j.memsci.2015.10.040>

Shi, L., Hu, Y., Xie, S., Wu, G., Hu, Z., Zhan, X., 2018. Recovery of nutrients and volatile fatty acids from pig manure hydrolysate using two-stage bipolar membrane electro dialysis. *Chem. Eng. J.* 334, 134–142.

<https://doi.org/10.1016/j.cej.2017.10.010>

Sleutels, T.H.J.A., Hamelers, H.V.M., Rozendal, R.A., Buisman, C.J.N., 2009. Ion transport resistance in Microbial Electrolysis Cells with anion and cation exchange membranes. *Int. J. Hydrogen Energy* 34, 3612–3620.

<https://doi.org/https://doi.org/10.1016/j.ijhydene.2009.03.004>

Smil, V., 2000. Phosphorus in the Environment : Natural Flows and Human Interferences 53–88.

Snyder, S., Westerhoff, P., Yoon, Y., Sedlak, D., 2003. Disruptors in Water : Implications for the Water Industry. *Environ. Eng. Sci.* 20, 449–469.

<https://doi.org/doi:10.1089/109287503768335931>

Son, M., Kim, T., Yang, W., Gorski, C.A., Logan, B.E., 2019. Electro-Forward Osmosis. *Environ. Sci. Technol.* 53, 8352–8361. <https://doi.org/10.1021/acs.est.9b01481>

Song, H., Xie, F., Chen, W., Liu, J., 2018. FO/MD hybrid system for real dairy wastewater recycling. *Environ. Technol.* 39, 2411–2421.

<https://doi.org/10.1080/09593330.2017.1377771>

Spångberg, J., Tidåker, P., Jönsson, H., 2014. Environmental impact of recycling nutrients in human excreta to agriculture compared with enhanced wastewater

treatment. *Sci. Total Environ.* 493, 209–219.

<https://doi.org/10.1016/j.scitotenv.2014.05.123>

Suárez, A., Fernández, P., Ramón Iglesias, J., Iglesias, E., Riera, F.A., 2015. Cost assessment of membrane processes: A practical example in the dairy wastewater reclamation by reverse osmosis. *J. Memb. Sci.* 493, 389–402.

<https://doi.org/10.1016/j.memsci.2015.04.065>

Sutzkover-Gutman, I., Hasson, D., 2010. Feed water pretreatment for desalination plants.

*Desalination* 264, 289–296. <https://doi.org/10.1016/j.desal.2010.07.014>

Tan, X., Acquah, I., Liu, H., Li, W., Tan, S., 2019. A critical review on saline wastewater treatment by membrane bioreactor (MBR) from a microbial perspective.

*Chemosphere* 220, 1150–1162. <https://doi.org/10.1016/j.chemosphere.2019.01.027>

Tang, L., Iddya, A., Zhu, X., Dudchenko, A. V., Duan, W., Turchi, C., Vanneste, J., Cath, T.Y., Jassby, D., 2017. Enhanced Flux and Electrochemical Cleaning of Silicate Scaling on Carbon Nanotube-Coated Membrane Distillation Membranes Treating Geothermal Brines. *ACS Appl. Mater. Interfaces* 9, 38594–38605.

<https://doi.org/10.1021/acsami.7b12615>

Telzhensky, M., Birnhack, L., Lehmann, O., Windler, E., Lahav, O., 2011. Selective separation of seawater Mg<sup>2+</sup> ions for use in downstream water treatment processes.

*Chem. Eng. J.* 175, 136–143. <https://doi.org/10.1016/j.cej.2011.09.082>

Terán, R.A.S., Orozco, C. de la M., Acuña, I.J.G., Rosales, S.G., Araujo, G.D., Arias, H.O.R., 2017. Removing organic matter and nutrients from swine wastewater after anaerobic-aerobic treatment. *Water (Switzerland)* 9, 1–11.

<https://doi.org/10.3390/w9100726>

Ternes, T.A., Bonerz, M., Herrmann, N., Teiser, B., Andersen, H.R., 2007. Irrigation of treated wastewater in Braunschweig, Germany: An option to remove pharmaceuticals and musk fragrances. *Chemosphere* 66, 894–904.

<https://doi.org/10.1016/j.chemosphere.2006.06.035>

Thomas, N., Sreedhar, N., Al-Ketan, O., Rowshan, R., Abu Al-Rub, R.K., Arafat, H., 2018. 3D printed triply periodic minimal surfaces as spacers for enhanced heat and mass transfer in membrane distillation. *Desalination* 443, 256–271.

<https://doi.org/10.1016/j.desal.2018.06.009>

Tijing, L.D., Woo, Y.C., Choi, J.S., Lee, S., Kim, S.H., Shon, H.K., 2015. Fouling and its control in membrane distillation-A review. *J. Memb. Sci.*

<https://doi.org/10.1016/j.memsci.2014.09.042>

Tran, A.T.K., Zhang, Y., De Corte, D., Hannes, J.-B., Ye, W., Mondal, P., Jullok, N., Meesschaert, B., Pinoy, L., Van der Bruggen, B., 2014. P-recovery as calcium phosphate from wastewater using an integrated selectrodialysis/crystallization process. *J. Clean. Prod.* 77, 140–151.

<https://doi.org/https://doi.org/10.1016/j.jclepro.2014.01.069>

Van Der Bruggen, B., Luis, P., 2015. Forward osmosis: Understanding the hype. *Rev. Chem. Eng.* 31, 1–12. <https://doi.org/10.1515/revce-2014-0033>

Vaneeckhaute, C., Lebuf, V., Michels, E., Belia, E., Vanrolleghem, P.A., Tack, F.M.G., Meers, E., 2017. Nutrient Recovery from Digestate: Systematic Technology Review and Product Classification. *Waste and Biomass Valorization* 8, 21–40.

<https://doi.org/10.1007/s12649-016-9642-x>

Vélez-Pérez, L.S., Ramirez-Nava, J., Hernández-Flores, G., Talavera-Mendoza, O., Escamilla-Alvarado, C., Poggi-Varaldo, H.M., Solorza-Feria, O., López-Díaz, J.A., 2020. Industrial acid mine drainage and municipal wastewater co-treatment by dual-chamber microbial fuel cells. *Int. J. Hydrogen Energy* 45, 13757–13766.

<https://doi.org/10.1016/j.ijhydene.2019.12.037>

Villano, M., Scardala, S., Aulenta, F., Majone, M., 2013. Carbon and nitrogen removal and enhanced methane production in a microbial electrolysis cell. *Bioresour. Technol.* 130, 366–371.

<https://doi.org/https://doi.org/10.1016/j.biortech.2012.11.080>

Volpin, F, Chekli, L., Phuntsho, S., Ghaffour, N., Vrouwenvelder, J.S., Shon, H.K., 2019. Optimisation of a forward osmosis and membrane distillation hybrid system for the treatment of source-separated urine. *Sep. Purif. Technol.* 212, 368–375.

<https://doi.org/https://doi.org/10.1016/j.seppur.2018.11.003>

Volpin, Federico, Heo, H., Hasan Johir, M.A., Cho, J., Phuntsho, S., Shon, H.K., 2019. Techno-economic feasibility of recovering phosphorus, nitrogen and water from dilute human urine via forward osmosis. *Water Res.* 150, 47–55.

<https://doi.org/10.1016/j.watres.2018.11.056>

von Münch, E., Winker, M., 2011. Technology review of urine diversion components 32.

Wang, C.C., Hao, X. Di, 2009. Small-scale formation of struvite by electrochemical deposition and its characterization, in: 3rd International Conference on Bioinformatics and Biomedical Engineering, ICBBE 2009. pp. 1–4.

<https://doi.org/10.1109/ICBBE.2009.5163406>

Wang, C.C., Hao, X.D., Guo, G.S., van Loosdrecht, M.C.M., 2010. Formation of pure struvite at neutral pH by electrochemical deposition. *Chem. Eng. J.* 159, 280–283.

<https://doi.org/10.1016/j.cej.2010.02.026>

Wang, H., Ren, Z.J., 2013a. A comprehensive review of microbial electrochemical systems as a platform technology. *Biotechnol. Adv.* 31, 1796–1807.

<https://doi.org/10.1016/j.biotechadv.2013.10.001>

Wang, H., Ren, Z.J., 2013b. A comprehensive review of microbial electrochemical systems as a platform technology. *Biotechnol. Adv.* 31, 1796–1807.

<https://doi.org/https://doi.org/10.1016/j.biotechadv.2013.10.001>

Wang, J., Burken, J.G., Zhang, X. (Jackie), Surampalli, R., 2005. Engineered struvite precipitation: Impacts of component-ion molar ratios and pH. *J. Environ. Eng.* 131, 1433–1440. [https://doi.org/10.1061/\(ASCE\)0733-9372\(2005\)131:10\(1433\)](https://doi.org/10.1061/(ASCE)0733-9372(2005)131:10(1433))

Wang, J., Wang, Z., Liang, J., He, Z., 2021. Electrolysis-assisted recovery of reverse-fluxed solutes in forward osmosis. *Desalination* 520, 115346.

<https://doi.org/10.1016/j.desal.2021.115346>

Wang, W., Zhang, Y., Esparra-Alvarado, M., Wang, X., Yang, H., Xie, Y., 2014. Effects of pH and temperature on forward osmosis membrane flux using rainwater as the makeup for cooling water dilution. *Desalination* 351, 70–76.

<https://doi.org/10.1016/j.desal.2014.07.025>

Wang, X.J., Xia, S.Q., Chen, L., Zhao, J.F., Renault, N.J., Chovelon, J.M., 2006.

Nutrients removal from municipal wastewater by chemical precipitation in a moving bed biofilm reactor. *Process Biochem.* 41, 824–828.

<https://doi.org/10.1016/j.procbio.2005.10.015>

Wang, Y.-J., Huang, L., Fang, Z., Wang, X.-M., Gao, M., Liu, H.-Q., Li, W.-W., Huang, T.-Y., 2022. Electrochemically self-cleanable carbon nanotube interlayered membrane for enhanced forward osmosis in wastewater treatment. *J. Environ. Chem. Eng.* 10, 107399. <https://doi.org/10.1016/j.jece.2022.107399>

Watkinson, A.J., Murby, E.J., Costanzo, S.D., 2007. Removal of antibiotics in conventional and advanced wastewater treatment: Implications for environmental discharge and wastewater recycling. *Water Res.* 41, 4164–4176. <https://doi.org/10.1016/j.watres.2007.04.005>

Watson, V.J., Saito, T., Hickner, M.A., Logan, B.E., 2011. Polymer coatings as separator layers for microbial fuel cell cathodes. *J. Power Sources* 196, 3009–3014. <https://doi.org/10.1016/j.jpowsour.2010.11.105>

Wick, K., Heumesser, C., Schmid, E., 2012. Groundwater nitrate contamination: Factors and indicators. *J. Environ. Manage.* 111, 178–186. <https://doi.org/10.1016/j.jenvman.2012.06.030>

Woo, Y.C., Kim, Y., Yao, M., Tijjng, L.D., Choi, J.-S., Lee, S., Kim, S.-H., Shon, H.K., 2018. Hierarchical Composite Membranes with Robust Omniphobic Surface Using Layer-By-Layer Assembly Technique. *Environ. Sci. Technol.* 52, 2186–2196. <https://doi.org/10.1021/acs.est.7b05450>

Wu, X., Modin, O., 2013. Ammonium recovery from reject water combined with

- hydrogen production in a bioelectrochemical reactor. *Bioresour. Technol.* 146, 530–536. <https://doi.org/10.1016/j.biortech.2013.07.130>
- Wu, Z., Zou, S., Zhang, B., Wang, L., He, Z., 2018. Forward osmosis promoted in-situ formation of struvite with simultaneous water recovery from digested swine wastewater. *Chem. Eng. J.* 342, 274–280. <https://doi.org/10.1016/j.cej.2018.02.082>
- Xie, M., Nghiem, L.D., Price, W.E., Elimelech, M., 2014. Toward Resource Recovery from Wastewater: Extraction of Phosphorus from Digested Sludge Using a Hybrid Forward Osmosis-Membrane Distillation Process. *Environ. Sci. Technol. Lett.* 1, 191–195. <https://doi.org/10.1021/ez400189z>
- Xie, M., Nghiem, L.D., Price, W.E., Elimelech, M., 2013. A Forward Osmosis–Membrane Distillation Hybrid Process for Direct Sewer Mining: System Performance and Limitations. *Environ. Sci. Technol.* 47, 13486–13493. <https://doi.org/10.1021/es404056e>
- Xie, M., Shon, H.K., Gray, S.R., Elimelech, M., 2016. Membrane-based processes for wastewater nutrient recovery: Technology, challenges, and future direction. *Water Res.* 89, 210–221. <https://doi.org/10.1016/j.watres.2015.11.045>
- Xu, M., Zhao, P., Tang, C.Y., Yi, X., Wang, X., 2022. Preparation of electrically enhanced forward osmosis (FO) membrane by two-dimensional MXenes for organic fouling mitigation. *Chinese Chem. Lett.* 33, 3818–3822. <https://doi.org/10.1016/j.ccllet.2021.11.071>
- Xu, Y., Peng, X., Tang, C.Y., Fu, Q.S., Nie, S., 2010. Effect of draw solution concentration and operating conditions on forward osmosis and pressure retarded

- osmosis performance in a spiral wound module. *J. Memb. Sci.* 348, 298–309.  
<https://doi.org/10.1016/j.memsci.2009.11.013>
- Yan, T., Ye, Y., Ma, H., Zhang, Y., Guo, W., Du, B., Wei, Q., 2018. A critical review on membrane hybrid system for nutrient recovery from wastewater. *Chem. Eng. J.* 348, 143–156. <https://doi.org/10.1016/j.cej.2018.04.166>
- Yang, L., Huang, T., Zhou, Y., Wang, H., Zhang, Z., Pang, Z., 2011. Technology progresses of swine wastewater treatment from large-scale pig farms, in: *ISWREP 2011 - Proceedings of 2011 International Symposium on Water Resource and Environmental Protection*. pp. 947–950.  
<https://doi.org/10.1109/ISWREP.2011.5893167>
- Yao, M., Woo, Y.C., Tijing, L.D., Choi, J.S., Shon, H.K., 2018. Effects of volatile organic compounds on water recovery from produced water via vacuum membrane distillation. *Desalination* 440, 146–155. <https://doi.org/10.1016/j.desal.2017.11.012>
- Ye, Y., Hao, H., Guo, W., Liu, Y., Woong, S., 2019. Feasibility study on a double chamber microbial fuel cell for nutrient recovery from municipal wastewater. *Chem. Eng. J.* 358, 236–242. <https://doi.org/10.1016/j.cej.2018.09.215>
- You, K., Ge, F., Wu, X., Song, K., Yang, Z., Zhang, Q., Liu, Y., Ruan, R., Zheng, H., 2021. Nutrients recovery from piggery wastewater and starch wastewater via microalgae-bacteria consortia. *Algal Res.* 60, 102551.  
<https://doi.org/https://doi.org/10.1016/j.algal.2021.102551>
- Yuan, H., Abu-Reesh, I.M., He, Z., 2016. Mathematical modeling assisted investigation of forward osmosis as pretreatment for microbial desalination cells to achieve

- continuous water desalination and wastewater treatment. *J. Memb. Sci.* 502, 116–123. <https://doi.org/10.1016/j.memsci.2015.12.026>
- Yuan, H., Abu-Reesh, I.M., He, Z., 2015. Enhancing desalination and wastewater treatment by coupling microbial desalination cells with forward osmosis. *Chem. Eng. J.* 270, 437–443. <https://doi.org/10.1016/j.cej.2015.02.059>
- Yuan, H., He, Z., 2015. Integrating membrane filtration into bioelectrochemical systems as next generation energy-efficient wastewater treatment technologies for water reclamation: A review. *Bioresour. Technol.* 195, 202–209. <https://doi.org/10.1016/j.biortech.2015.05.058>
- Zang, G.-L., Sheng, G.-P., Li, W.-W., Tong, Z.-H., Zeng, R.J., Shi, C., Yu, H.-Q., 2012. Nutrient removal and energy production in a urine treatment process using magnesium ammonium phosphate precipitation and a microbial fuel cell technique. *Phys. Chem. Chem. Phys.* 14, 1978–1984. <https://doi.org/10.1039/C2CP23402E>
- Zhang, S., Wang, P., Fu, X., Chung, T.S., 2014. Sustainable water recovery from oily wastewater via forward osmosis-membrane distillation (FO-MD). *Water Res.* 52, 112–121. <https://doi.org/10.1016/j.watres.2013.12.044>
- Zhang, X., Li, C., Wang, Y., Luo, J., Xu, T., 2011. Recovery of acetic acid from simulated acetaldehyde wastewaters: Bipolar membrane electro dialysis processes and membrane selection. *J. Memb. Sci.* 379, 184–190. <https://doi.org/10.1016/j.memsci.2011.05.059>
- Zhang, Y., Angelidaki, I., 2014. ScienceDirect Microbial electrolysis cells turning to be versatile technology : Recent advances and future challenges. *Water Res.* 56, 11–25.

<https://doi.org/10.1016/j.watres.2014.02.031>

Zhao, F., Harnisch, F., Schröder, U., Scholz, F., Bogdanoff, P., Herrmann, I., 2006.

Challenges and Constraints of Using Oxygen Cathodes in Microbial Fuel Cells.

Environ. Sci. Technol. 40, 5193–5199. <https://doi.org/10.1021/es060332p>

Zhao, Z.-P., Xu, L., Shang, X., Chen, K., 2013. Water regeneration from human urine by

vacuum membrane distillation and analysis of membrane fouling characteristics.

Sep. Purif. Technol. 118, 369–376.

<https://doi.org/https://doi.org/10.1016/j.seppur.2013.07.021>

Zhou, K.G., Vasu, K.S., Cherian, C.T., Neek-Amal, M., Zhang, J.C., Ghorbanfekr-

Kalashami, H., Huang, K., Marshall, O.P., Kravets, V.G., Abraham, J., Su, Y.,

Grigorenko, A.N., Pratt, A., Geim, A.K., Peeters, F.M., Novoselov, K.S., Nair, R.R.,

2018. Electrically controlled water permeation through graphene oxide membranes.

Nature 559, 236–240. <https://doi.org/10.1038/s41586-018-0292-y>

Zhu, Z.L., Chen, D.L., 2002. Nitrogen fertilizer use in China - Contributions to food

production, impacts on the environment and best management strategies. Nutr. Cycl.

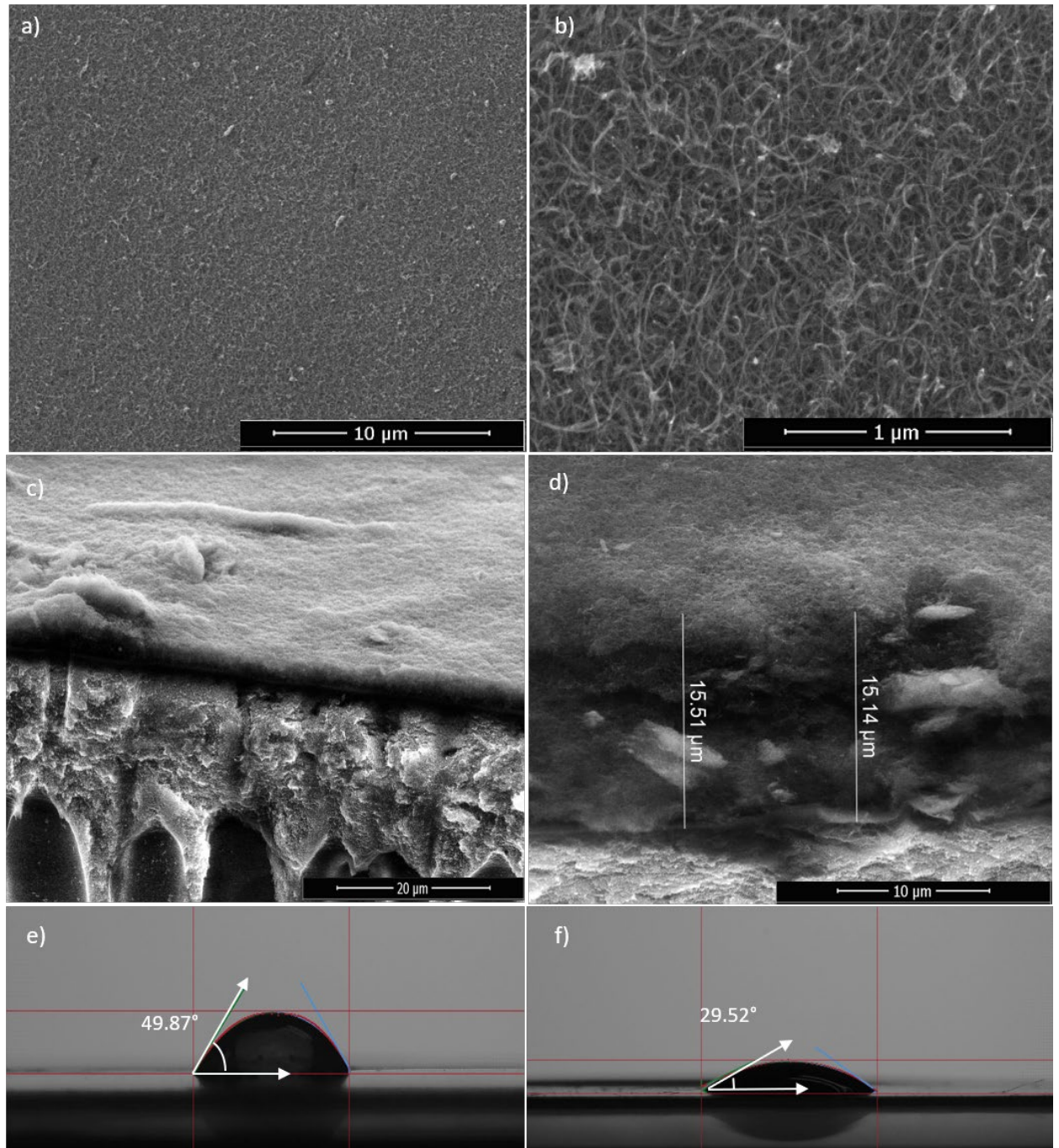
Agroecosystems 63, 117–127. <https://doi.org/10.1023/A:1021107026067>

Zou, S., He, Z., 2017. Electrolysis-assisted mitigation of reverse solute flux in a three-

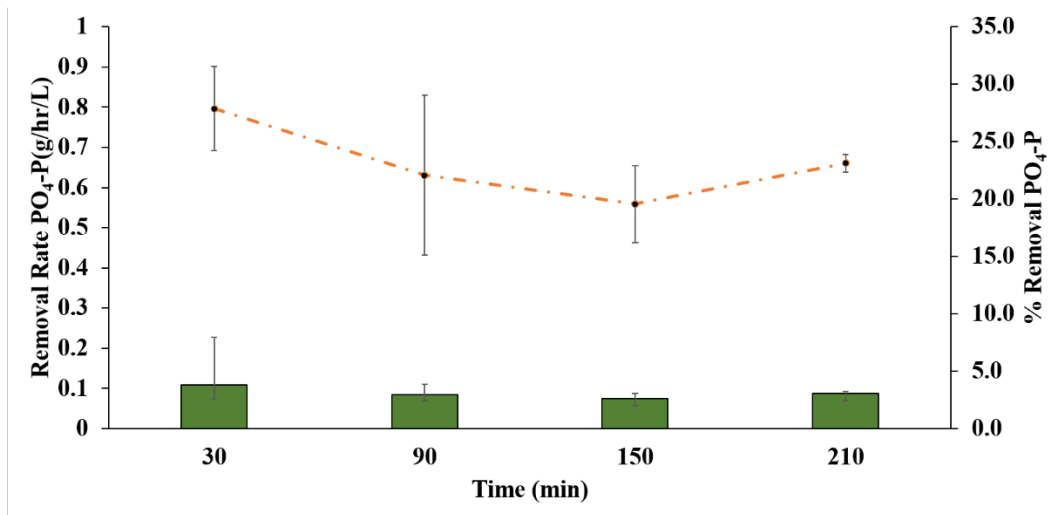
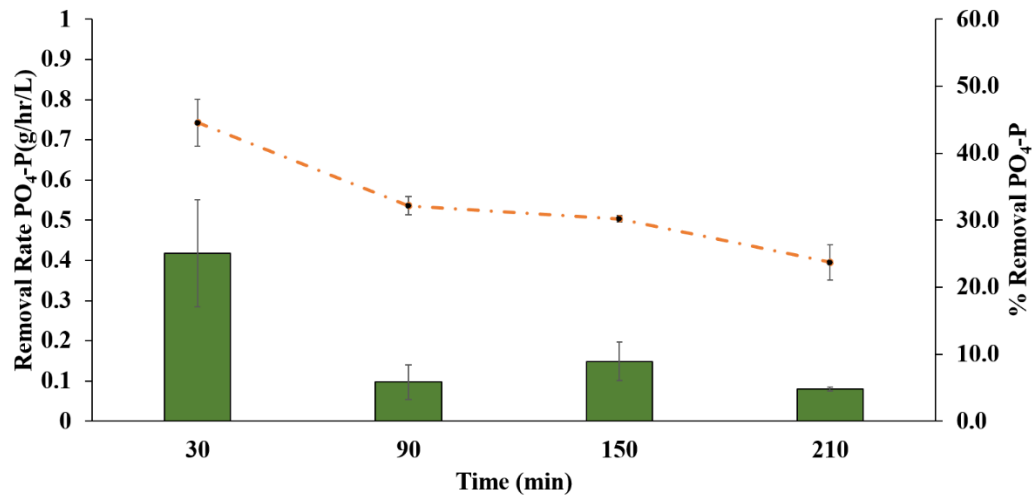
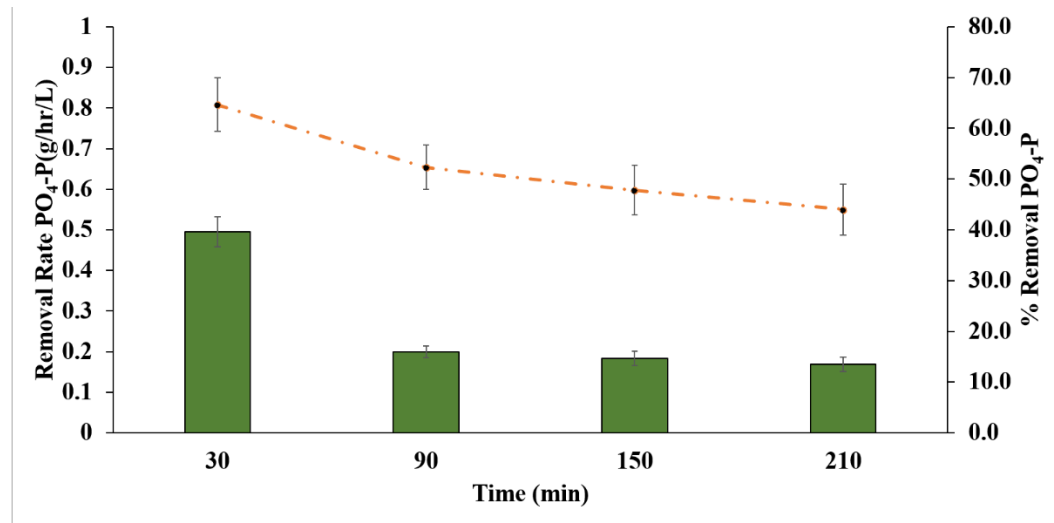
chamber forward osmosis system. Water Res. 115, 111–119.

<https://doi.org/10.1016/j.watres.2017.02.060>

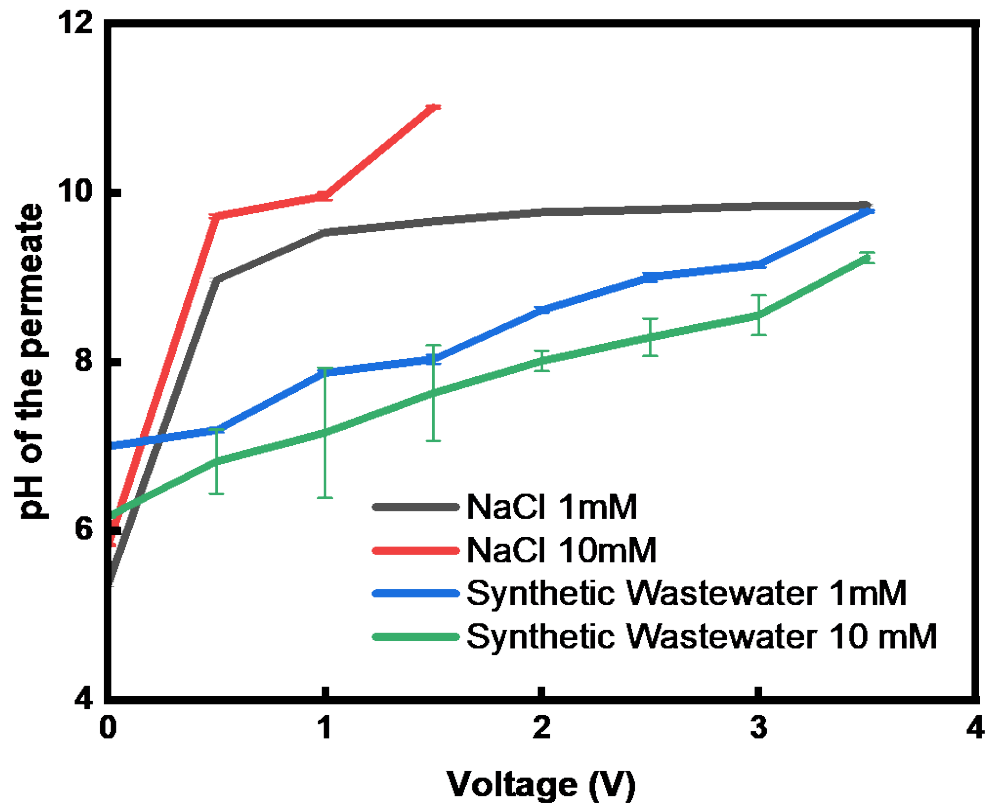
## APPENDIX A. SUPPLEMENTARY MATERIAL



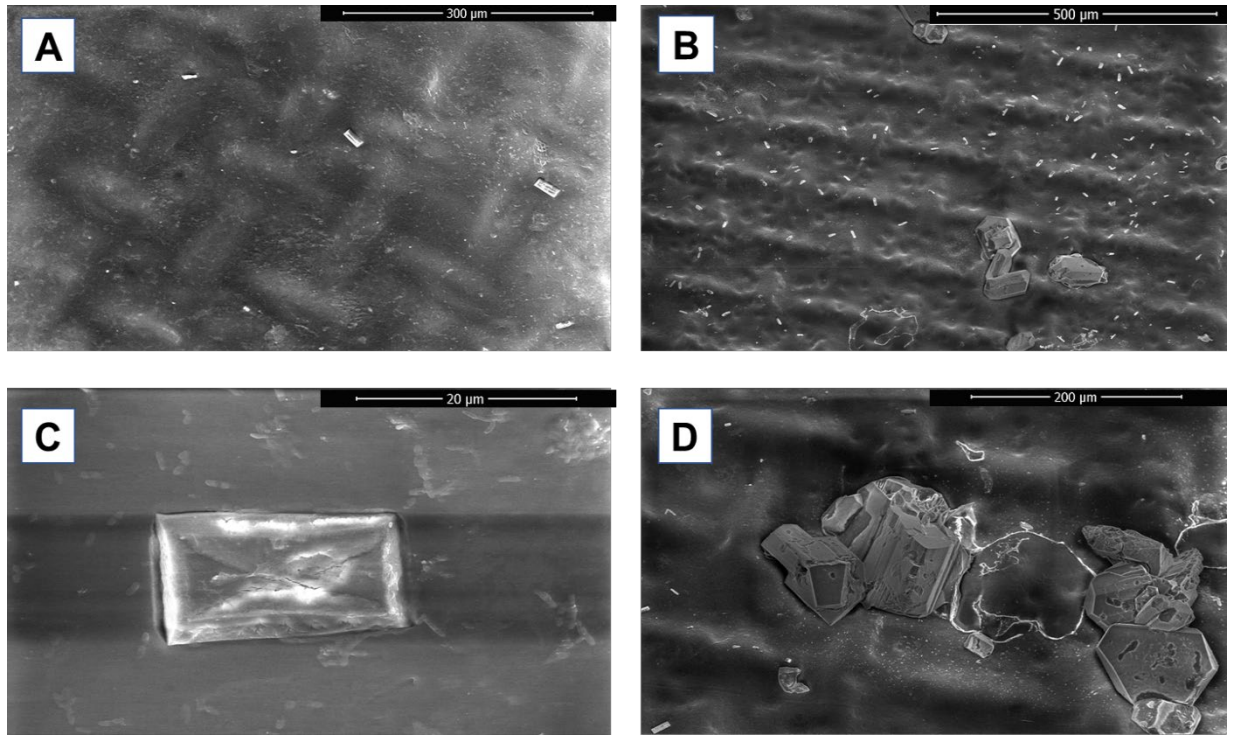
**FigA1.** a) & b) Scanning electron microscopy image of membrane surface c) & d) Cross section of the CNT membrane e) goniometer analysis of uncoated membrane f) goniometer analysis of coated membrane.



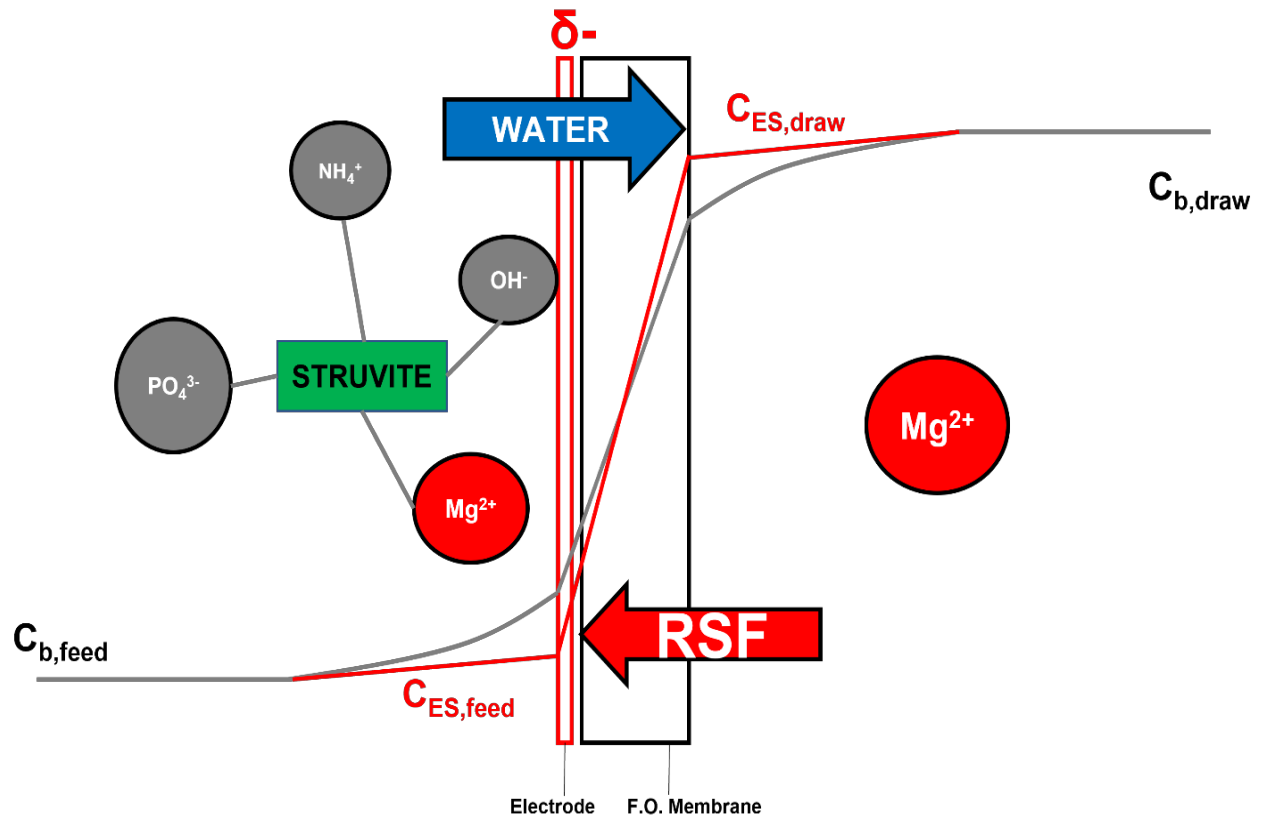
FigA2. Phosphate removal over successive cycles.



**FigA3.** Changes in pH based on voltage application and solution concentration



**FigA4.** a) Struvite precipitation after 5 hour operation b) struvite precipitation after 24 hour operation c) struvite crystal formed during 5 hour operation d) clusters of struvite precipitated after 24 hours



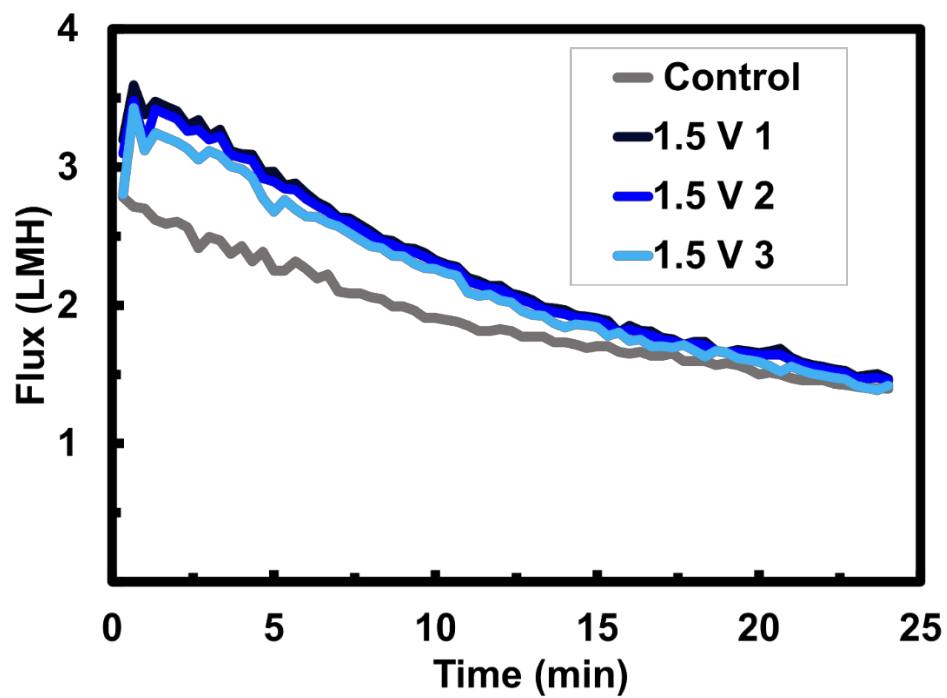
**FigA5.** Electricity assisted forward osmosis process



**FigA6.** Struvite precipitation on forward osmosis membrane system



FigA7. a) Struvite precipitation when electricity is applied b) Salt precipitation without voltage application



FigA8. Successive use of cellulose triacetate forward osmosis membrane under voltage and no voltage conditions